

**LIQUOR COMPOSITION EFFECTS ON
CORROSION RATES IN KRAFT WHITE LIQUOR**

Project 3556

**Report Three
A Progress Report
to**

MEMBERS OF THE INSTITUTE OF PAPER CHEMISTRY

September 11, 1985

NOTICE & DISCLAIMER

The Institute of Paper Chemistry (IPC) has provided a high standard of professional service and has exerted its best efforts within the time and funds available for this project. The information and conclusions are advisory and are intended only for the internal use by any company who may receive this report. Each company must decide for itself the best approach to solving any problems it may have and how, or whether, this reported information should be considered in its approach.

IPC does not recommend particular products, procedures, materials, or services. These are included only in the interest of completeness within a laboratory context and budgetary constraint. Actual products, procedures, materials, and services used may differ and are peculiar to the operations of each company.

In no event shall IPC or its employees and agents have any obligation or liability for damages, including, but not limited to, consequential damages, arising out of or in connection with any company's use of, or inability to use, the reported information. IPC provides no warranty or guaranty of results.

THE INSTITUTE OF PAPER CHEMISTRY

Appleton, Wisconsin

LIQUOR COMPOSITION EFFECTS ON CORROSION RATES
IN KRAFT WHITE LIQUOR

Project 3556

Report Three

A Progress Report

to

MEMBERS OF THE INSTITUTE OF PAPER CHEMISTRY

September 11, 1985

TABLE OF CONTENTS

	Page
ABSTRACT	1
SUMMARY FOR THE NONSPECIALIST	2
INTRODUCTION	4
EXPERIMENTAL PROCEDURES	9
RESULTS	11
Polysulfide	11
Thiosulfate	21
DISCUSSION	32
Polysulfide	32
Thiosulfate	40
Implications for Pulp Mill Operations	42
CONCLUSIONS	43
ACKNOWLEDGMENTS	44
REFERENCES	45
APPENDIX I: EVALUATION OF EXPERIMENTAL PROCEDURES	47
APPENDIX II: CORROSION POTENTIAL DURING WEIGHT LOSS TESTS	52
APPENDIX III: DATA FROM POLARIZATION CURVES	86

THE INSTITUTE OF PAPER CHEMISTRY

Appleton, Wisconsin

LIQUOR COMPOSITION EFFECTS ON CORROSION RATES
IN KRAFT WHITE LIQUOR

ABSTRACT

The effects of additions of elemental sulfur and sodium thiosulfate on corrosion rates of 1018 carbon steel in alkaline sulfide solutions have been determined by long term weight loss tests. The polarization behavior of 1018 steel and gold in the solutions was investigated.

Elemental sulfur, which forms polysulfide, had a transient effect at low concentration, increasing corrosion rate initially. After further exposure the corrosion potential increased, the electrode passivated, and corrosion rate decreased. At higher concentrations, passivation was immediate.

Thiosulfate increased corrosion rates dramatically by placing the corrosion potential at the active-passive transition, where iron dissolution is greatest. Passivation was impaired by thiosulfate.

SUMMARY FOR THE NONSPECIALIST

Corrosion of carbon steel in kraft white liquors reduces the service life of equipment and causes unexpected failures to occur. There is a need to understand the fundamental causes of this corrosion as a first step in reducing corrosion costs. This work addresses that need by providing information on the effects of variation in liquor chemistry.

In general, corrosion rates depend on the concentrations of corrosive species in the solution. This is true of kraft pulping liquors. Changes in concentration of corrosive species will influence the rate of corrosion. The magnitude of this effect will depend on the role a particular species plays in the corrosion process. If the effect on corrosion rate for a range of anticipated concentrations of various corrosive species is known, it should be possible to predict the effect of changes in process chemistry on corrosion rates in the mill. The objective of this work has been to measure the effects on corrosion rates of varying the concentration of important corrosive species in solution.

Specimens were exposed in $\text{NaOH} + \text{Na}_2\text{S}$ aqueous solutions containing polysulfide or thiosulfate, both known to influence corrosion rate. Polysulfide and thiosulfate are common white liquor contaminants resulting from incomplete reduction in the recovery boiler or from air oxidation. Weight losses were measured after 2, 4, 6, and 8 weeks, and corrosion rates were calculated. In the solutions containing low concentrations of polysulfides, there was a high rate of corrosion initially, but the rate decreased to a very low level after a period of exposure, apparently because the electrode formed a passivating oxide film. Dramatic increases in corrosion rate were observed in solutions containing thiosulfate, with the increase in proportion to the thiosulfate concentration.

When steel is exposed in white liquor it develops an electrochemical potential due to the corrosion reactions occurring on its surface. This corrosion potential will depend on the concentration of corrosive species and temperature and therefore will vary depending on the conditions where the steel is exposed. It is possible to obtain information on expected behavior in a variety of conditions by varying this electrochemical potential and observing the behavior. At low potential, the steel actively corrodes; this is the 'active' region. At higher (more noble) potential, the surface becomes partially protected by the formation of an oxide film. Iron sulfides interfere with proper formation of the passive oxide film, and dissolution of the steel continues through the poorly formed film. At still higher potential, a protective or 'passive' oxide film forms and the corrosion rate is very low. Depending on the corrosion potential, dissolution or passivation of the steel occurs. This can account for some of the variation of corrosion rates that may be observed in white liquors. The effects of varying concentrations of polysulfide and thiosulfate on this behavior have been investigated to provide better information on how chemistry can be manipulated to cause passivation of steel in kraft white liquor.

INTRODUCTION

The seriousness of corrosion and stress corrosion cracking in white liquor streams in the kraft pulp mills has been recognized and has received considerable attention in efforts to reduce the costs of corrosion. Nevertheless, no thorough investigation of the effects of liquor composition on corrosion rate has been published.

As early as 1951, corrosion in kraft mills was investigated in Sweden. Ruus and Stockman¹ found that increasing concentrations of sodium sulfide (Na_2S), sodium hydroxide (NaOH), sodium thiosulfate ($\text{Na}_2\text{S}_2\text{O}_3$), and sodium polysulfide (Na_2S_x) stimulated corrosion. Corrosion was also related to the amount of oxygen present in the (batch) digester.²

An account of a U.S. study indicated that poor reproducibility of weight loss test results that had been observed could be related to whether or not the steel was passivated by a protective oxide film.³

Haegland and Roald⁴ suggested that corrosion rates were controlled by the rate of diffusion of polysulfide to the surface, where it was cathodically reduced while anodic dissolution of the steel occurred. Thiosulfate increased polysulfide concentration and sulfite decreased it, apparently by equilibration. Roald⁵ developed an equation relating corrosion rate to the rate of diffusion of polysulfide to the surface. Corrosivity was a function of NaOH , Na_2S , Na_2SO_3 , and Na_2SO_3 (sodium sulfite) concentrations.

Mueller⁶ utilized anodic polarization curves to determine the active-passive nature of steel in white liquor. A large active-passive peak was observed between the active and the passive potential ranges as illustrated in Fig. 1. Higher concentrations of oxidizing species could shift the potential

into the passive range where corrosion rates were lower. The surface is 'passivated' by formation of a thin oxide layer which protects the surface from dissolution. Thus corrosion rates would depend on whether the electrode was passivated or not and this could account for some of the great variation between mill and laboratory. In a subsequent publication, Mueller⁷ stated that stirring doubled the size of the active-passive peak.

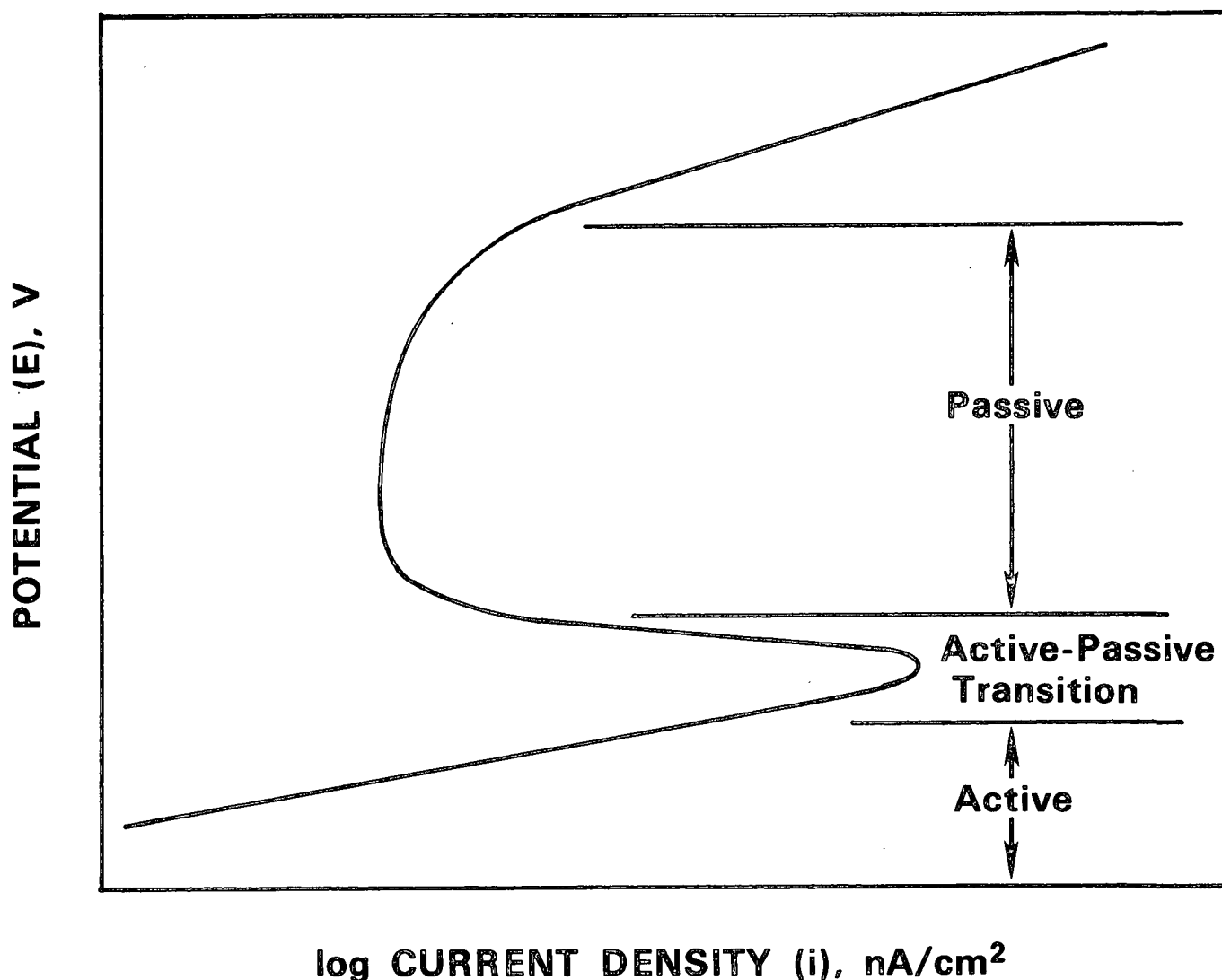


Figure 1. Schematic anodic polarization curve of steel.

At The Institute of Paper Chemistry, Kesler and Bakken⁸ determined that carbonate (Na_2CO_3), chloride (NaCl), and sulfate (Na_2SO_4) slightly depressed the

maximum anodic current density at the active-passive peak. Corrosion was increased only if Na_2SO_3 concentration was < 1 g/L. The additives had a negligible or slightly inhibitive effect when sulfite content was higher. These peak currents could have been influenced by the value of the corrosion potential, with a high cathodic current masking an increase in anodic currents associated with higher actual corrosion rates. They performed weight loss tests and found that corrosion rate correlated with Roald's equation only when liquors contained > 1 g/L Na_2SO_3 .

Landmark and Roald⁹ determined that increasing concentrations of polysulfides decreased the size of the active-passive peak, making passivation easier, and attributed this decrease to the simultaneous cathodic reduction of polysulfide.

The polarization behavior of steel in white liquors was studied by Wensley and Charlton¹⁰ in an effort to determine the effect of various species. Sulfide and thiosulfate impaired passivation. Sulfate and sulfite had no effect. The corrosion potential was controlled by polysulfide concentration.

Tromans¹¹ investigated the polarization behavior of carbon steel in $\text{NaOH} + \text{Na}_2\text{S}$ solutions in an effort to better understand the processes causing corrosion. Passivation was found to be inhibited by the incorporation of sulfide into the passivating Fe_3O_4 film. This effort was extended by Crowe,¹² in a study at high temperature. Passivation required the formation of an Fe_2O_3 film, and sulfide impaired the formation of this film. The formation of a soluble iron sulfide species was associated with the active-passive peak.

In the research of stress corrosion cracking in kraft white liquor, Singbeil and Garner³¹ found that inorganic constituents present in spent liquor inhibited cracking. Their result suggests that inorganics may influence corrosion rates.

IPC has undertaken the task of obtaining information on the effect of liquor composition on corrosion rate. Some of these results for NaOH + Na₂S solutions have been described in a previous progress report.¹⁴ At higher NaOH concentration, passivation in sulfide solutions was slower or did not occur, thus resulting in higher corrosion rates. The corrosion rates after 8 week exposures are summarized in the isocorrosion plot in Fig. 2. Active corrosion was balanced by hydrogen reduction. Corrosion potential in the passive region corresponded to the S²⁻/S₂²⁻ redox potential. Intermediate polysulfide concentrations (0.5-2.0 g/L S) increased corrosion rate, but higher concentrations did not. Thiosulfate additions increased the corrosion rate substantially, and copious NaFeS₂ formed on the electrode.

The objective of the present work has been to determine the effect of a range of concentrations of the oxidized sulfur species S_x²⁻ and S₂O₃²⁻ on long-term corrosion rate and to investigate the effects on the polarization behavior. The polarization behavior of gold was investigated to determine which features of the polarization curve of steel are due to reduction and oxidation reactions of sulfides in solution; the gold itself is inert.

The chemistry of alkaline sulfide solutions is complicated by the number of oxidized sulfur species which form, including S_x²⁻, S₂O₃²⁻, SO₃²⁻ and SO₄²⁻. Polysulfide can be formed by addition of elemental sulfur to sulfide solution where it will combine with sulfide. This polysulfide is present in a range of sizes: S₂²⁻, S₃²⁻, S₄²⁻, and S₅²⁻, in equilibrium with each other. Sulfide in its most reduced form is present in alkaline solutions as HS⁻ or S²⁻. The bisulfide ion, HS⁻, is considered to be the predominant form of reduced sulfide at the pH of white liquor,^{12,15,16} and for this reason electrochemical equilibria have been written in terms of HS⁻ in the present work.

The accuracy of experimental methods used in the work was appraised as summarized in Appendix I.

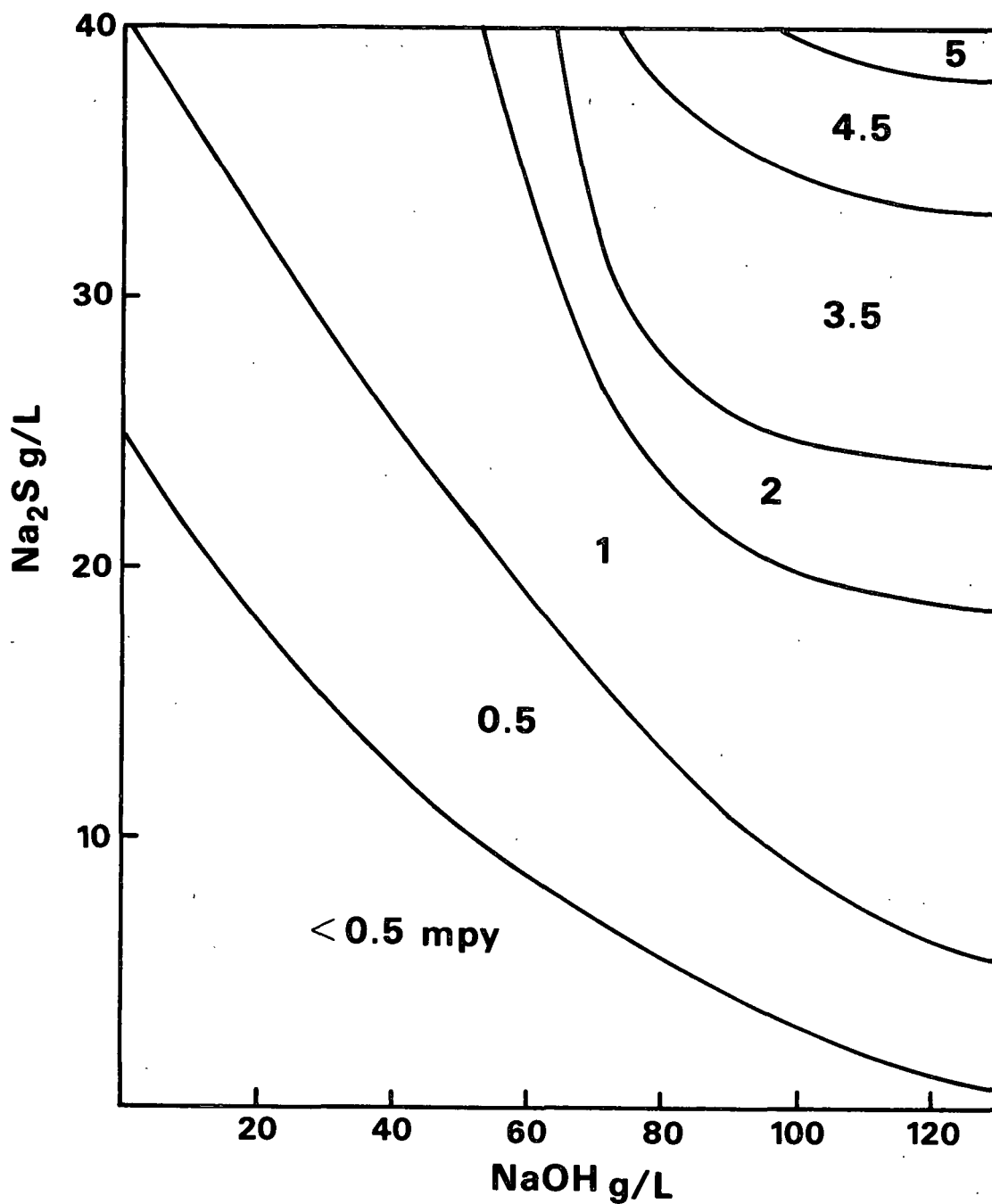


Figure 2. Isocorrosion plot for NaOH + Na₂S solutions.

EXPERIMENTAL PROCEDURES

Corrosion rates were investigated in the present work by exposing 1018 steel weight loss coupons to liquors at 90°C containing NaOH (60-120 g/L), Na₂S (10-40 g/L), S (0-10 g/L), and Na₂S₂O₃ (0-50 g/L) for 2, 4, 6, and 8 weeks.

Experiments were performed in 180 mL Teflon™ beakers with screw-top lids as described in a previous report.¹⁴ The cylindrical electrodes were 3/8-inch in diameter with a surface area of 9 cm², tapped at one end and polished to 120 grit and degreased. The composition of the 1018 steel has been listed previously.¹⁴ The electrode holders were constructed of Teflon™. The electrode was isolated from the holder by a Hypalon™ gasket. Each cell contained four electrodes to be removed at two week intervals and a silver-silver sulfide reference electrode. After the test the electrodes were carefully blasted clean before weighing. The experimental procedures and cleaning methods were evaluated as described in Appendix I.

Polysulfide solutions were prepared in a purged flask using analytical reagents and distilled water. Thiosulfate solutions were purged after make-up. In the series using elemental sulfur to form S_x²⁻, solutions were changed every three days to ensure that polysulfide concentrations were not decreased by oxidation. Solutions containing thiosulfate, considered more stable, were changed at two week intervals. The solutions were changed in a glove bag under a nitrogen atmosphere to prevent oxidation by air. Solutions were maintained at 90°C throughout the test. The open circuit or corrosion potentials of the specimens were recorded daily and plotted.

Anodic and cathodic polarization curves were obtained for steel and gold in each liquor composition at 90°C. Potential was scanned at 1 mV/s using a

Princeton Applied Research Model 350 corrosion measurement system. All measured potentials have been quoted with respect to the silver-silver sulfide electrode, V(SSSE), or have been converted to the standard hydrogen scale, V(SHE). These potentials may be related by the equation:

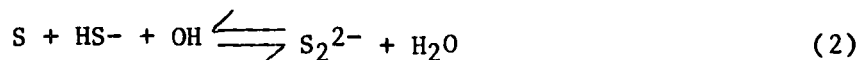
$$V(SHE) = V(SSSE) - 0.7125 - 0.039 \log ([Na_2S]/858) \quad (1)$$

where $[Na_2S]$ is the sodium sulfide concentration in g/L, as described previously.¹⁷

RESULTS

POLYSULFIDE

Elemental sulfur was added to sulfide solutions to form polysulfide via



The effect of S_x^{2-} on corrosion weight loss is summarized in Table 1. Low concentrations of polysulfide (0.5-2.0 g/L S) caused a substantial increase in corrosion initially, but the rate declined after some exposure time, presumably due to passivation of the surface. This effect was more pronounced at high HS^- concentrations and to a lesser extent at high OH^- concentrations. After eight weeks exposure, the differences were reduced, apparently because the electrodes spent most of their exposure in the passive condition. Figures 3 and 4 illustrate the 5 mpy isocorrosion surface in the $NaOH + Na_2S + S$ solutions after 2 and 8 weeks, respectively. Corrosion rates in solutions of compositions located inside the isocorrosion surface exceeded 5 mpy. Solutions with compositions located on the surface caused corrosion rates of 5 mpy. The figures illustrate that the average corrosion rate is above 5 mpy for a smaller range of solutions after 8 weeks exposure, and the range corresponds to the range of much higher rates measured after the 2 week test.

The effect of S additions on corrosion rate (after 2 weeks exposure) is shown dramatically in Fig. 5 for 120 g/L NaOH solution with a range of Na_2S concentrations.

The variation of the corrosion potential of the electrodes with time is plotted in Fig. 6 for the range of S_x^{2-} concentrations in 100 g/L NaOH + 30 g/L Na_2S . The plot indicates that the potential became more noble after a period of

Table 1. White liquor studies - polysulfide weight loss results.

NaOH, g/L	Na ₂ S, g/L	S as elemental sulfur, g/L						
		0	0.5	1.0	1.5	2.0	5.0	10.0
2 Weeks, mpy								
60	10	2.3	5.0	3.6	0.6	0.9	0.5	0.8
	20	2.1	6.1	9.5	0.8	18.2	3.3	3.8
	30	4.3	17.7	15.4	13.3	18.9	3.8	3.3
	40	5.2	21.8	19.7	14.4	15.4	6.4	1.1
80	10	2.2	5.3	0.5	0.7	1.1	0.4	0.6
	20	2.9	7.6	8.8	12.4	20.4	1.7	2.2
	30	3.4	21.7	13.9	19.1	18.6	2.0	2.4
	40	4.5	15.7	14.2	17.1	22.0	4.8	2.4
100	10	3.4	7.7	10.8	1.7	7.7	1.2	1.2
	20	2.7	10.2	15.9	22.5	17.9	1.1	1.2
	30	4.3	9.0	24.7	19.0	20.3	11.8	2.6
	40	4.1	20.9	35.0	51.3	62.4	9.4	2.1
120	10	5.1	7.2	10.4	14.3	9.7	2.0	2.0
	20	5.1	15.6	9.5	14.0	19.4	5.9	3.8
	30	6.5	21.2	38.9	19.4	19.9	12.8	7.2
	40	5.5	19.9	39.0	16.8	20.8	16.6	14.1
4 Weeks, mpy								
60	10	0.6	2.6	0.8	1.0	0.5	0.6	0.5
	20	—	4.9	4.3	12.6	1.3	2.0	2.1
	30	3.6	8.7	6.0	6.0	1.6	1.8	1.9
	40	4.1	12.4	19.9	14.8	9.7	0.8	0.7
80	10	2.1	3.0	9.6	0.7	0.8	1.0	0.8
	20	2.6	4.0	4.5	6.7	8.5	2.1	1.5
	30	3.3	16.1	7.3	9.7	14.7	1.4	1.8
	40	5.4	18.0	7.1	10.2	11.9	6.7	2.1
100	10	4.4	4.9	6.3	1.9	1.4	1.2	1.2
	20	3.6	10.3	11.6	14.0	21.5	2.0	1.7
	30	3.6	8.2	14.0	10.2	11.0	3.4	1.7
	40	4.8	21.7	35.1	26.5	37.6	4.9	1.9
120	10	4.1	4.2	5.9	7.7	6.3	1.8	1.6
	20	5.9	10.8	4.9	7.3	13.5	5.1	2.2
	30	5.4	20.2	34.1	10.4	25.8	7.4	8.8
	40	5.1	19.3	34.6	8.6	10.5	6.6	7.0

Table 1 (Continued). White liquor studies - polysulfide weight loss results.

NaOH, g/L	Na ₂ S,g/L	S as elemental sulfur, g/L						
		0	0.5	1.0	1.5	2.0	5.0	10.0
6 weeks, mpy								
60	10	0.6	1.6	0.7	0.6	0.5	0.6	3.4
	20	2.1	2.5	2.8	0.6	1.2	0.9	0.9
	30	2.7	5.0	3.6	3.6	6.5	0.6	0.4
	40	3.1	15.7	6.4	10.8	5.3	0.7	0.6
80	10	2.0	2.1	6.6	0.8	0.9	0.6	0.9
	20	2.4	3.0	3.6	4.3	7.0	2.0	1.3
	30	4.0	17.8	5.7	7.4	3.6	0.9	1.0
	40	4.1	13.6	4.4	6.8	8.7	4.6	1.1
100	10	2.8	2.6	4.1	4.9	3.0	0.6	0.8
	20	2.8	11.1	10.9	11.6	9.5	1.5	1.5
	30	3.5	5.5	9.3	14.6	7.4	1.3	1.3
	40	5.6	19.4	37.6	14.8	23.4	3.4	0.9
120	10	3.9	2.8	4.0	5.0	4.1	1.1	0
	20	13.6	8.0	3.4	4.7	7.5	6.6	1.5
	30	5.5	20.8	36.4	6.3	6.5	4.4	6.2
	40	5.5	24.5	31.8	5.0	6.6	3.0	4.1
8 Weeks, mpy								
60	10	0.9	1.5	0.6	0.7	0.7	0.8	0.6
	20	2.0	—	2.4	5.5	1.0	0.9	0.8
	30	2.7	3.4	2.5	3.1	5.3	1.7	0.5
	40	3.7	4.2	2.5	4.8	4.7	0.7	0.6
80	10	1.6	1.9	0.8	0.7	0.6	0.5	0.7
	20	3.1	2.2	2.6	3.9	4.6	1.4	1.3
	30	4.1	15.3	4.6	5.5	6.6	2.5	0.7
	40	4.8	10.6	3.7	6.2	6.3	3.2	0.8
100	10	1.9	2.0	3.0	0.9	1.0	0.8	1.1
	20	2.8	8.6	8.1	9.0	9.1	1.5	1.3
	30	4.7	4.0	6.6	10.6	4.3	1.1	1.1
	40	5.3	19.5	33.8	14.4	22.2	3.0	0.7
120	10	2.9	2.5	3.5	4.2	3.3	1.3	1.9
	20	6.9	6.9	3.0	4.0	6.3	4.5	1.3
	30	5.3	21.1	40.4	5.0	3.8	3.6	3.7
	40	5.8	11.1	34.2	3.8	4.8	3.5	3.1

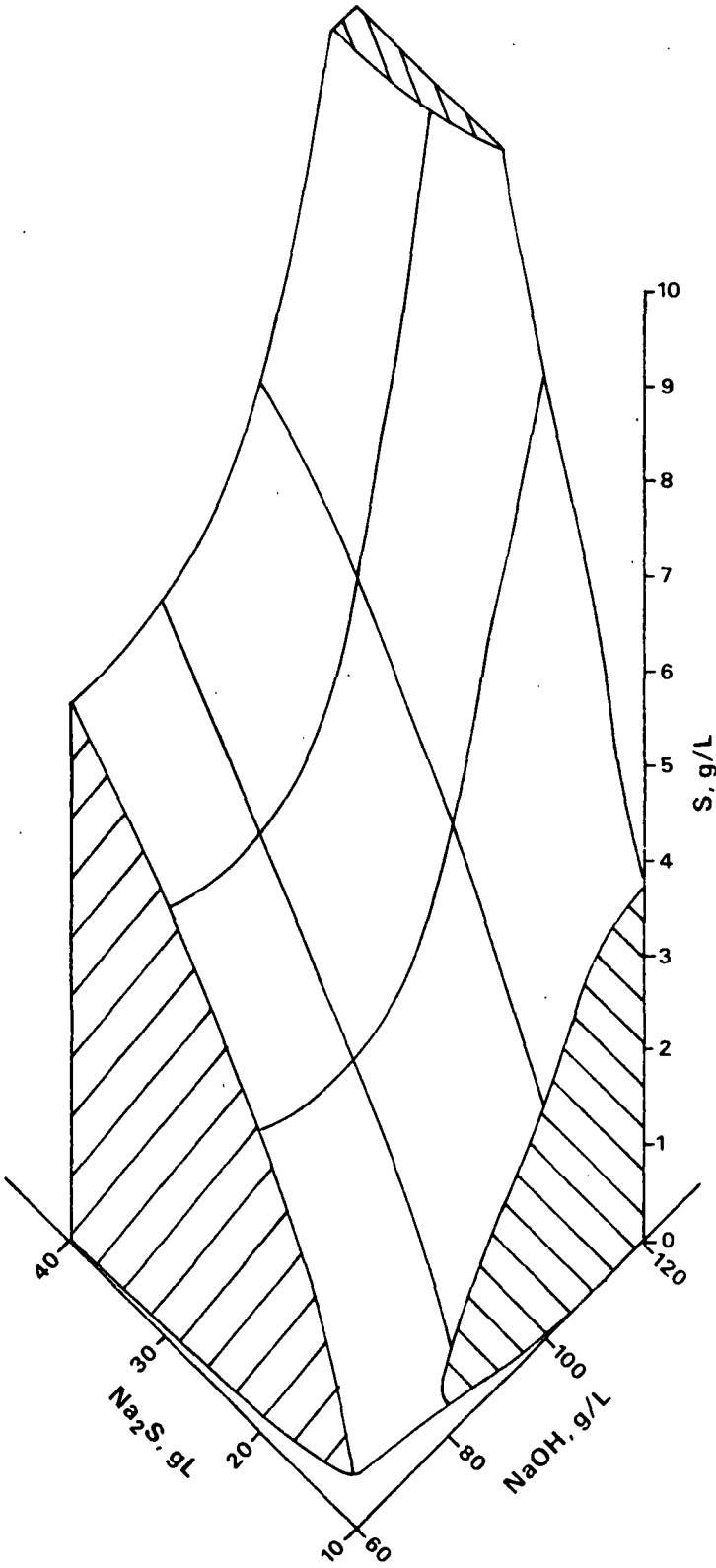


Figure 3. Isocorrosion surface 5 mpy in NaOH + Na₂S + S solution after 2 weeks exposure.

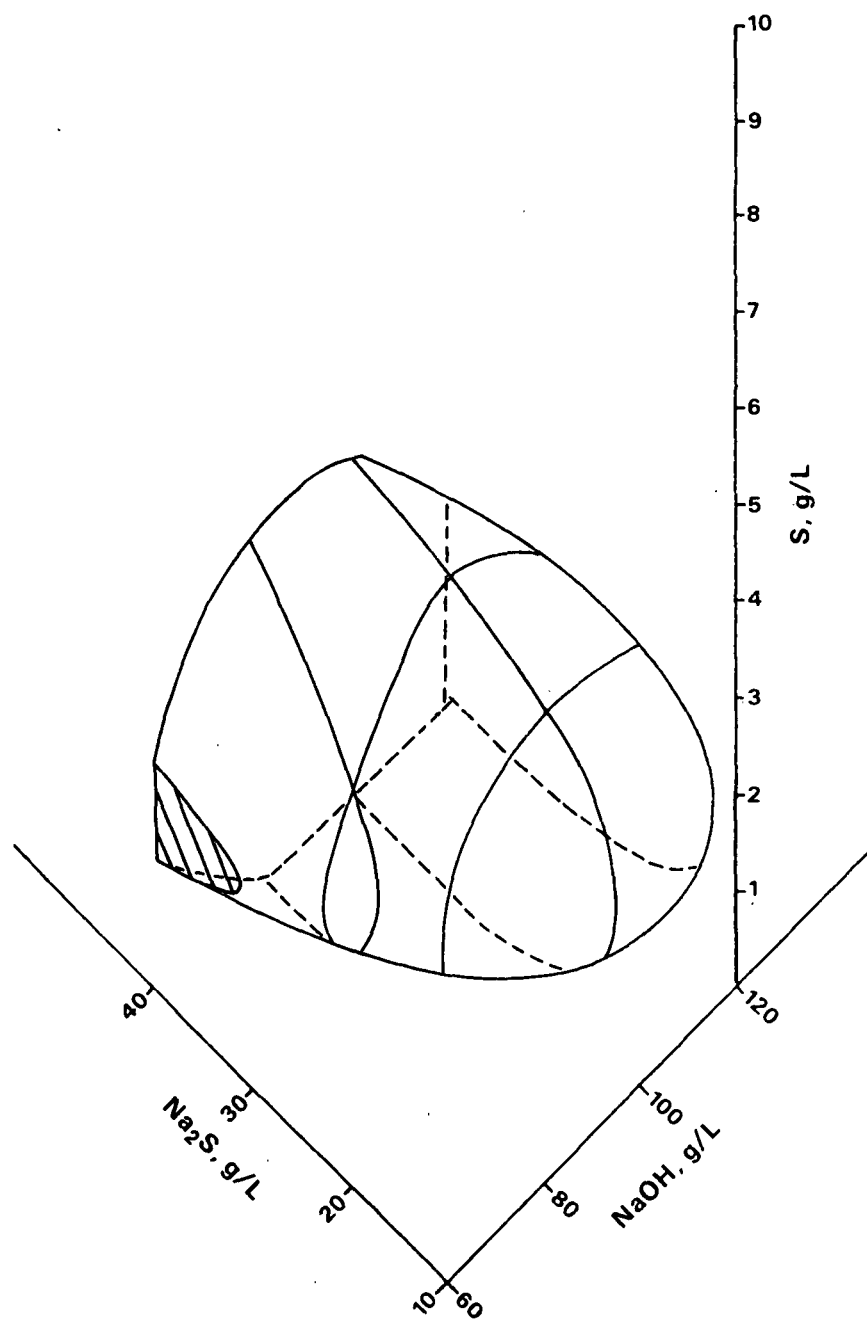


Figure 4. Isocorrosion surface 5 mpy in NaOH + Na₂S + S solution after 8 weeks exposure.

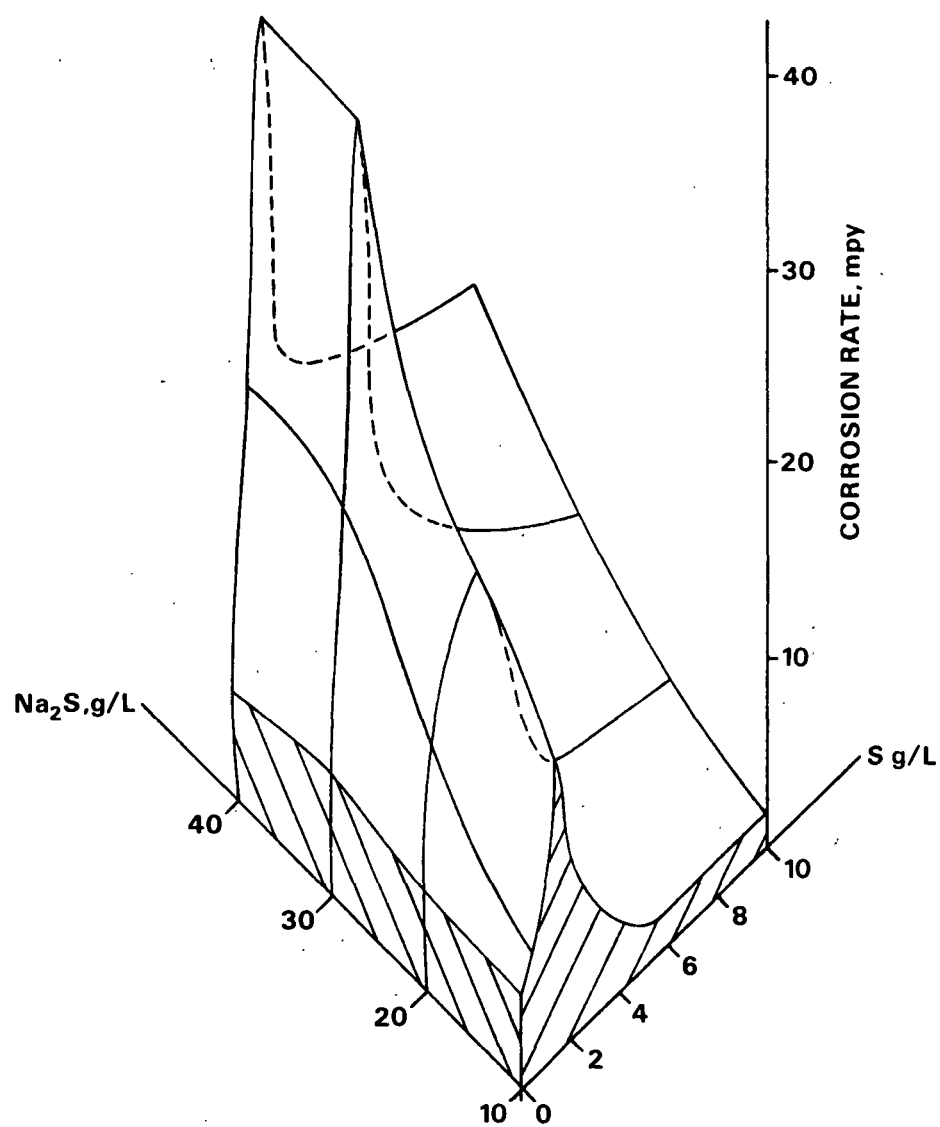


Figure 5. Corrosion rates in $\text{Na}_2\text{S} + \text{S} + 120 \text{ g/L NaOH}$ solution after 2 week exposure.

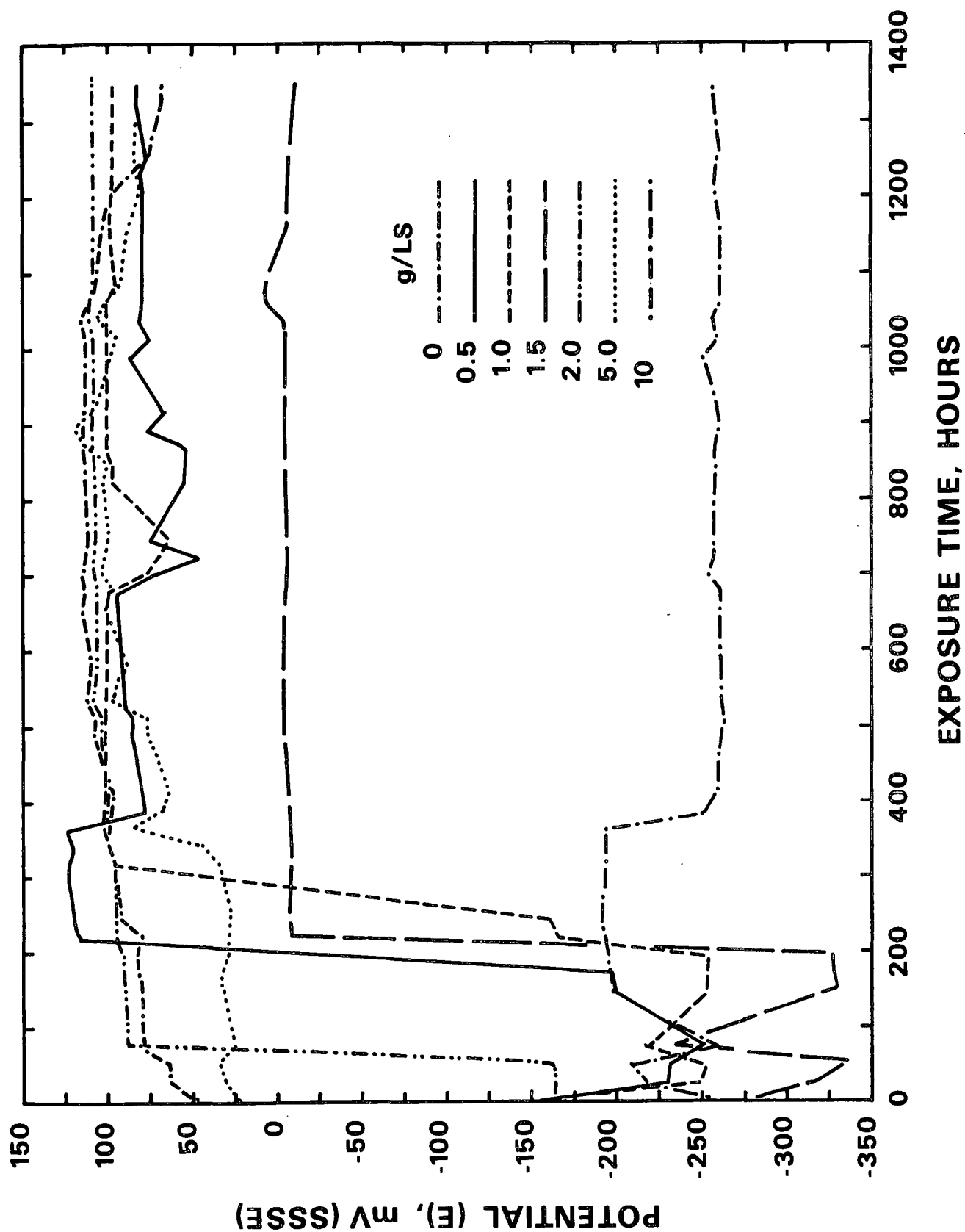


Figure 6. Corrosion potential as a function of exposure time in 100 g/L NaOH + 30 g/L Na_2S + 0-10 g/L S.

time in the polysulfide solutions, corresponding with passivation of the electrode. The time to achieve passivation depended on the polysulfide concentration. As seen in Fig. 6, if no S was added, the electrode remained active. Fluctuations of potential were especially noticeable as the electrode moved from the active to the passive condition. Representative plots for all solution compositions are contained in Appendix II.

As the OH⁻ and HS⁻ concentration increased, the amount of S_x²⁻ needed to cause immediate passivation was increased. In the solution 100 g/L NaOH + 30 g/L Na₂S, passivation was immediate in a solution containing 5 g/L S. In lower concentration 60 g/L NaOH + 10 g/L Na₂S solution, only 1 g/L S was necessary to cause immediate passivation, but in 120 g/L NaOH + 10 g/L Na₂S, 5 g/L S was required to cause immediate passivation. When no sulfur was added, the electrode remained active.

Electrodes which experienced a high corrosion rate spent a significant portion of their life at corrosion potentials ranging from -200 to -150 mV(SSSE).

Polarization behavior of steel was investigated in each solution composition. Data from the polarization curves are summarized in Appendix III. The corrosion potentials on steel were clustered around four values as shown in Fig. 7. The value of corrosion potential was more noble for higher S concentrations. Representative anodic and cathodic polarization curves for steel are presented in Fig. 8. Three major current peaks were observed repeatedly, although the peaks shifted slightly as the solution composition was varied. Typically, the peaks were located at 70, -40 and -150 mV(SSSE), although the peaks at -150 mV were somewhat indistinct. These peaks are associated with oxidation reactions: dissolution or formation of solid products such as oxide films.

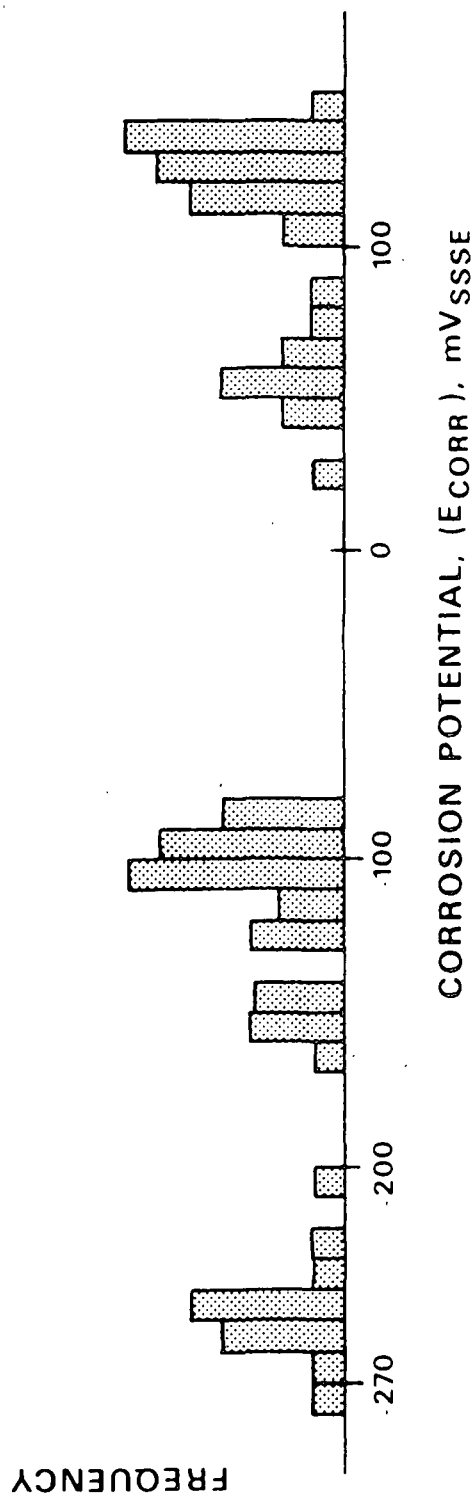


Figure 7. Frequency of different corrosion potentials on steel in all solutions prior to polarization.

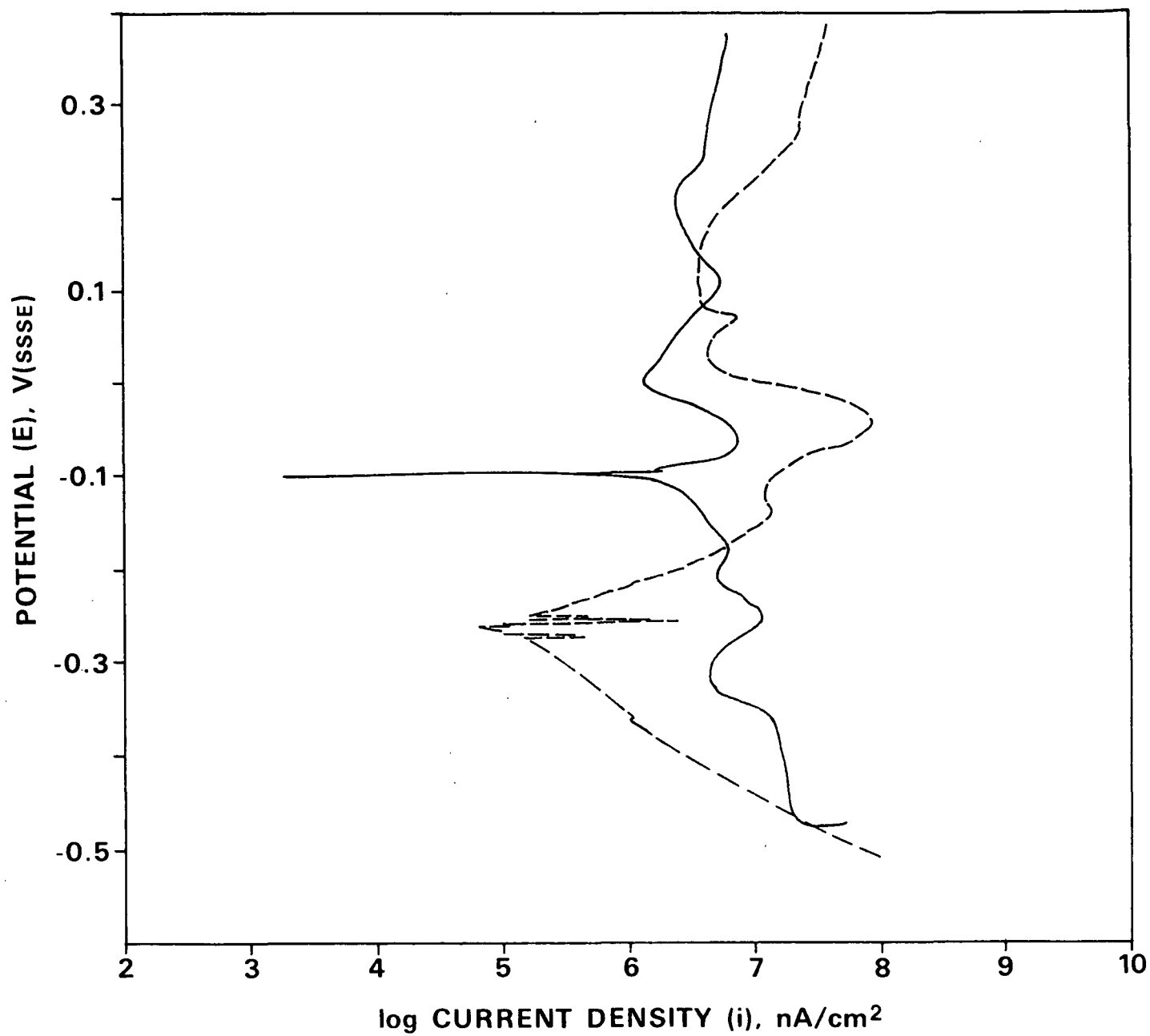


Figure 8. Polarization curves for 1018 steel, 90 C, 1 mV/s in 100 g/L NaOH + 20 g/L Na₂S with (—) and without (---) added S.

The polysulfide obscured the features of the anodic polarization curve of steel compared to plain NaOH + Na₂S solutions. At high S concentrations, E_{corr} was very high and anodic peaks were located below E_{corr} . The slope of the polarization curve, in mV/logarithmic unit of current, is related to the charge passed during the electrochemical reaction or reactions occurring at that potential, and therefore can provide some information on the corrosion process, useful in understanding the fundamental causes of the corrosion. The anodic Tafel slope, β_A , on steel was 64 mV (av. 26 values, $s = 34$ where s is the standard deviation). The cathodic Tafel slope, β_C , was 128 mV (av. of 18 values, $s = 47$).

The polarization behavior of gold was similar in all solutions. Data from the polarization curves are summarized in Appendix III. The cathodic polarization curves had two or more sections as seen in Fig. 9, indicating that a number of reduction steps occur for the sulfides in solution. At higher S_x^{2-} concentrations, the current densities were increased and the current density reached a plateau, suggesting concentration polarization. The anodic Tafel slope, β_A , was 78 mV (av. of 56 values, $s = 18$), with a trend to slightly lower values at high S_x^{2-} concentrations. The cathodic Tafel slope, β_C , was 125 mV (av. of 70 values, $s = 34$), with a general decrease with decreasing OH⁻ and HS⁻ concentration. This is the opposite trend to the anodic Tafel slopes on gold. The lower section of the gold cathodic polarization curve had a slope of 38 mV (av. of 11 values, $s = 4.5$). At these potentials gas evolution was observed at the electrodes.

THIOSULFATE

Additions of thiosulfate increased the corrosion rate significantly as summarized in Table 2. This effect was more pronounced at higher OH⁻ and HS⁻

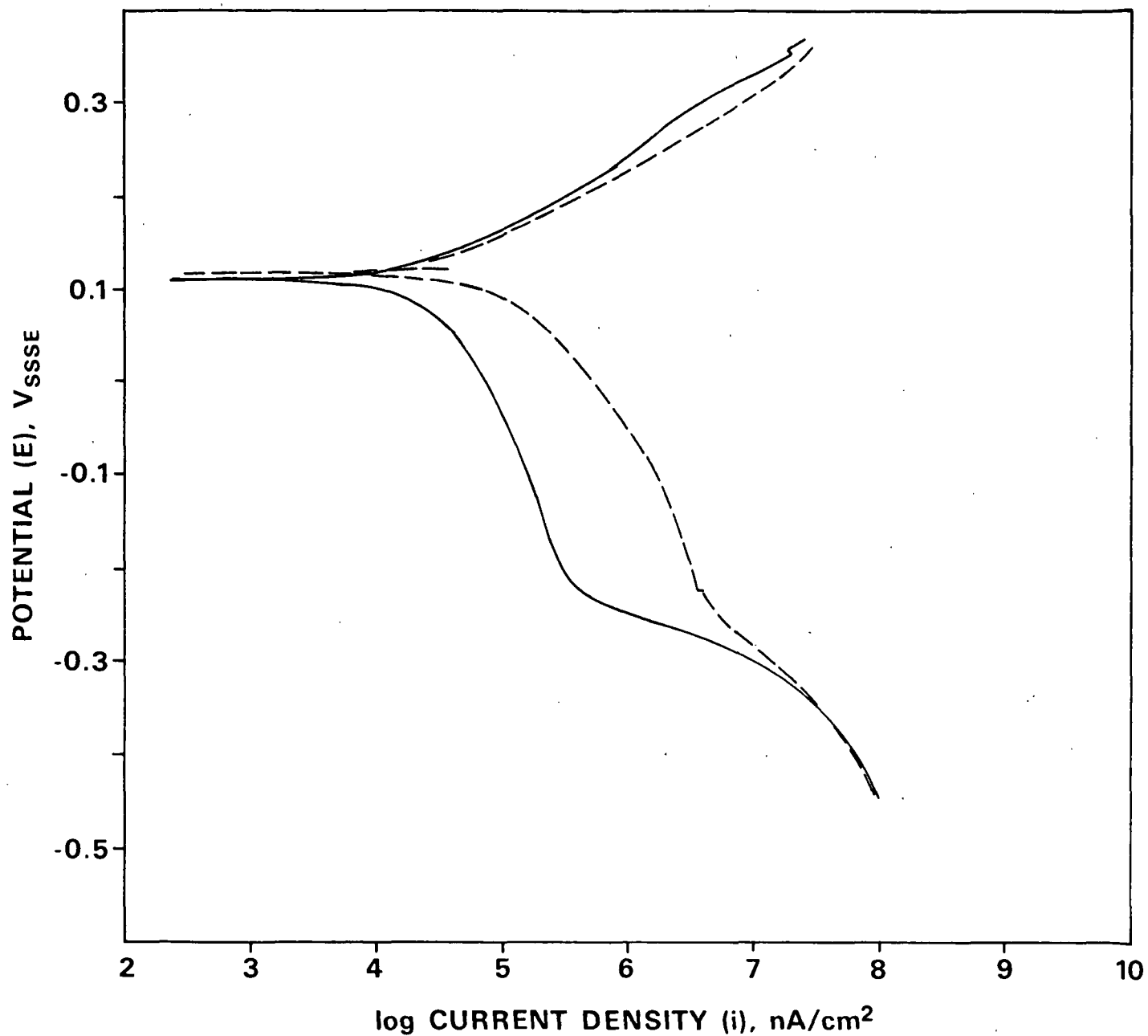


Figure 9. Polarization curve for gold, 90 C, 1 mV/s in 100 g/L NaOH + 30 g/L Na₂S with 0.5 g/L S (—) and 1.5 g/L S (---) additions.

concentrations. Thiosulfate increased the corrosion rate more than did polysulfide. At higher HS- concentration the corrosion rate did not fall with time, suggesting that passivation never occurred. Weight loss was much greater than in polysulfide, especially after long exposure times. This is illustrated schematically in Fig. 10 and 11 for 2 and 8 weeks exposure, respectively, which show the 15 mpy isocorrosion surface. This region, enclosing higher corrosion rates than the 5 mpy isocorrosion surface drawn for the polysulfide solutions, covers a large range of solution compositions, and within that area corrosion rates are as high as 60-80 mpy.

Table 2. White liquor studies - thiosulfate weight loss results.

NaOH, g/L	Na ₂ S, g/L	S ₂ O ₃ --, g/L					
		0	2.5	5.0	10.0	25.0	50.0
2 Weeks, mpy							
60	10	3.1	2.7	4.4	9.1	9.9	15.9
	20	3.9	3.3	4.6	8.6	14.5	30.3
	30	8.6	6.6	5.6	9.3	20.6	41.6
	40	8.3	9.1	7.1	9.9	29.2	44.6
80	10	5.0	11.4	16.9	10.1	10.5	12.0
	20	5.5	10.5	14.7	6.3	22.6	39.6
	30	--	10.5	16.8	15.5	21.7	45.0
	40	--	11.9	20.9	14.3	27.8	50.6
100	10	--	13.4	14.1	24.8	6.6	12.4
	20	--	10.0	18.8	32.6	30.1	58.8
	30	--	22.0	33.0	33.5	23.7	58.1
	40	--	13.9	22.7	30.1	36.	62.6
120	10	--	13.8	16.2	28.6	8.7	15.0
	20	--	15.0	24.7	40.4	38.9	69.5
	30	--	--	--	--	--	--
	40	--	16.0	45.5	34.6	43.8	76.9

Table 2 (Continued). White liquor studies - thiosulfate weight loss results.

NaOH, g/L	Na ₂ S, g/L	S ₂ O ₃ —, g/L					
		0	2.5	5.0	10.0	25.0	50.0
4 Weeks, mpy							
60	10	1.4	1.9	2.2	4.4	5.4	7.6
	20	2.2	3.1	4.4	8.4	17.1	35.3
	30	4.1	4.2	4.2	8.8	23.4	47.5
	40	3.9	6.0	6.8	9.8	29.3	53.4
80	10	3.1	5.0	10.1	6.1	5.4	6.8
	20	3.6	11.6	8.5	9.8	24.6	42.4
	30	—	12.8	8.9	18.4	26.1	49.8
	40	—	13.4	16.5	19.1	30.6	61.8
100	10	—	6.7	7.6	12.6	4.0	7.0
	20	—	12.3	23.6	16.8	34.9	63.5
	30	—	13.0	32.4	19.9	27.2	66.3
	40	—	14.0	22.0	25.5	36.1	67.2
120	10	—	7.7	9.9	13.1	3.8	7.9
	20	—	11.8	13.8	21.9	46.6	39.0
	30	—	—	—	—	—	—
	40	—	14.4	37.9	31.7	41.5	52.9
6 Weeks, mpy							
60	10	4.3	2.7	4.7	3.2	4.2	5.3
	20	2.2	3.1	4.6	8.5	23.0	39.8
	30	2.9	3.6	3.9	9.8	24.5	52.4
	40	3.0	5.2	6.5	9.9	31.5	61.8
80	10	2.7	4.5	7.8	4.5	4.3	5.0
	20	6.0	8.6	7.0	10.3	26.6	49.5
	30	—	8.6	7.0	12.7	16.9	33.9
	40	—	17.1	11.8	18.3	36.0	74.6
100	10	—	6.8	5.3	13.7	3.2	5.3
	20	—	12.6	6.4	17.0	43.7	72.0
	30	—	13.5	34.5	20.4	33.9	72.5
	40	—	9.6	14.2	26.4	39.7	78.9
120	10	—	6.8	6.4	9.1	3.6	6.7
	20	—	9.0	12.3	13.7	54.7	29.1
	30	—	—	—	—	—	—
	40	—	23.4	40.3	29.1	40.4	30.2

Table 2 (Continued). White liquor studies - thiosulfate weight loss results.

NaOH, g/L	Na ₂ S, g/L	S ₂ O ₃ --, g/L					
		0	2.5	5.0	10.0	25.0	50.0
8 Weeks, mpy							
60	10	0.6	2.3	3.5	2.2	2.3	3.5
	20	1.9	2.5	5.7	9.2	24.6	38.1
	30	4.4	3.4	4.1	10.4	26.3	57.6
	40	3.6	5.1	7.0	11.3	35.6	65.1
80	10	1.9	3.5	5.7	2.2	3.0	3.3
	20	6.5	7.1	7.0	10.5	27.8	52.5
	30	--	6.4	5.0	9.6	36.1	26.8
	40	--	5.5	19.6	20.8	43.2	86.5
100	10	--	7.1	4.0	9.4	2.1	4.2
	20	--	15.1	12.5	22.8	52.6	79.0
	30	--	19.3	20.3	21.5	43.1	81.9
	40	--	7.4	11.3	26.0	45.2	70.3
120	10	--	4.2	4.7	6.6	2.4	5.8
	20	--	7.5	17.1	10.7	61.5	19.0
	30	--	--	--	--	--	--
	40	--	26.4	44.0	27.4	35.0	25.4

Corrosion potential, E_{corr} , of the electrodes was monitored throughout the exposure and is plotted in Fig. 12 for a range of $\text{S}_2\text{O}_3^{2-}$ concentrations in 80 g/L NaOH + 40 g/L Na_2S . Representative plots of corrosion potential vs. time are shown in Appendix II. Shifts of E_{corr} occurred in conjunction with change of electrodes, perhaps due to the momentary loss of temperature or the agitation associated with specimen removal¹⁴ or because of some drying of the electrode as it was transferred to the fresh solution.

Polarization curves for steel were obtained for each liquor composition. A representative curve is shown in Fig. 13. Data for the polarization curves are summarized in Appendix III. Generally, as the thiosulfate concentration was increased, the corrosion potential increased from -240 to approximately -140 mV. The E_{corr} was slightly more noble in lower HS^- concentrations. This range of

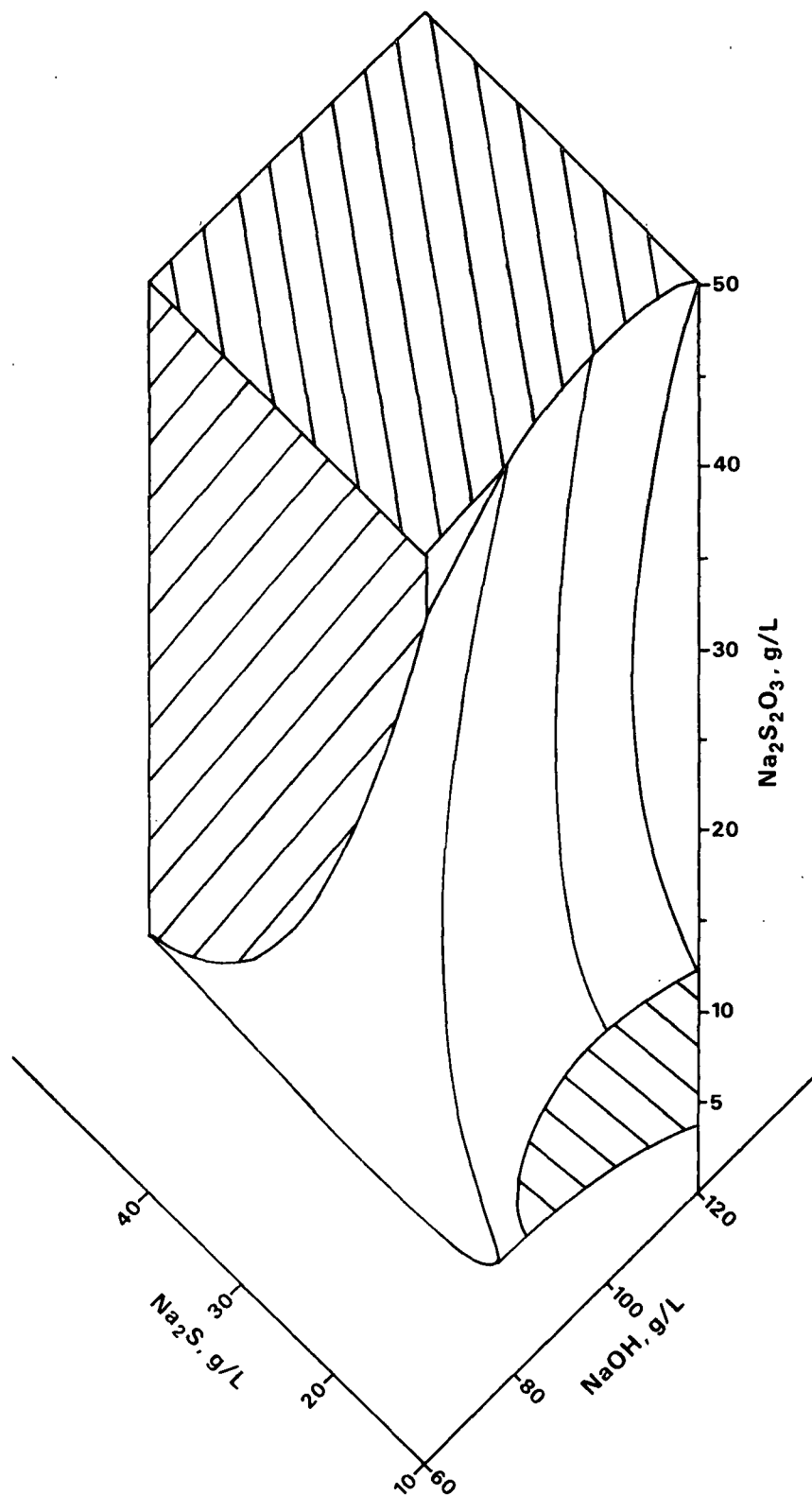


Figure 10. Isocorrosion plot of 15 mpy surface in $\text{NaOH} + \text{Na}_2\text{S} + \text{Na}_2\text{S}_2\text{O}_3$ solutions after 2 weeks exposure.

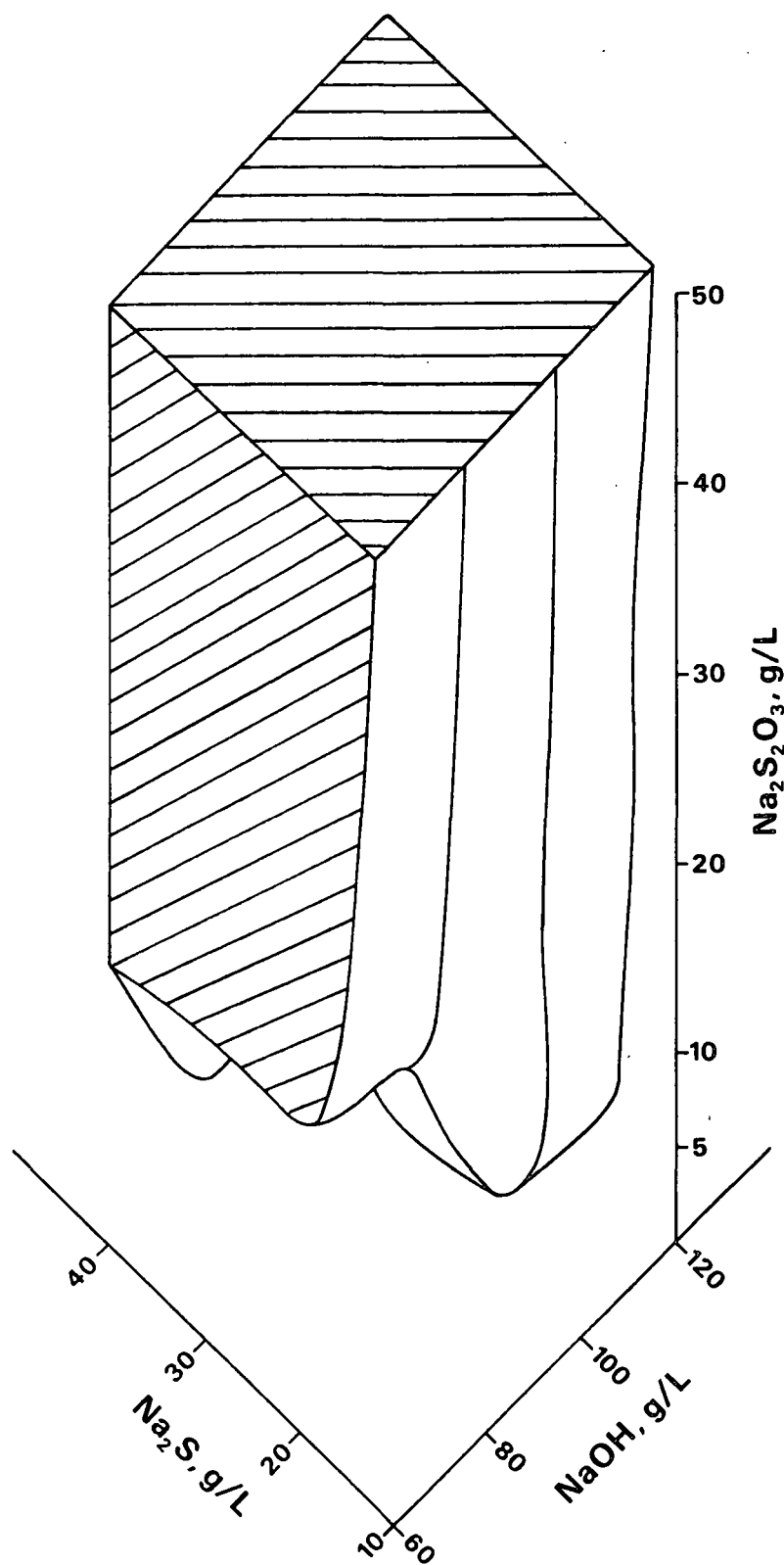


Figure 11. Isocorrosion plot of 15 mpy surface in $\text{NaOH} + \text{Na}_2\text{S} + \text{Na}_2\text{S}_2\text{O}_3$ solutions after 8 weeks exposure.

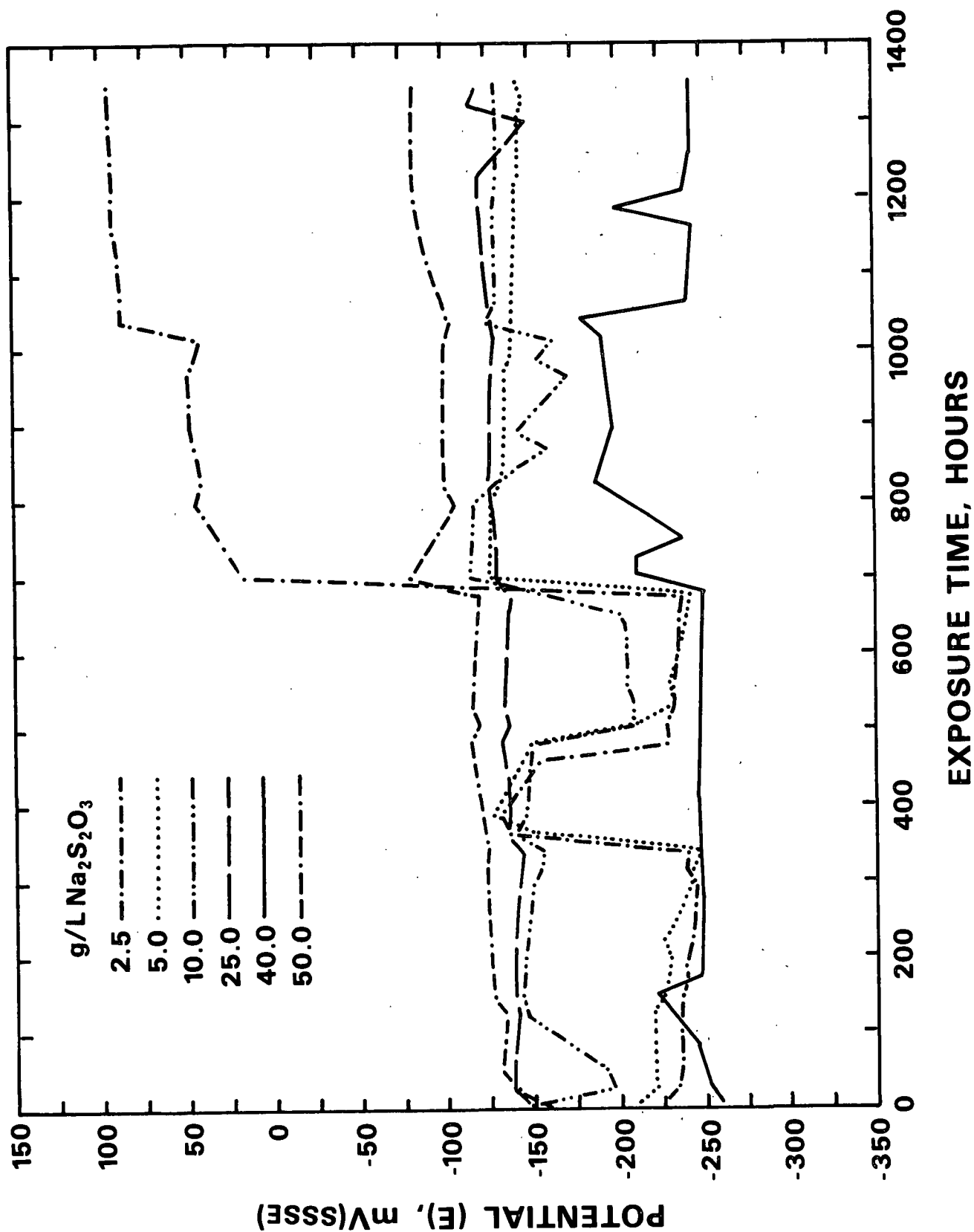


Figure 12. Corrosion potential during exposure in 80 g/L NaOH + 40 g/L Na_2S + 0-50 g/L $\text{Na}_2\text{S}_2\text{O}_3$.

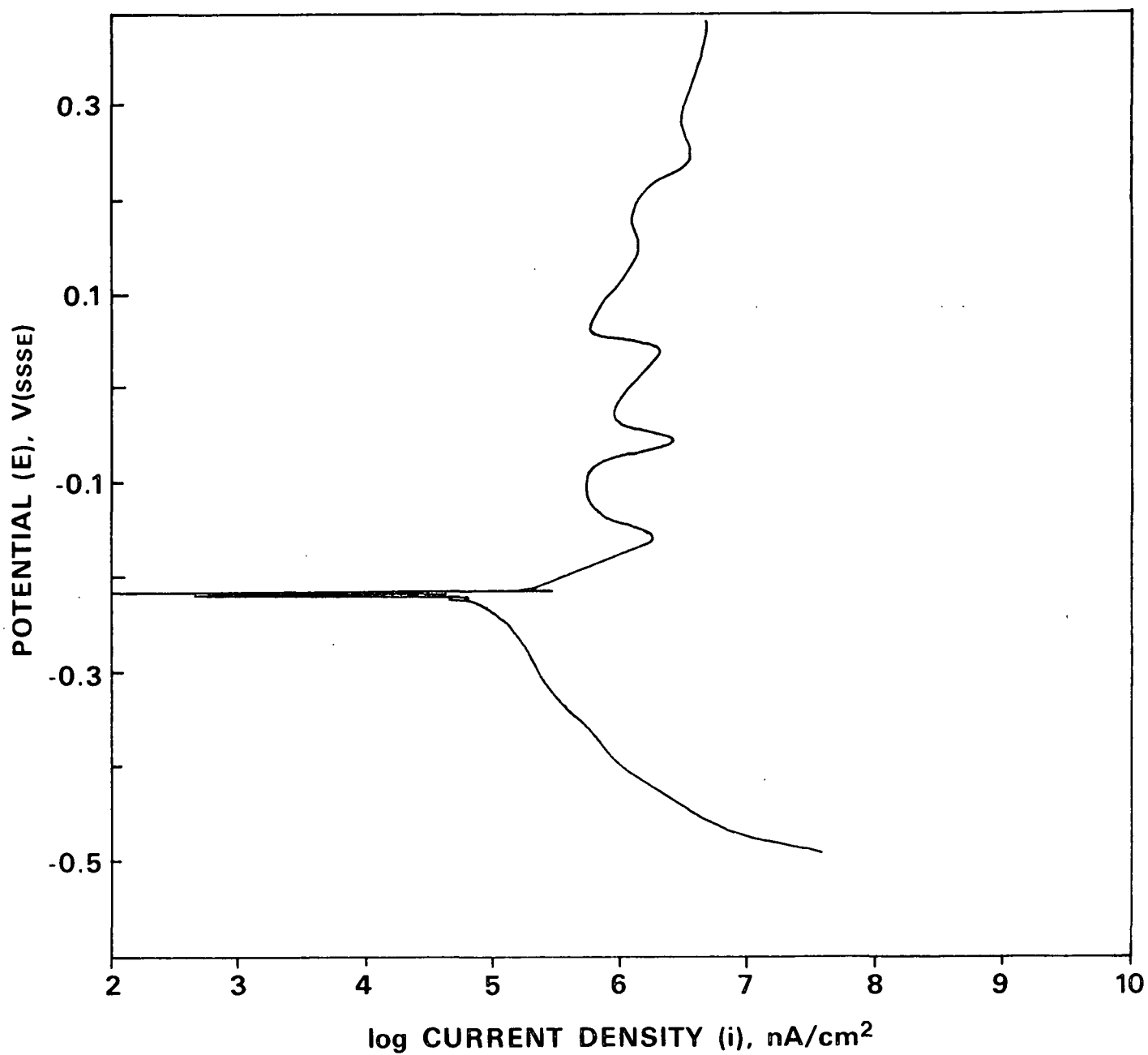


Figure 13. Polarization curve of steel in 100 g/L NaOH + 10 g/L Na₂S + 10 g/L Na₂S₂O₃, 90°C, 1 mV/S.

potential was in the active-passive transition, very close to one of the peaks where dissolution rates were high. There was no trend in either the anodic or cathodic Tafel slopes, and they varied from test to test. In solutions containing no thiosulfate, the anodic Tafel slope was approximately the same as in polysulfide solution. Otherwise, there was no consistency in either the anodic or cathodic Tafel slopes on steel. At -240 mV(SSSE), a peak was generally observed in the cathodic scan. Anodic peaks were located at approximately -150, -50, 75 and 165 mV(SSSE).

Corrosion potential on gold was comparable to S_x^{--} solutions. It was comparatively unaffected by $S_2O_3^{2-}$, but declined at higher HS^- concentration. Data from the polarization curves are summarized in Appendix III. The anodic Tafel slope, β_A , on gold was 59 mV (av. of 66 values, $s = 9$). At higher potential, the Tafel slope was 263 mV (av. of 55 values, $s = 91$); these values varied widely. The cathodic Tafel slope was 51 mV (av. of 72 values, $s = 10$). A representative polarization curve for gold in $NaOH + Na_2S + Na_2S_2O_3$ solution is illustrated in Fig. 14.

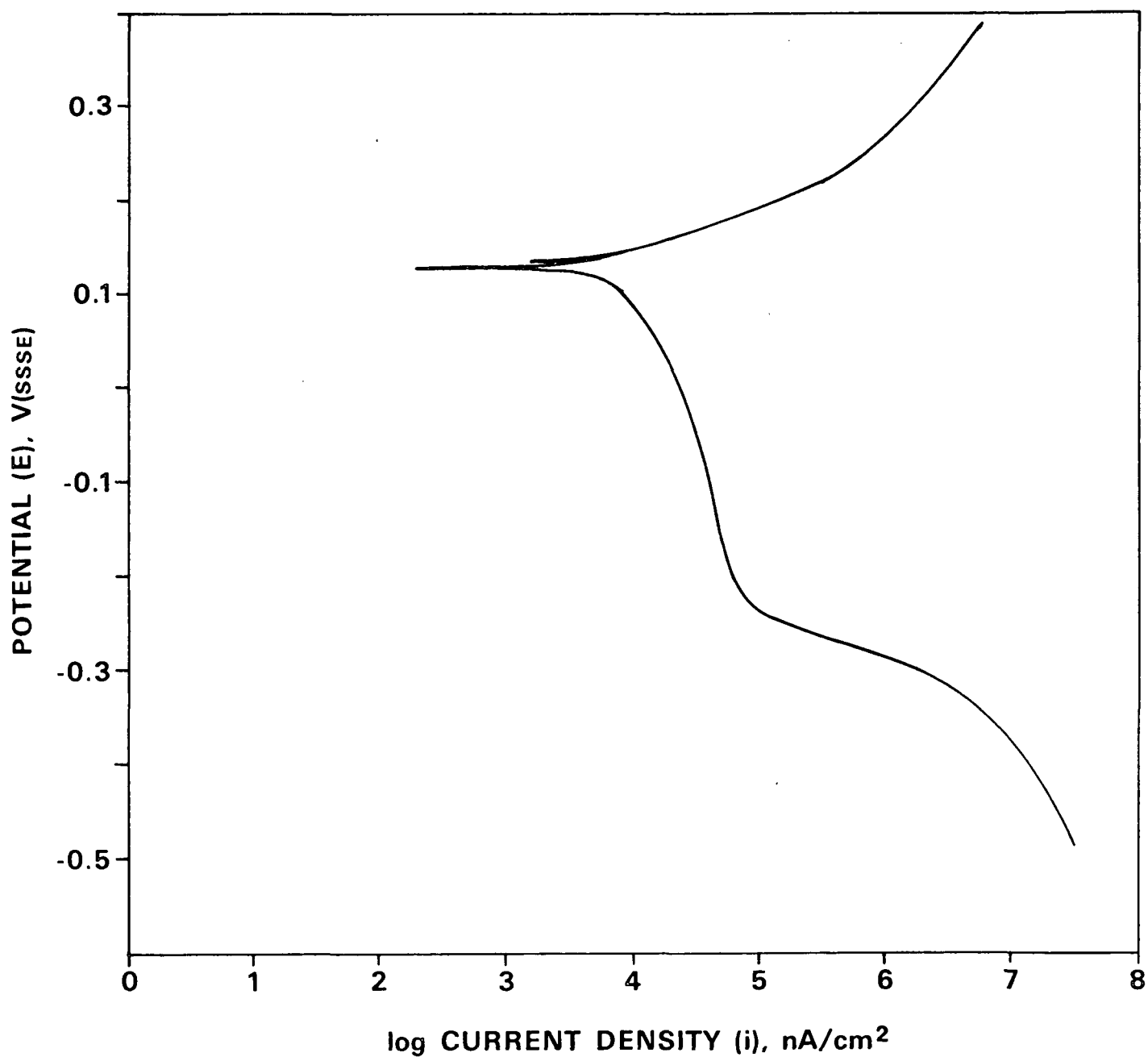


Figure 14. Polarization curve of gold in 100 g/L NaOH + 10 g/L Na₂S + 10 g/L Na₂S₂O₃ solution.

DISCUSSION

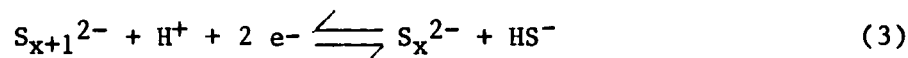
POLYSULFIDE

High initial corrosion rates were a transient effect in low concentration polysulfide solutions (0.5-2.0 g/L S), and rates decreased dramatically when passivation occurred as seen by comparing Fig. 3 and 4. The isocorrosion surface encloses fewer solutions after 8 weeks than after 2 weeks, and these are mostly solutions in which very much higher corrosion rates were observed after the two-week exposure test. Figure 5 shows how corrosion rates were much higher in solutions with low concentrations of S. The passivation process is well illustrated by the plot of the rest potential, E_{corr} , vs. exposure time (Fig. 6), where it can be seen that the potential moves from the active region, -240 mV(SSSE), to the passive region, 100 mV(SSSE), after a period of time. After the steel became passivated, the corrosion rate was decreased to 2.5 mpy. At high polysulfide concentrations (5-10 g/L S), immediate passivation occurred and no period of high corrosion rate was observed.

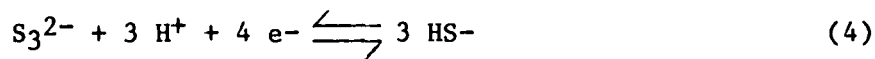
The increase of corrosion rate at higher sulfide concentration may be attributed to increased difficulty of passivation in these solutions. This increased difficulty of passivation can be rationalized by consideration of the polarization curve. Anodic peak heights are larger in higher sulfide concentration solutions.^{10,12} As the electrodes passivate, the potential must increase through the range of potentials of this peak where the increased currents are associated with increased dissolution. The peak current is known as the critical current for passivation, $i_{\text{(crit)}}$. More corrosion occurs before passivation is complete, that is, $i_{\text{(crit)}}$ is larger for higher sulfide concentrations. Indeed, electrodes which experienced high corrosion rates spent considerable time in the peak potential range from -150 to -200 mV(SSSE) before passivating.

At high sulfide concentrations, more polysulfide was required to passivate the electrode within a given period. In combinations of high OH⁻ and HS⁻ (120 g/L NaOH + 40 g/L Na₂S, 100 g/L NaOH + 40 g/L Na₂S), corrosion rates were high even after 8 weeks due to the difficulty of passivation.

Polysulfides stimulate passivation by their oxidizing nature. The redox potential for the half-cell



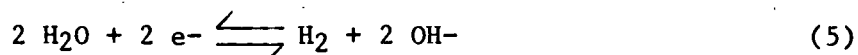
is located at a noble potential. For example, for



the reversible potential at 90°C in 100 g/L NaOH + 30 g/L Na₂S is 136 mV(SSSE). This reaction and similar reactions for other polysulfides form a mixed potential. On an inert electrode, it has been shown¹² that these polysulfides also form a mixed potential with thiosulfate in solution and that this mixed potential of polysulfides and thiosulfate is located at a potential slightly below the mixed potential for the polysulfides alone. At higher temperature, this potential moves closer to the thiosulfate equilibrium. The mixed potential of polysulfides and thiosulfate in sulfide solution has been described in more detail elsewhere.¹² At the mixed potential, polysulfides are reduced. The reduction of polysulfides comes to electrochemical equilibrium with oxidation of iron at the corrosion potential, E_{corr} , in the solution. Apparently, sufficient current to maintain the passive oxide film on steel can be supplied by S_x^{2-} reduction. If large quantities of polysulfide are available, their reduction can provide current to passivate the surface immediately, as was observed in high polysulfide solutions. Thus the polysulfide reduction supplies current just as an anodic protection system would.

The change of E_{corr} with time of exposure is not related to changes in the solution composition due to oxidation of the polysulfide; solutions were changed frequently to ensure that polysulfide concentrations were maintained. Passivation may take longer in some cases because some transformation of the film must occur to make it protective. New films may contain significant sulfide, making them nonprotective. Some period may be required to convert this film to a protective one by replacing the sulfide with protective oxide. This is supported by the observation that the film is more adherent after a long exposure than newly formed film.

The corrosion potentials of electrodes prior to polarization were observed to attain values distributed around -250, -100, 60 and 130 mV(SSSE), (Fig. 7). The lowest value coincides with reduction of hydrogen. At this mixed rest potential (-250), the anodic dissolution of the steel is balanced by the hydrogen evolution reaction:¹⁴



as illustrated schematically in Fig. 15. The mixed potential is in the active region of steel. The theoretical potential for hydrogen evolution may be calculated using the Nernst equation:

$$E = E_0 - (2.303RT/2F) \log(a_{\text{H}_2}) - (2.303 RT/F)\text{pH} \quad (6)$$

The pH is approximately 12.9 in these solutions at 90°C.¹⁸ The potential for hydrogen evolution at 90°C is calculated to be -929 mV(SHE) or -279 mV(SSSE), which is in fairly good agreement considering that hydrogen activity was unknown and errors due to liquid junction potential were neglected.

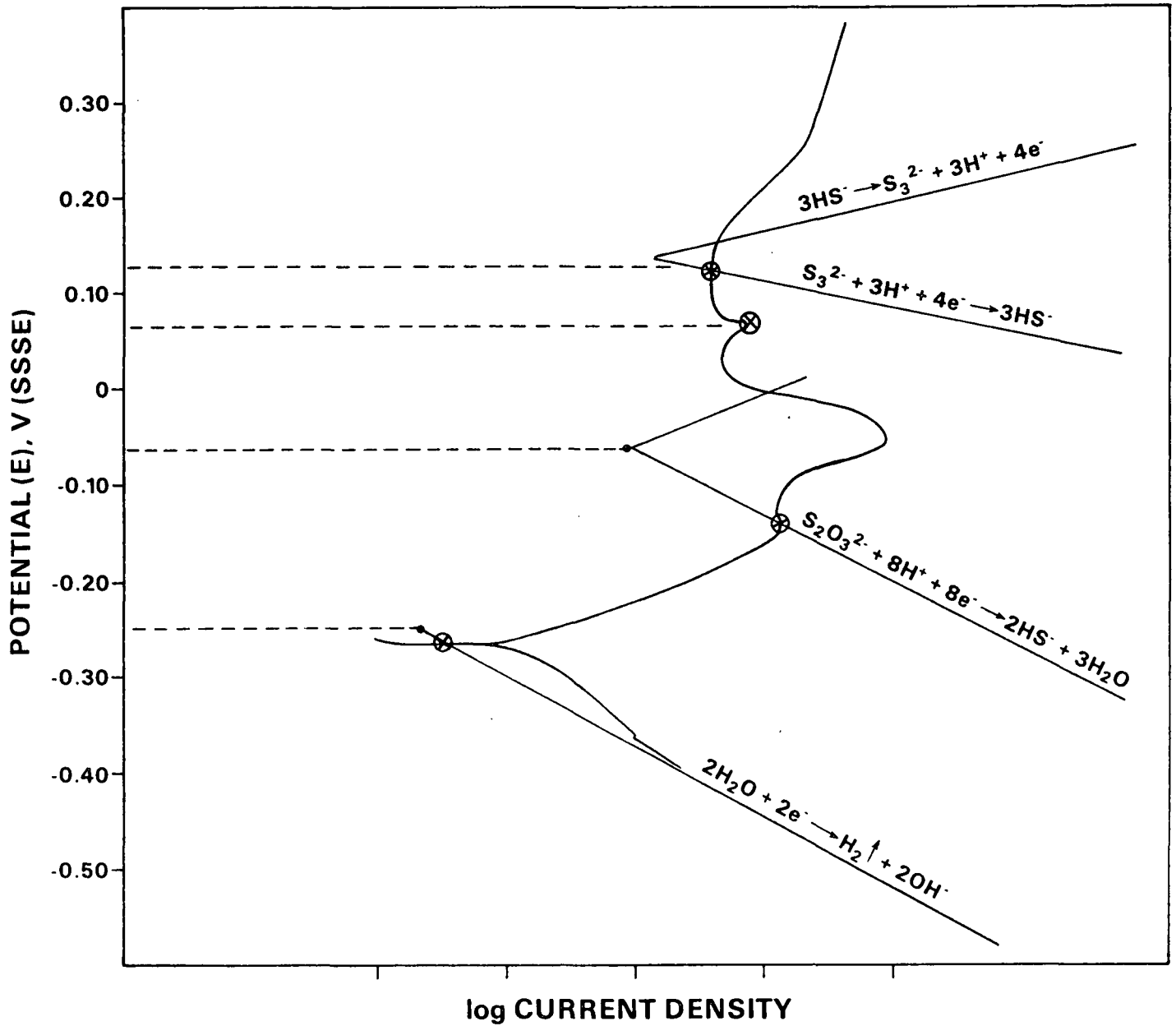
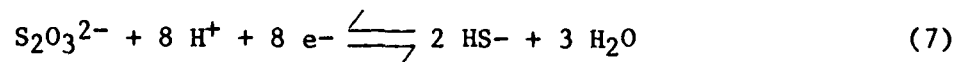


Figure 15. Schematic diagram illustrating the reactions which may control the corrosion potential.

The E_{corr} at -100 mV(SSSE) corresponds closely with the active-passive peak. This corrosion potential also coincides with the half-cell:



The reversible potential of this reaction is calculated to be -699 mV(SHE) at 90°C or -55 mV(SSSE) in 100 g/L NaOH + 30 g/L Na₂S solution with an impurity level of 0.001 g/L Na₂S₂O₃. The mixed potential with steel would be expected at a lower potential as was observed (-100) because the thiosulfate would be reduced as the iron oxidizes. Thus the corrosion potential in this range results from a balance of oxidation reactions of the steel and the reduction of thiosulfate as illustrated in Fig. 15. Electrodes which attained a rest potential in this region experienced a high corrosion rate because this also corresponded to the active-passive peak of the steel.

The highest values of E_{corr} (60, 130) were close to the polysulfide equilibrium, [Eq. (3)]. The highest potential, 130 mV, is close to the reversible potential for reaction 4. The lower potential, 60 mV, may result from mixed potential of reaction 4 with reaction 7. In this case, iron oxidation is apparently balanced by reduction of polysulfide as shown in Fig. 15. At high concentrations of polysulfide, the corrosion potential attained noble values, close to the polysulfide equilibrium, as would be expected.

The polarization curves for steel were significantly affected by additions of polysulfide. As illustrated in Fig. 8, the current density of the peaks was decreased in polysulfide solutions. The applied current of a polarization curve is the difference between spontaneous oxidation and reduction currents. A decrease in current may result from a decrease in the oxidation current or an increase in the reduction current. The current for the oxidation

of steel (due to film formation or dissolution) may have the same value as in polysulfide-free solution, but when summed with the reduction current for the polysulfide which is of opposite sign, the total current is decreased. Thus the critical current for passivation is decreased by reduction of polysulfide.

The anodic peaks have been discussed by Crowe¹² and can be identified with reasonable confidence. The peak at -150 mV(SSSE) was close to the potential for formation of Fe_3O_4 , and some of the current may result from dissolution to $\text{Fe}(\text{OH})_3^-$. The peak at -40 mV(SSSE) corresponded with FeS_2 formation from FeS . The peak at 70 mV(SSSE) was consistent with the formation of Fe_2O_3 or FeOOH , which forms a protective passive surface film. These reactions may be seen by reference to an E-pH diagram for the Fe-S- H_2O system at 100°C,¹² Fig. 16. This diagram illustrates the stability regions of species satisfactorily at 90°C. In these solutions, at 100°C the pH is approximately 13.¹⁸ At this pH, indicated by the vertical arrows, iron is stable as a number of forms, depending on the potential. As the potential increases the species stable at that potential forms: first, soluble $\text{Fe}(\text{OH})_3^-$, then oxide Fe_3O_4 , and finally Fe_2O_3 which is a passive layer. Note that the FeS_2 region is nearby and may extend to higher pH in the potential range of the peak if the activities of the species are different than assumed in constructing the diagram. The FeS_2 may prevent the formation of the protective passive film.

The anodic Tafel slope of 64 mV indicated that the rate determining step for oxidation involves the passage of a doubly charged species away from the surface. This may be for oxidation of the steel or the sulfides in solution. The cathodic reaction may be limited by a step involving a singly charged species as evidenced by the larger Tafel slope (128 mV).

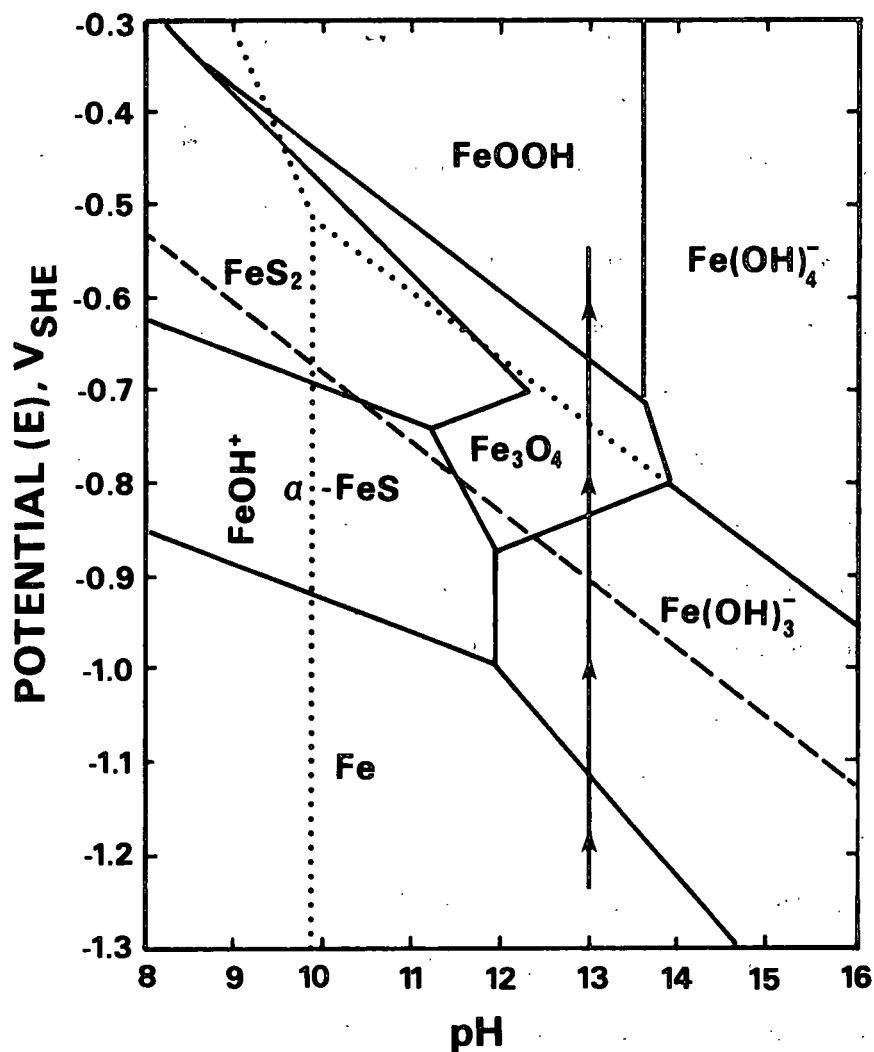


Figure 16. E-pH diagram for the Fe-S-H₂O system at 100 C.¹²

The polarization behavior of gold results from the oxidation and reduction reactions of the constituents of the solution only because the gold itself is inert and does not participate. The cathodic polarization curve had two sections, indicating that at least two reduction reactions were taking place when the electrode was polarized. The lower section was consistent with H⁺ reduction¹⁴ and was confirmed by visual observation. The Tafel slope was 38 mV which was fairly consistent with a mechanism for hydrogen evolution described by O'Brien and Seto.¹⁹ The upper section of the cathodic polarization curve is consistent

with reduction of S_x^{2-} to HS^- as described by Yeske.¹⁴ There may also be some reduction of $S_2O_3^{2-}$ at lower potentials. The large cathodic Tafel slope in this range was suggestive of concentration polarization. The linear portions observed in this range would result from the various sulfide species present in the solution which could be oxidized. This was supported by the observation of an increase in current with increasing S concentration seen in Fig. 9.

The anodic Tafel slope on gold (~78) was close to 75, indicating that a doubly charged species was moving through the double layer, which would be consistent with oxidation of HS^- to S_x^{2-} .¹² Thus the high currents at these potentials are principally due to oxidation of sulfide to form polysulfide. The cathodic Tafel slope was higher (125 mV), indicating that movement of single charged species (perhaps HS^-) was involved in the rate determining step.

Polysulfides exert a strong influence on the corrosion potential as observed by others.^{10,20} Low concentrations of polysulfides accelerate corrosion by shifting the corrosion potential into the active-passive region, and high concentrations cause spontaneous passivation. The present study has shown that passivation eventually occurs even with low concentrations. Ahlers²¹ found that low concentrations of polysulfide increased the corrosion rate in batch cooks. The surface would be exposed to the air between cooks and the passive layer would be damaged. Thus, the transient effect would be repeated in each cook cycle, resulting in a much higher corrosion rate than would be expected for a continuous exposure. Polysulfide may also be very important when upsets occur frequently or where the surface passive film is repeatedly damaged. Frequent damage to the film would occur due to high flow rate or mechanical abrasion. The transient effect of S_x^{2-} on corrosion rate is of importance to the problem

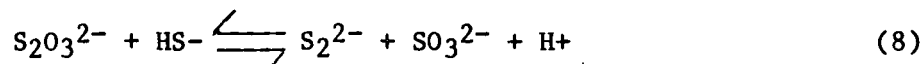
of stress corrosion, too. In polysulfide solutions of low concentration, dissolution rates may be very high at the tips of stress corrosion cracks where deformation repeatedly breaks the passive film. Competing repassivation processes may be slow, as indicated by the long period for passivation to occur in weight loss tests. The effect of polysulfide on long-term exposure is to passivate the electrode, thereby decreasing corrosion rate.

THIOSULFATE

Thiosulfate increased the corrosion rate significantly throughout the period of the exposure in proportion to the amount of thiosulfate in solution. The isocorrosion surface, 15 mpy, illustrated the large number of solution compositions in which the corrosion rate exceeds 15 mpy. This effect was again increased by higher HS⁻ concentrations, probably due to increased dissolution currents at the active/passive peak as were observed by Wensley.¹⁰ More corrosion would occur while the electrode was in the peak potential range.

The redox potential for the equilibrium $\text{HS}^-/\text{S}_2\text{O}_3^{2-}$ has a value of -699 mV(SHE) or -45 mV(SSSE) in 100 g/L NaOH + 30 g/L Na₂S + 5 g/L Na₂S₂O₃, which is very close to the active-passive peak potential of -50 mV(SSSE). The corrosion potential of the steel would rest in this potential range due to the thiosulfate equilibrium, and increased corrosion would take place. The active-passive peak is consistent with formation of FeS₂.¹² At higher potentials, passivation with an oxide film prevents dissolution. Thus thiosulfate stimulates corrosion by increasing the active/passive peak heights and by placing the corrosion potential into the active/passive range. Thiosulfate must delay the point of onset of passivation and thus stimulate larger active/passive peaks. Figures 10 and 11 illustrate that high corrosion rates were experienced for almost all solutions containing thiosulfate.

In low concentration of thiosulfate (2.5-5.0 g/L) or sulfide (10 g/L) corrosion rate decreased with time because the electrode became passive as can be seen in Fig. 12 for 2.5 g/L $\text{Na}_2\text{S}_2\text{O}_3$. It is possible that some of the thiosulfate is converted to polysulfide via the equilibrium:



The polysulfide thus formed may assist the electrode to passivate during a sufficient period of exposure. The passivation is presumably easier in low sulfide solution due to the smaller size of the active-passive transition in these solutions as described previously.

The polarization behavior on steel was almost the same as in polysulfide solution. Peaks were probably identified with the same reactions. The peak at 165 mV(SSSE) could not be identified due to the large number of reactions which may occur in this range. No conclusions could be drawn from the Tafel slopes observed on steel; presumably a number of reactions are occurring to cause the scatter in values.

Polarization behavior on gold was similar to that in polysulfide solutions, too. Nothing conclusive could be stated about the Tafel slopes. The high anodic Tafel slope was consistent with diffusion control.

Thiosulfate does not increase corrosion rate by generating low concentrations of polysulfide. If this were true, then very high concentrations of thiosulfate would generate a large amount of polysulfide and passivation should occur after a period of exposure. This was not observed.

The results obtained here are significant because they indicate that the corrosion rate will be high where thiosulfate is formed by oxidation of

sulfide, for example at the liquid-vapor line in pipes and tanks or where it is present as the result of poor reduction in the recovery boiler. Furthermore, thiosulfate impairs passivation and a high corrosion rate is maintained.

IMPLICATIONS FOR PULP MILL OPERATIONS

The results of the studies of liquor composition effects on corrosion rates in kraft white liquor have some practical implications for operations. These mostly concern the process chemistry.

The oxidized sulfide species have a considerable influence on corrosion rate. Therefore high reduction efficiency in recovery boilers is important to minimize concentrations of polysulfide and thiosulfate. Also, air should be excluded from the process to prevent formation of thiosulfate. The effect of air oxidation is especially noticeable in the wet/dry zone of tanks where corrosion rate underneath moisture films is high. Splashing should be minimized in the process to reduce the amount of contact with air.

Polysulfide, in sufficient quantities, may reduce corrosion rates. This confirms that polysulfide pulping may be beneficial in reducing corrosion. The addition of smaller amounts of emulsified sulfur make-up in the recausticizing area may place the polysulfide concentration at a low level, and a high transient corrosion rate will be experienced following the addition. This effect could extend for significant distances from the addition point, as the liquor is diluted. To avoid this problem, emulsified sulfur should be added in the black liquor area prior to reduction in the recovery boiler.

CONCLUSIONS

1) Low concentrations of polysulfide increase corrosion rates only initially, but assist passivation, thus decreasing corrosion rate in the long run. Their effect would be most pronounced when the steel surface is continuously exposed by abrasion, deformation or changing solution level.

2) Thiosulfate increases the corrosion rate throughout the exposure except at very low Na_2S and NaOH concentrations. Rest potential is controlled at the potential of the half cell reaction between HS^- and $\text{S}_2\text{O}_3^{2-}$ which is close to the potential of the active-passive transition peak.

3) Time of exposure has an influence on the corrosion rate. A protective passive layer is formed after a period of exposure which depends on the polysulfide and thiosulfate concentrations.

ACKNOWLEDGMENTS

The authors wish to acknowledge the diligence of Mr. Mike Heath in obtaining the experimental results and Mr. Craig Thompson for the appraisal of experimental procedures described in Appendix I.

REFERENCES

1. Ruus, L.; Stockman, L., Svensk Papperstid. 56:857(1953).
2. Stockman, L.; Ruus, L., Svensk Papperstid. 57:831(1954).
3. Hassler, J. W., Tappi 38:265-74(1955).
4. Haegland, B.; Roald, B., Norsk Skogind. 9:351-64(1955).
5. Roald, B., Norsk Skogind. 10:285-9(1956).
6. Mueller, W. A., Can. J. Tech. 34:162-81(1956).
7. Mueller, W. A., Tappi 40:129-40(1957).
8. Kesler, R. B.; Bakken, J. F., Tappi 41:97-102(1958).
9. Landmark, P.; Roald, B., Norsk Skogind. 15:342-7(1961).
10. Wensley, D. A.; Charlton, R. S., Corrosion 36:385-8(1980).
11. Tromans, D., J. Electrochem. Soc. 127:1253-6(1980).
12. Crowe, D. Ph.D. Thesis, The University of British Columbia, 1985.
13. Singbeil, D.; Garner, A. Final Semiannual Progress Report of the Research Program to Investigate Cracking of Continuous Digesters, Pulp and Paper Research Institute of Canada, Contract Report 6294, 1984.
14. Yeske, R. Corrosion rate measurements in kraft white liquor, Project 3556 Progress Report Two, The Institute of Paper Chemistry, May 21, 1984.
15. Ellis, A. J.; Giggenbach, W. Geochim. et Cosmochim Acta 35:247-60(1971).
16. Giggenbach, W., Inorg. Chem. 10:1333-8(1971).
17. Yeske, R. The silver/silver sulfide reference electrode for use in corrosion studies in kraft white liquor, Project 3556 Progress Report, The Institute of Paper Chemistry, February 15, 1984.
18. Macdonald, D. D.; McKubre, M. C. H. Temperature limitations of alkaline battery electrodes. Part II. The thermodynamic properties of iron, nickel and zinc in concentrated sodium hydroxide solutions, SRI International Project 7775. Final Report to DOE Contract EM-78C-01-5159, Menlo Park, California, 1979.
19. O'Brien, R. N.; Seto, P., J. Electrochem. Soc. 117:32-4(1970).
20. Singbeil, D.; Tromans, D. In: Pulp and Paper Industry Corrosion Problems, vol. 3, pp. 40-46, N.A.C.E., Houston, 1982.
21. Ahlers, P. E. In: Pulp and Paper Industry Corrosion Problems, vol. 4, pp. 53-55, N.A.C.E., Houston, 1983.

THE INSTITUTE OF PAPER CHEMISTRY

David C. Crowe

David C. Crowe
Research Fellow
Corrosion & Materials Engineering Section
Engineering Division

Ronald A. Yeske

Ronald A. Yeske
Section Leader
Corrosion & Materials Engineering Section
Engineering Division

Clyde H. Sprague

Clyde H. Sprague
Director
Engineering Division

APPENDIX I.

EVALUATION OF EXPERIMENTAL PROCEDURES.

The purpose of these studies was to determine possible sources of error in white liquor studies. The effects on weight loss of 1) removal of corrosion products by blasting versus abrasion methods, 2) initial surface condition, 3) liquor volume, 4) material of test container and 5) removal of corrosion products were studied. Surfaces were examined after blasting and chemical cleaning to determine if cleaning introduced impurities. A procedure for removal of corrosion products was adopted, as described below.

Electrodes were blasted with spherical silica glass beads at 20-30 psi in a Cyclo-blaster to remove the corrosion products. The rate of material loss from a bare specimen averaged about 100 mg/min of blast time. The rate of loss was somewhat higher if the initial surface was blasted rather than abraded. Abrasion of an electrode to remove a mark made by a felt marker pen resulted in roughly twice the weight loss from removal of the mark by blasting.

Initial surface condition influenced subsequent rate of weight loss, as illustrated in Fig. AI-1. Rate of weight loss in 100 g/L NaOH + 33 g/L Na₂S solution was higher for more coarsely abraded specimens. The blast-cleaned specimen lost weight at approximately the same rate as the specimen abraded to 120 grit.

A 120 grit finish has been established as the standard finish for the threaded, cylindrical type specimens. This finish is easily obtained by abrading the surface to 120 grit with silicon carbide paper while rotating the specimen via an electric motor. Periodic cooling with water will prevent metallurgical changes to the surface due to heat. After abrasion, the specimens

should be rinsed thoroughly with water and acetone. Air blasting will assist drying. Tissues or tweezers should be used to handle the specimens after this point to keep the samples clean. The specimens should be left for one hour to come to equilibrium with the room temperature and humidity level. Prior to weighing with the analytical balance, the specimens may be placed in snap cap vials and labeled.

Figure AI-2 shows that the volume of liquor in the test container had a significant effect on corrosion rate. This effect suggests that some corrosive reactant is depleted or corrosion products are accumulated, slowing the corrosion rate.

The material of construction of the test container (stainless steel or Teflon) may affect the corrosion rate, but the effect was not determined conclusively.

Corrosion products were removed with a paper towel or by blasting, but subsequent corrosion rate was essentially the same as for untouched specimens.

Analysis of surface composition by EDS/SEM showed no significant concentration of unusual or heavy elements. Some of the Si detected may have been due to deposition of glass (from the blasting beads) on the surface, and some due to background.

Cleaning in Clarke's solution ($10 \text{ g Sb}_2\text{O}_3 + 25 \text{ g SnCl}_2 + 500 \text{ mL HCl}(\text{sp. gr. } 1.19)$) generally resulted in surface staining. Surface analysis by EDS detected no Sn, and Sb and Cl were 0.5 and 1 % above background level, respectively. These low levels probably do not affect the corrosion rate significantly.

PROCEDURE FOR REMOVAL OF CORROSION PRODUCTS FROM CARBON STEEL WEIGHT LOSS SPECIMENS

Careful removal of corrosion products is critical in obtaining accurate, reproducible weight loss data. The following cleaning and handling techniques will aid in minimizing errors.

Corrosion products may be removed by blasting with a Cyclo-blast dry honer using glass beads. It is desirable that the specimens are hand-held and individually blasted at the lowest blast velocity that effectively removes the corrosion products from the surface. Careful attention is required to ensure that surfaces are not blasted any more than is necessary to remove visible deposits. Following blasting, the specimens are flushed with air. They are then rinsed in water, and the threaded hole is rinsed and cleaned with a pipe cleaner. The hole is then blasted with air to remove any water and pipe cleaner fibers. The entire specimen is then rinsed with acetone, air blasted dry, and allowed to sit for one hour before weighing.

Alternatively, corrosion deposits may be removed by a chemical cleaning method. Clarke's solution is prepared as noted above. The addition of an aldehyde such as formaldehyde, acetaldehyde, benzaldehyde, or glyoxal may prevent the evolution of toxic hydrogen sulfide gas from sulfide corrosion products. As a further precaution, preparation of the cleaning solution and the cleaning procedure should always be performed in a fume hood. The specimens may be supported by a perforated Teflon jar lid in the bottom of a beaker of cleaning solution at room temperature. The solution is vigorously stirred by means of a magnetic stir bar located underneath the perforated Teflon lid. The specimens are placed in the solution for about 15 minutes, then removed with tongs, rinsed in distilled water, and lightly brushed with an acid resistant brush. Specimens

are then placed back into solution for an additional 10 minutes. Finally, the electrodes are rinsed in water, cleaned with a pipe cleaner, rinsed in acetone, air blasted dry, and left to sit until weighing.

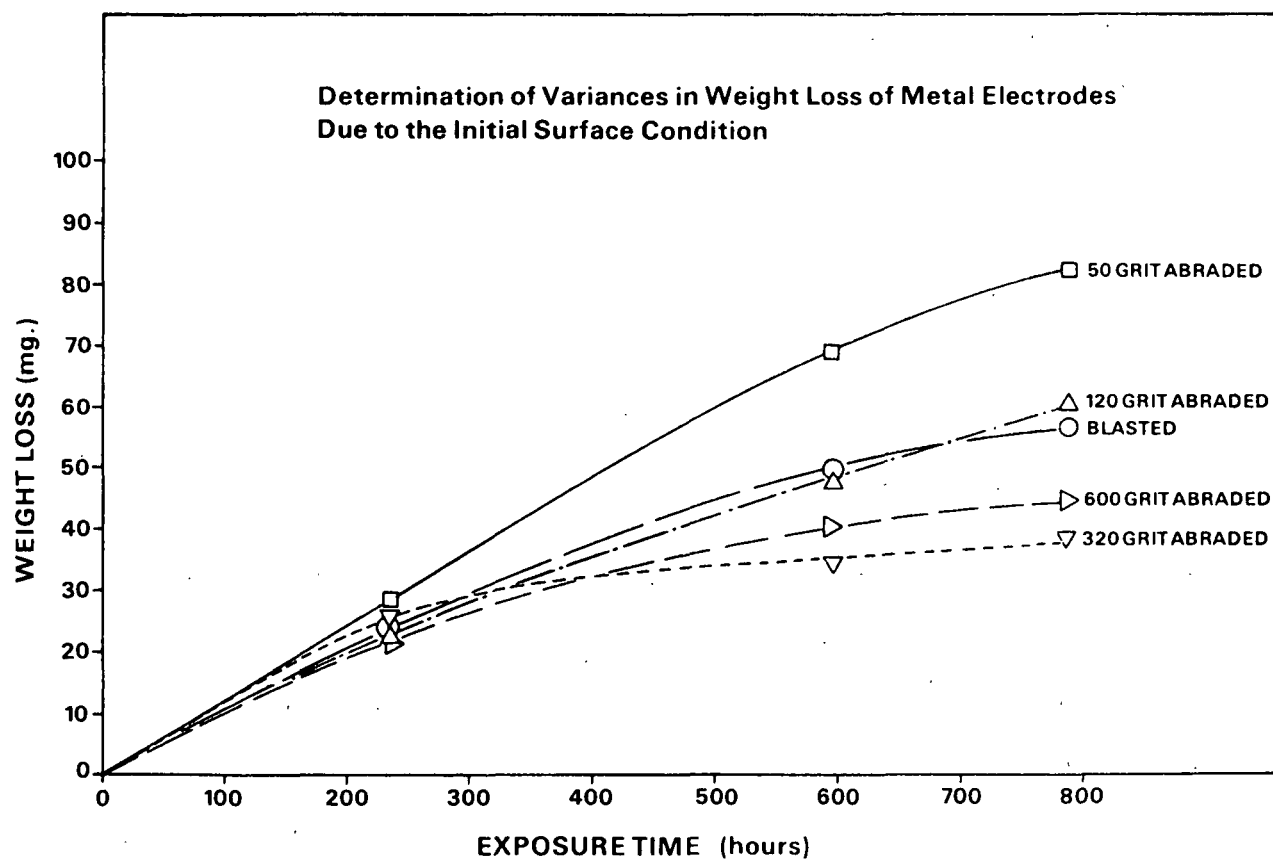


Figure AI-1. Determination of variances in weight loss of metal electrodes due to the initial surface condition.

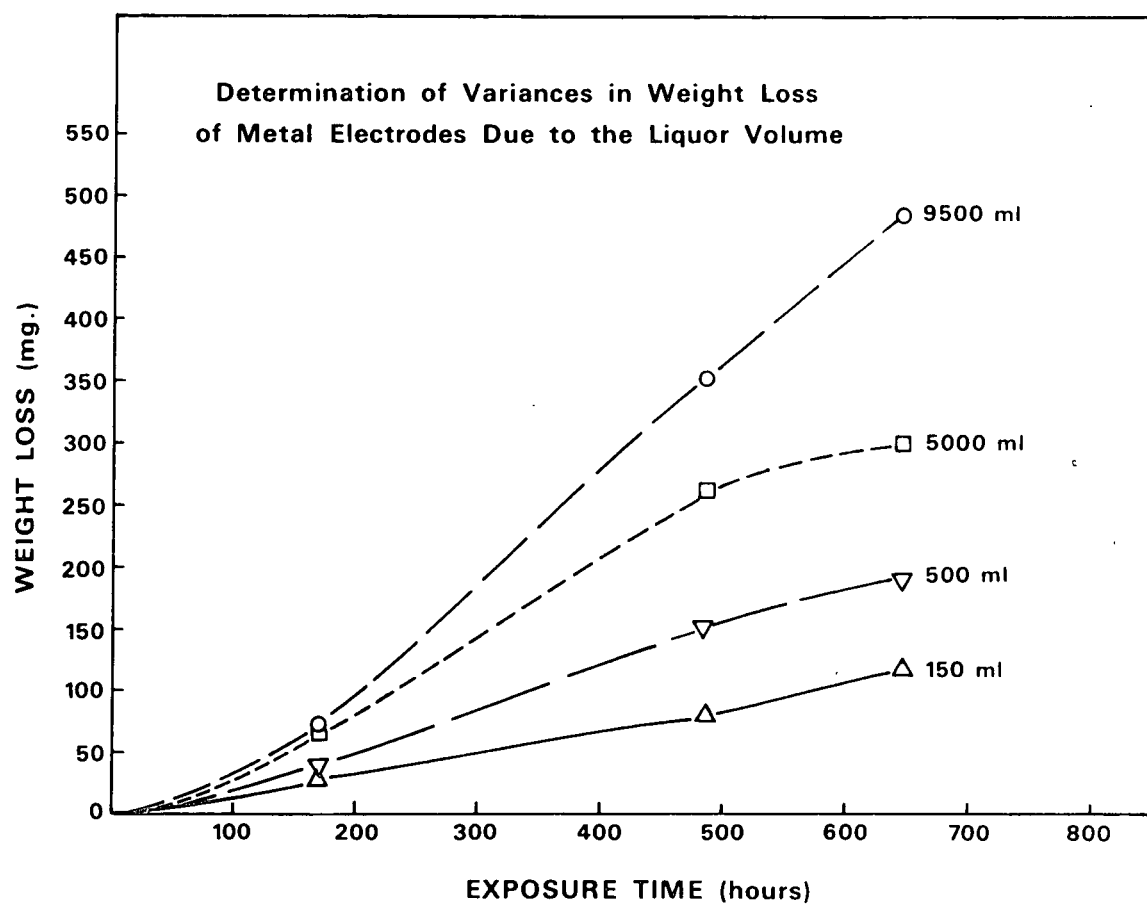
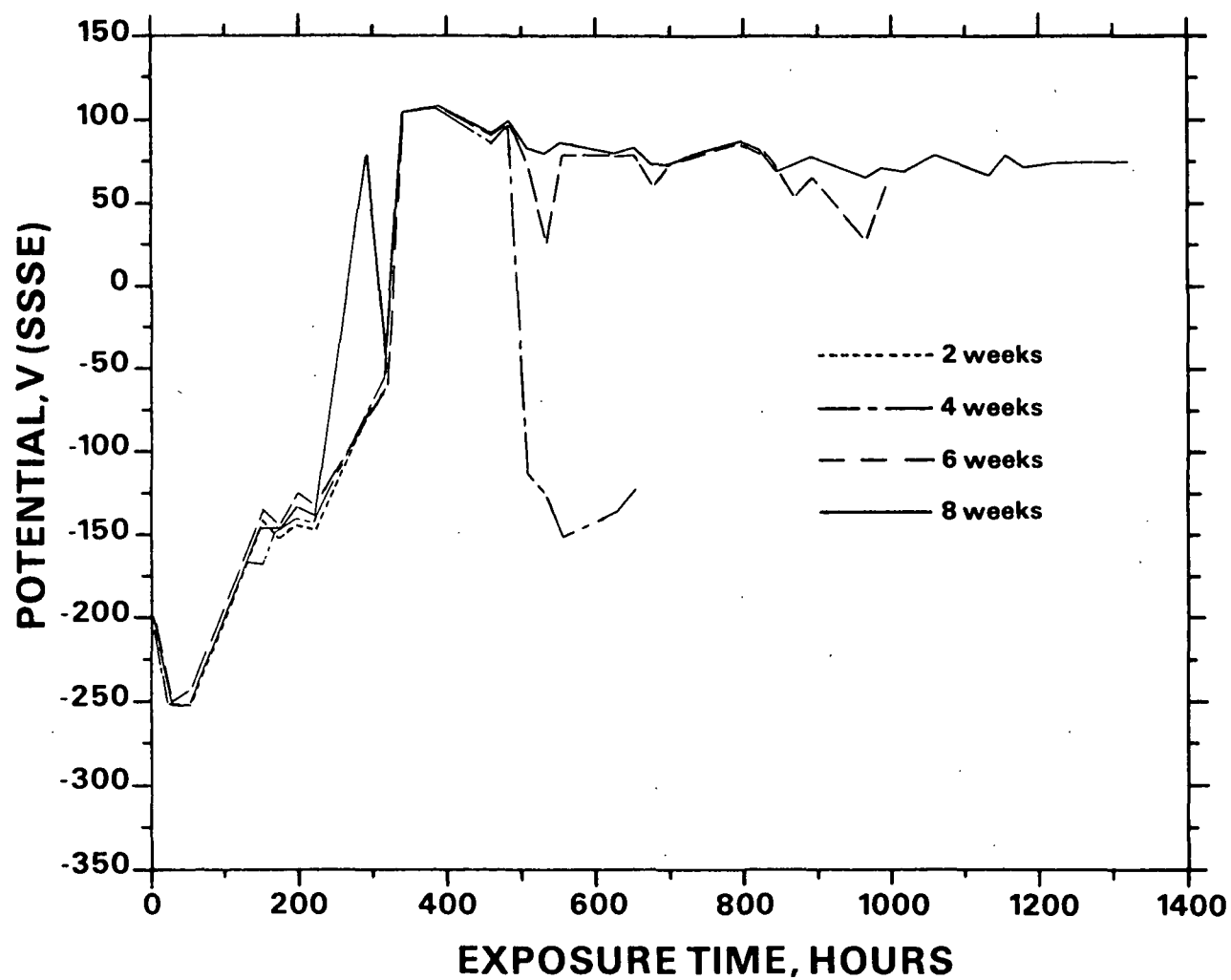


Figure AI-2. Determination of variances in weight loss of metal electrodes due to the liquor volume.

APPENDIX II

CORROSION POTENTIAL DURING WEIGHT LOSS TESTS

SOLUTIONS CONTAINING SULFUR ADDITIONS

Figure AII-1. Corrosion potential in 60 g/L NaOH + 10 g/L Na₂S.

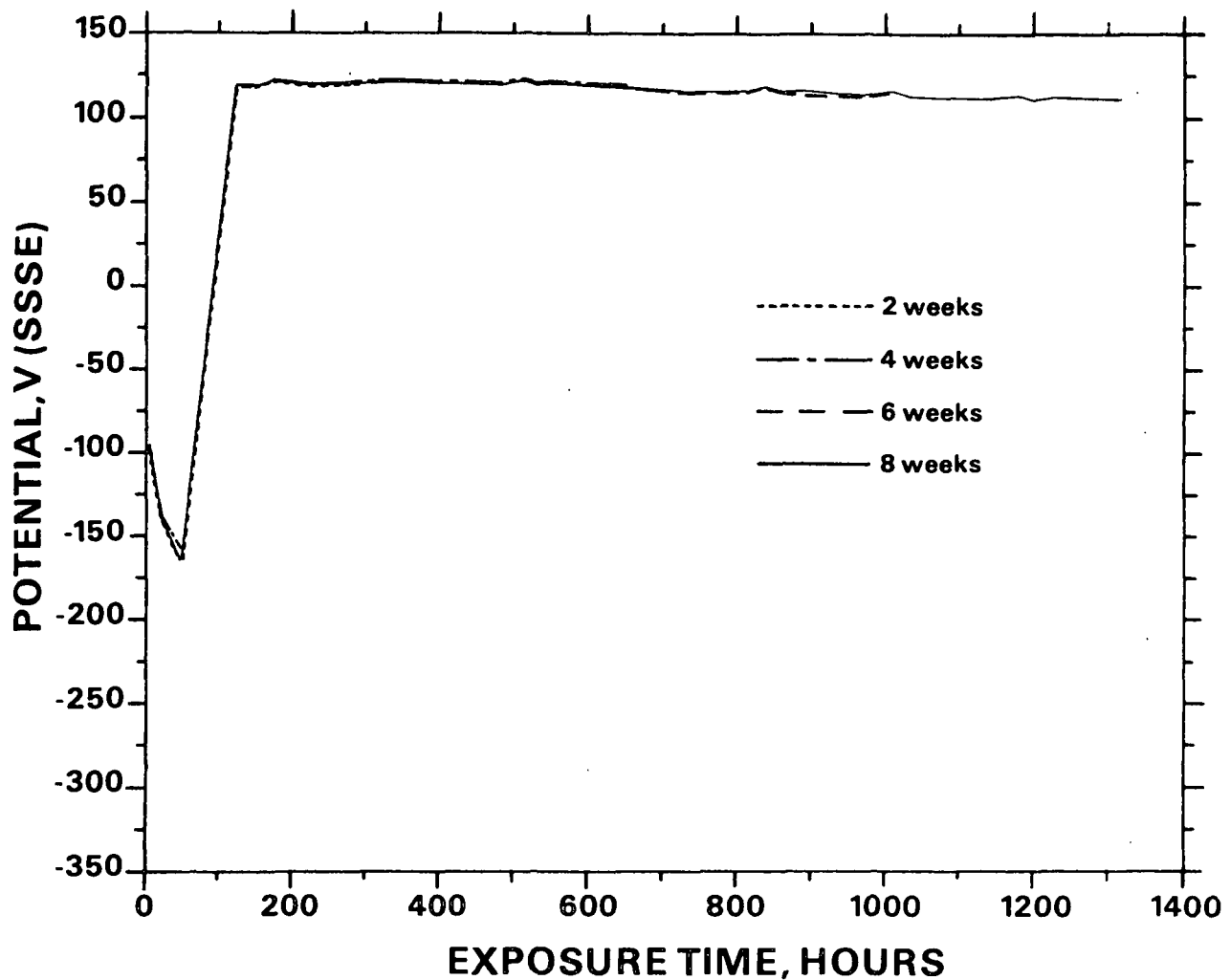


Figure AII-2. Corrosion potential in 60 g/L NaOH + 10 g/L Na₂S + 0.5 g/L S. Similar behavior was observed in the solutions of the following compositions:

NaOH, g/L	Na ₂ S, g/L	S, g/L
60	20	1.5
60	20	1
60	30	1.5
60	30	2
60	40	1.5
60	40	2
80	30	2
100	40	5
120	10	2

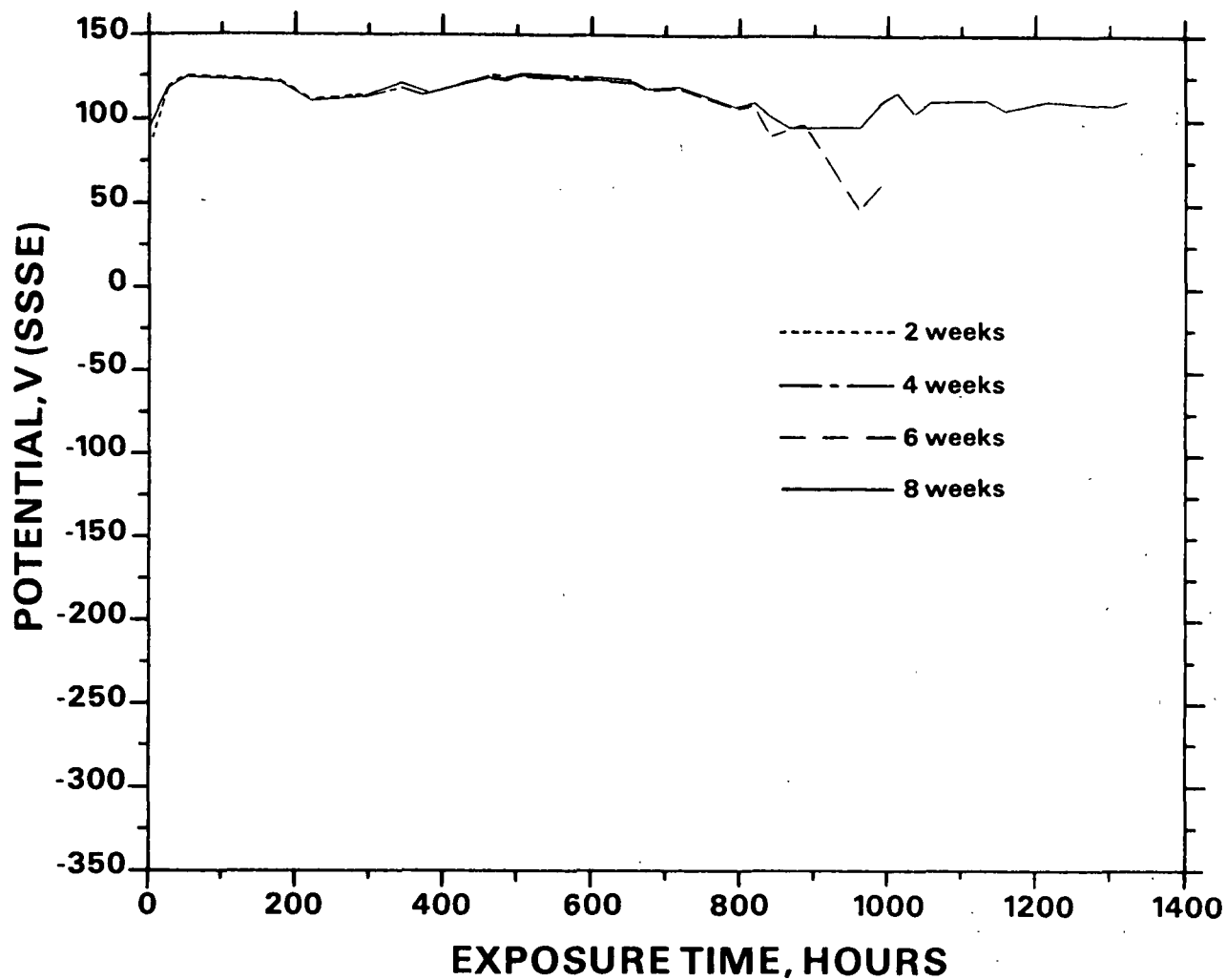


Figure AII-3. Corrosion potential in 60 g/L NaOH + 10 g/L Na₂S + 1 g/L S. Similar behavior was observed in solutions of the following compositions:

NaOH, g/L	Na ₂ S, g/L	S, g/L
60	10	1.5
60	10	2
60	10	5
60	10	10
60	20	2
80	10	1.5
80	10	2
80	10	5
80	10	10
100	10	1.5
100	10	5
100	10	10
100	20	5
100	20	10
120	10	5
120	10	10
120	20	10
120	30	5

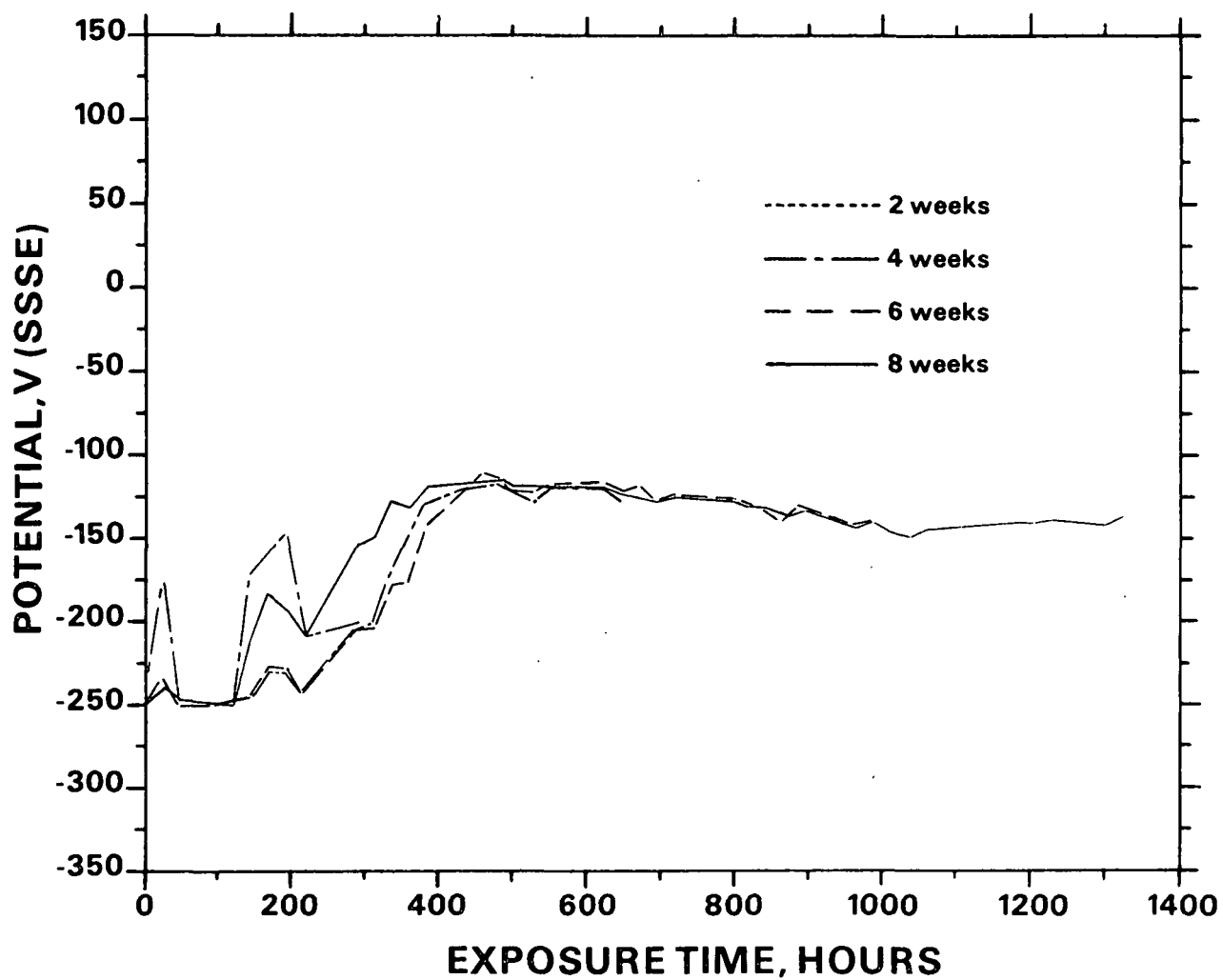


Figure AII-4. Corrosion potential in 60 g/L NaOH + 20 g/L Na₂S.

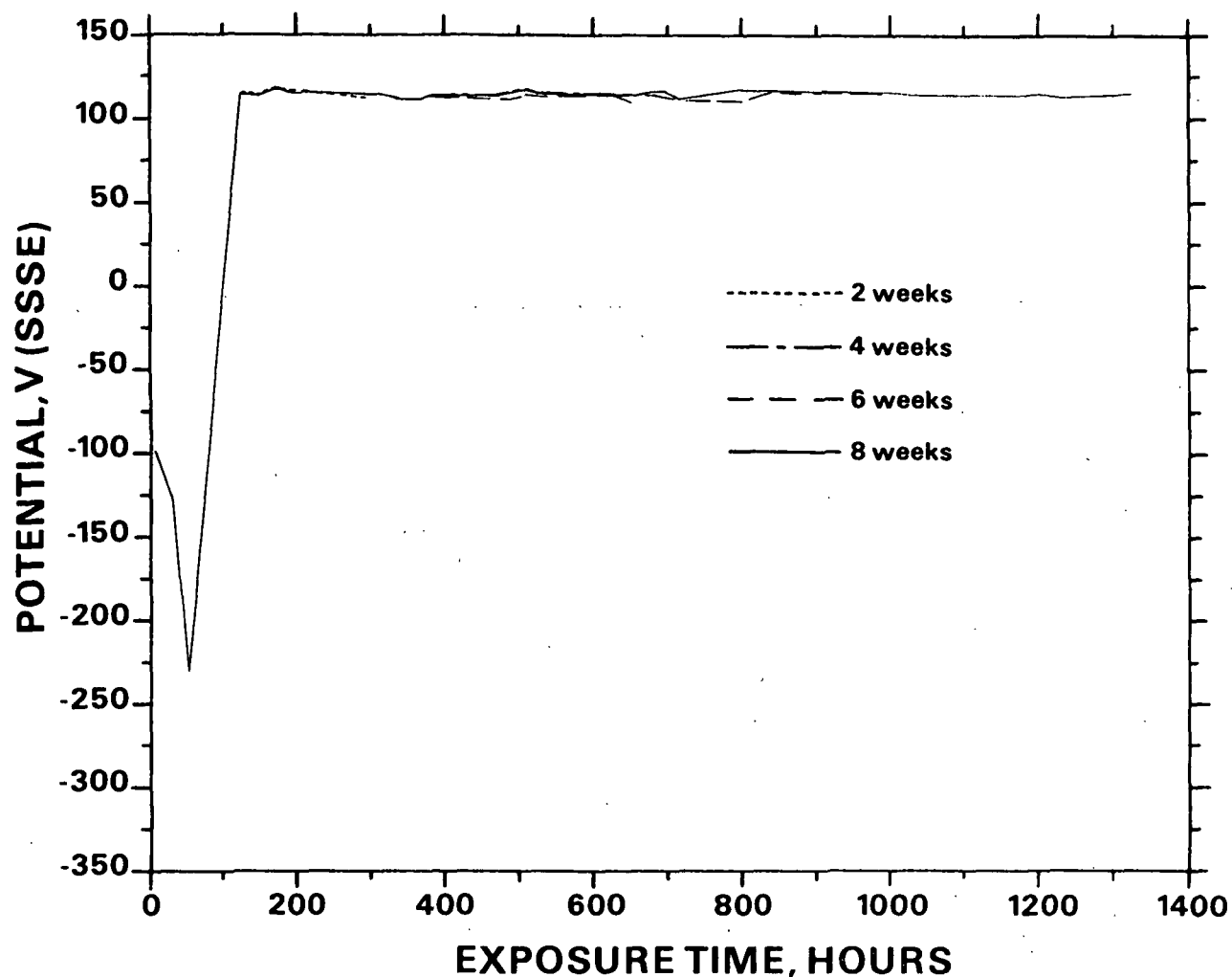


Figure AII-5. Corrosion potential in 60 g/L NaOH + 20 g/L Na₂S + 0.5 g/L S. Similar behavior was observed in solutions of the following compositions:

NaOH, g/L	Na ₂ S, g/L	S, g/L
60	30	1
60	40	1
80	30	1
80	40	1.5
80	40	2
100	10	0.5
120	10	0.5
120	20	1
120	20	1.5
120	20	2
120	30	1.5
120	30	2
120	40	1.5
120	40	2

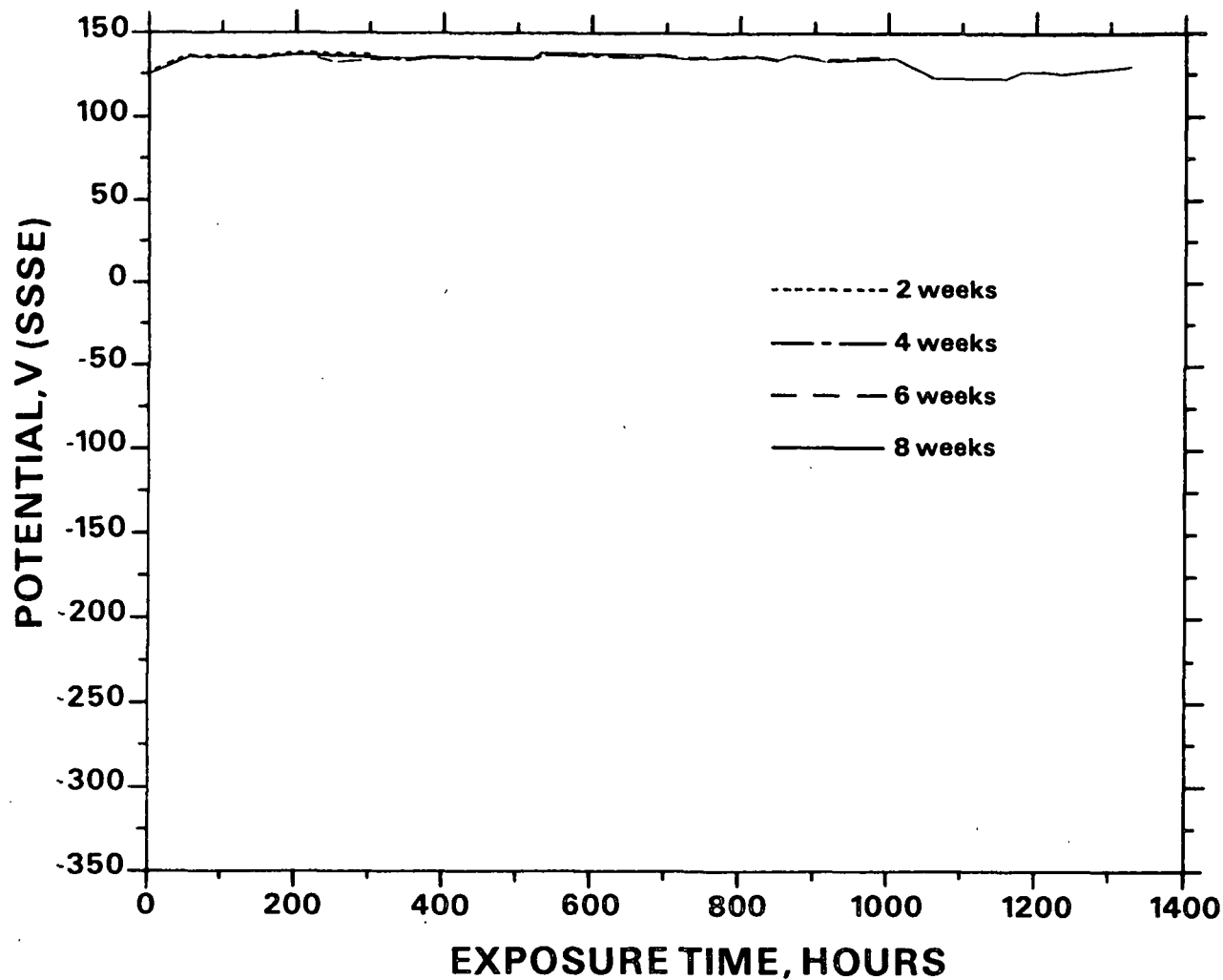


Figure AII-6. Corrosion potential in 60 g/L NaOH + 20 g/L Na₂S + 5 g/L S. Similar behavior was observed in solutions of the following compositions:

NaOH, g/L	Na ₂ S, g/L	S, g/L
60	20	10
60	30	5
60	30	10
60	40	5
60	40	10
80	40	5
80	40	10

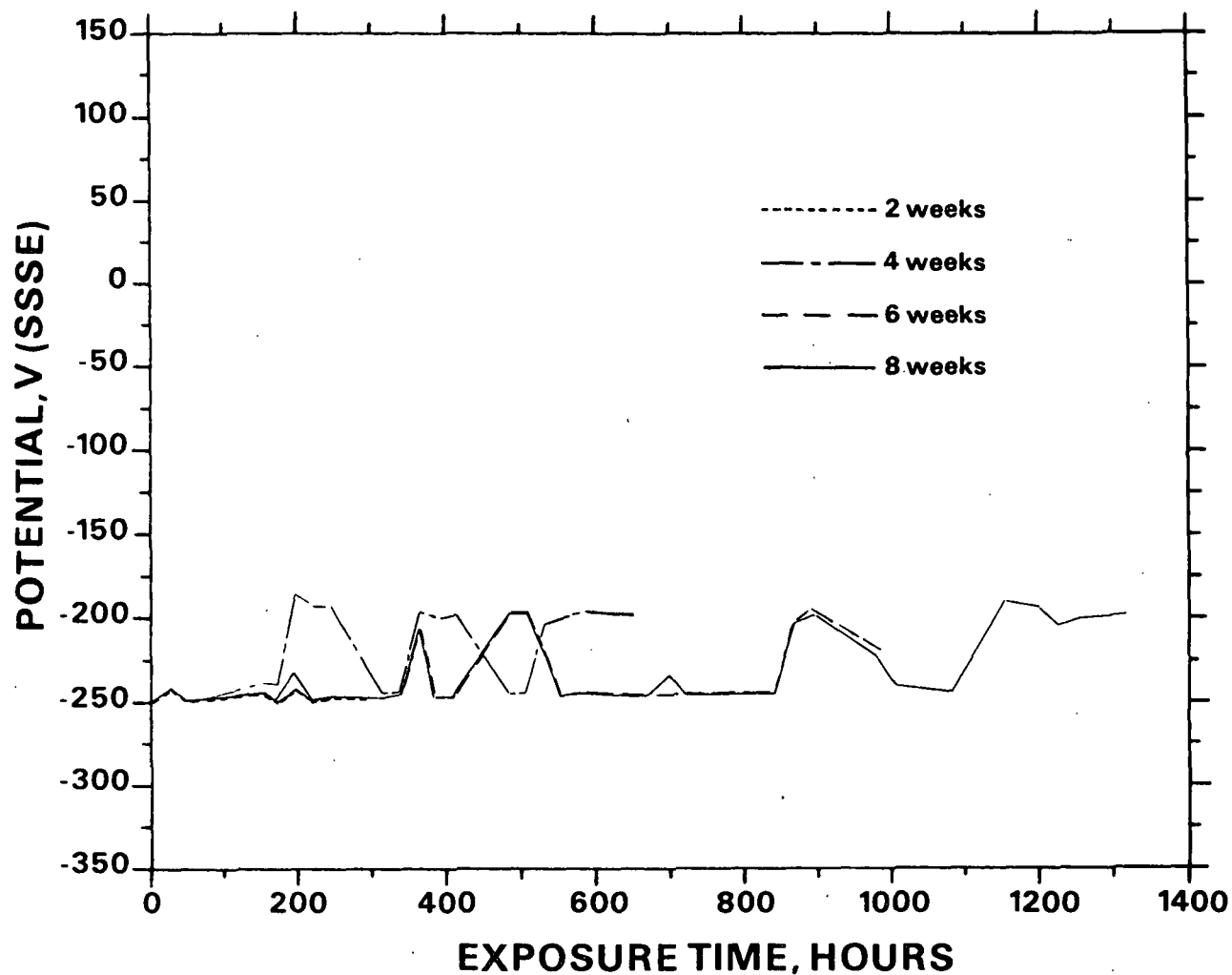


Figure AII-7. Corrosion potential in 60 g/L NaOH + 30 g/L Na₂S. Similar behavior was observed in solutions of the following compositions:

NaOH, g/L	Na ₂ S, g/L	S, g/L
60	40	
100	40	0.5
120	30	0.5

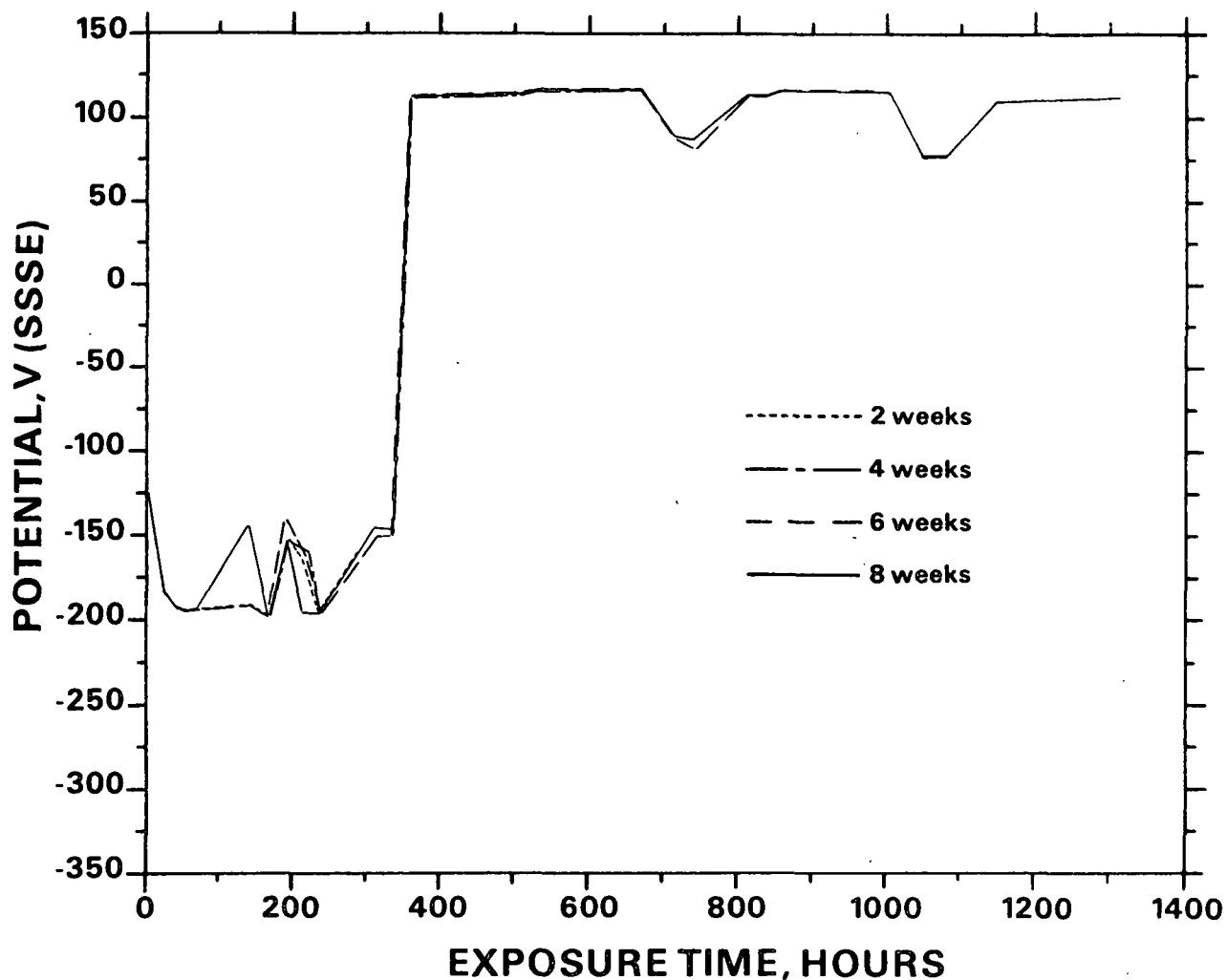


Figure AII-8. Corrosion potential in 60 g/L NaOH + 30 g/L Na₂S + 0.5 g/L S. Similar behavior was observed in solutions of the following compositions:

NaOH, g/L	Na ₂ S, g/L	S, g/L
60	40	0.5
100	40	1.5

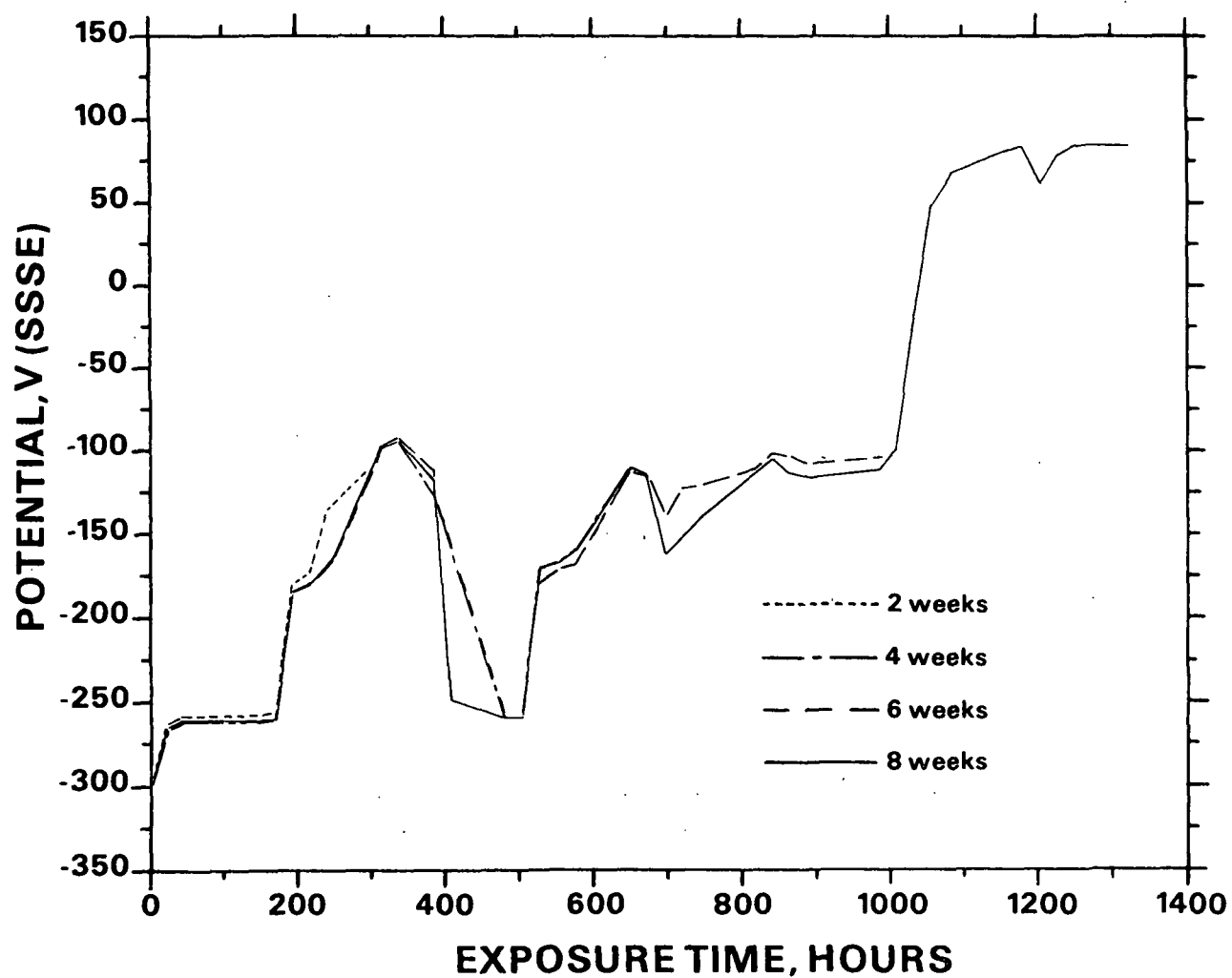


Figure AII-9. Corrosion potential in 80 g/L NaOH + 10 g/L Na₂S + 1 g/L S.

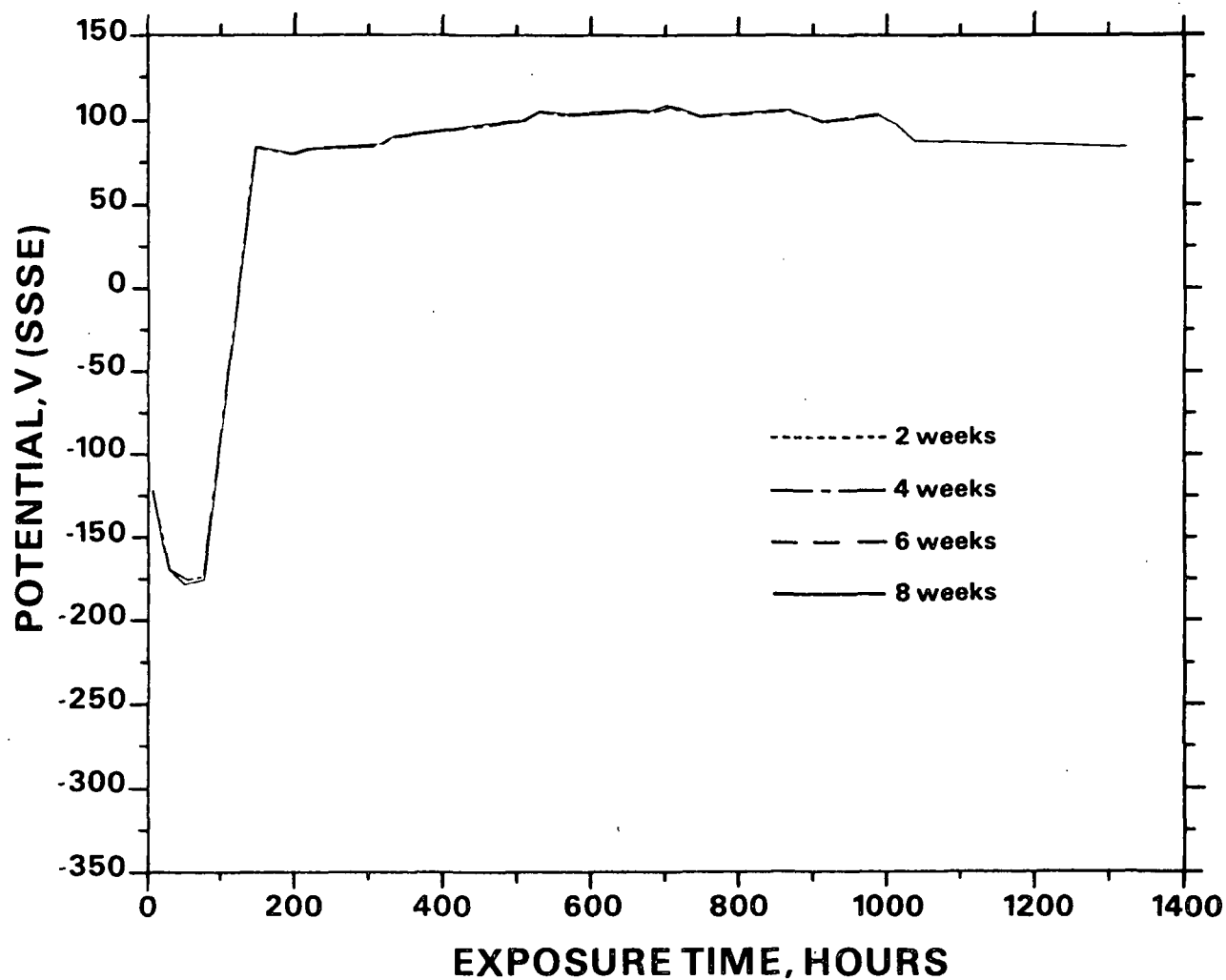


Figure AII-10. Corrosion potential in 80 g/L NaOH + 10 g/L Na₂S + 0.5 g/L S. Similar behavior was observed in solutions of the following compositions:

NaOH, g/L	Na ₂ S, g/L	S, g/L
80	20	0.5
80	20	2
100	10	1
120	10	1
120	10	1.5

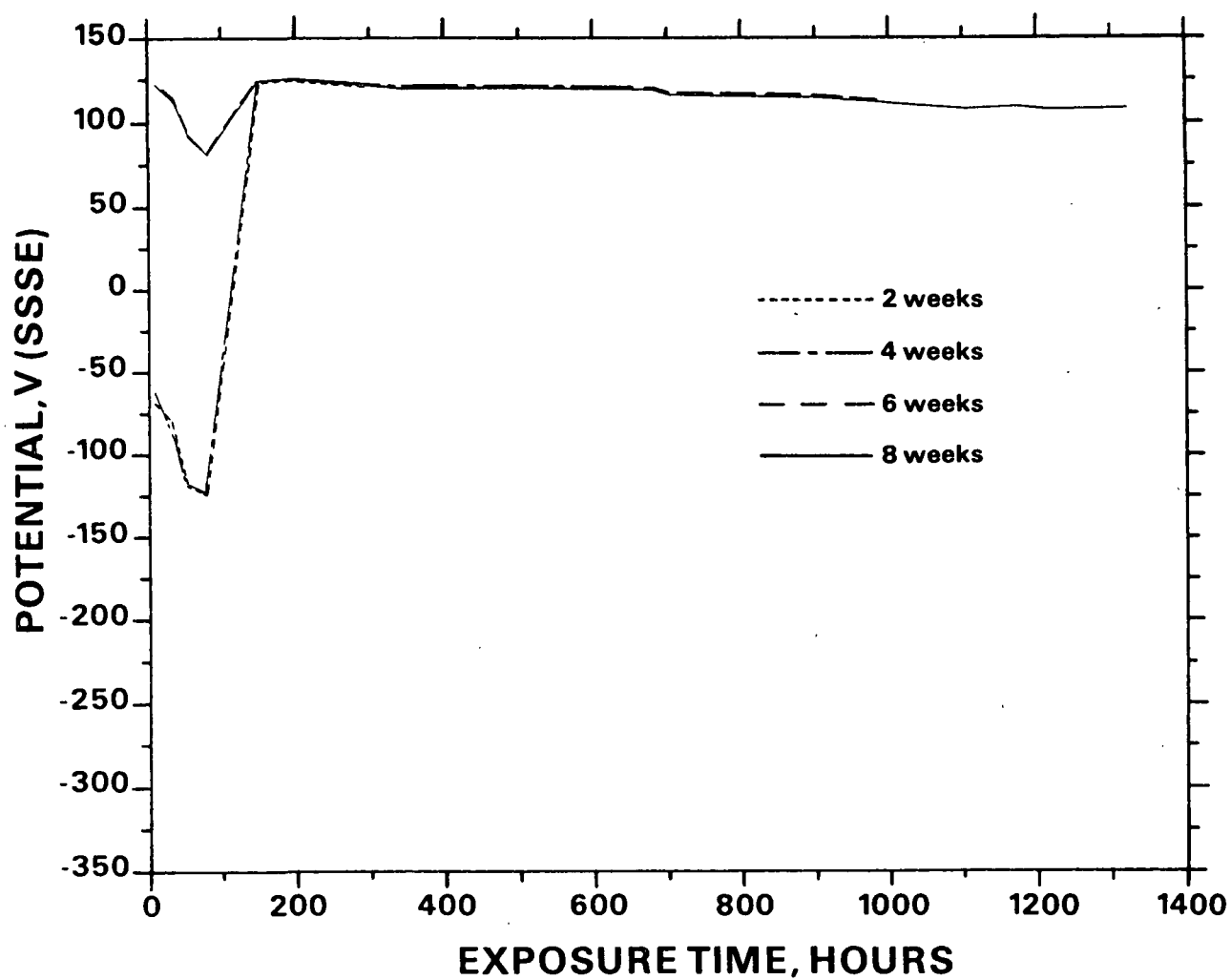


Figure AII-11. Corrosion potential in 80 g/L NaOH + 10 g/L Na₂S + 1 g/L S. Similar behavior was observed in solution containing 100 g/L NaOH + 10 g/L Na₂S.

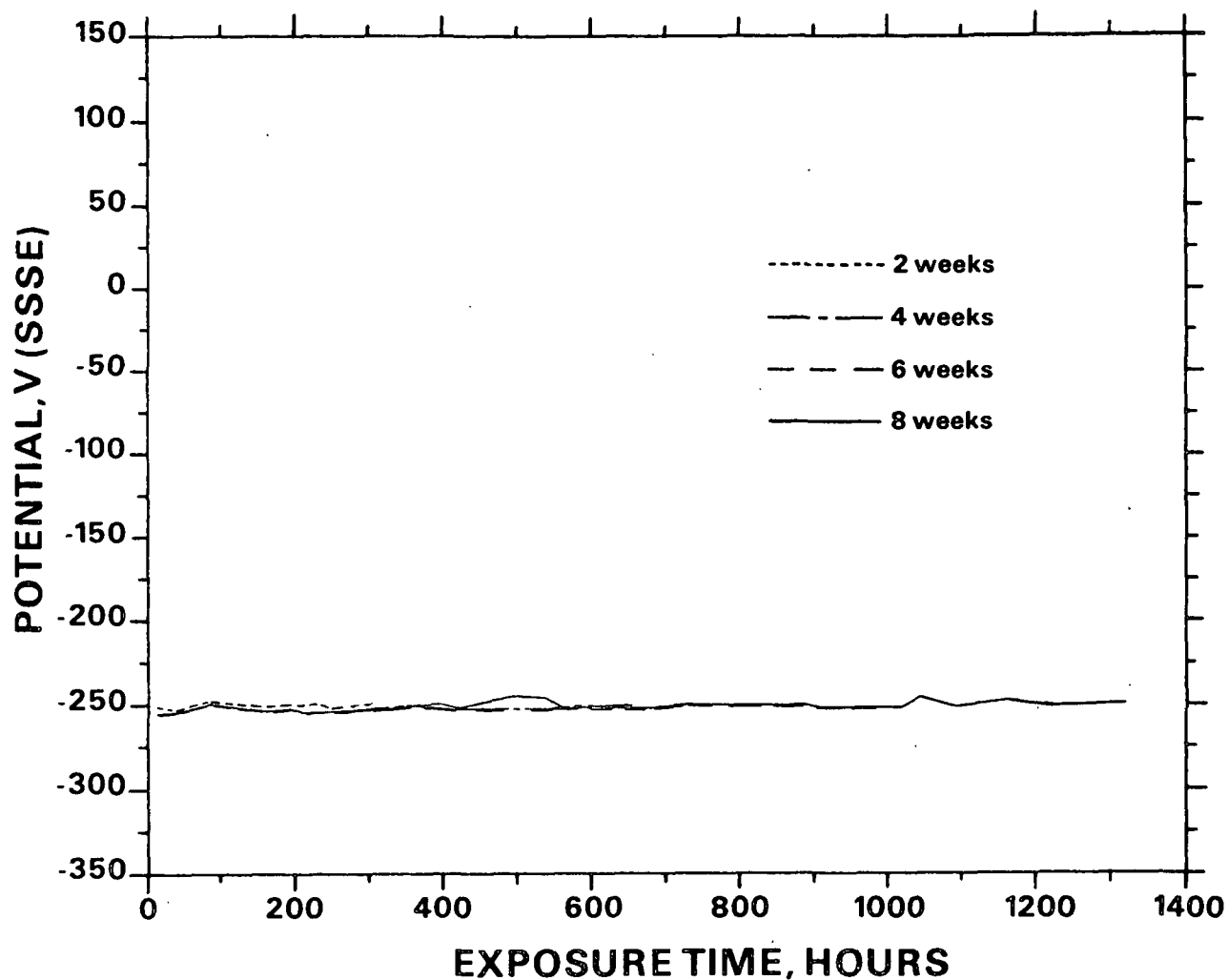


Figure AII-12. Corrosion potential in 80 g/L NaOH + 20 g/L Na₂S. Similar behavior was observed in solutions of the following compositions:

NaOH, g/L	Na ₂ S, g/L
80	30
100	40
120	20
120	30
120	40

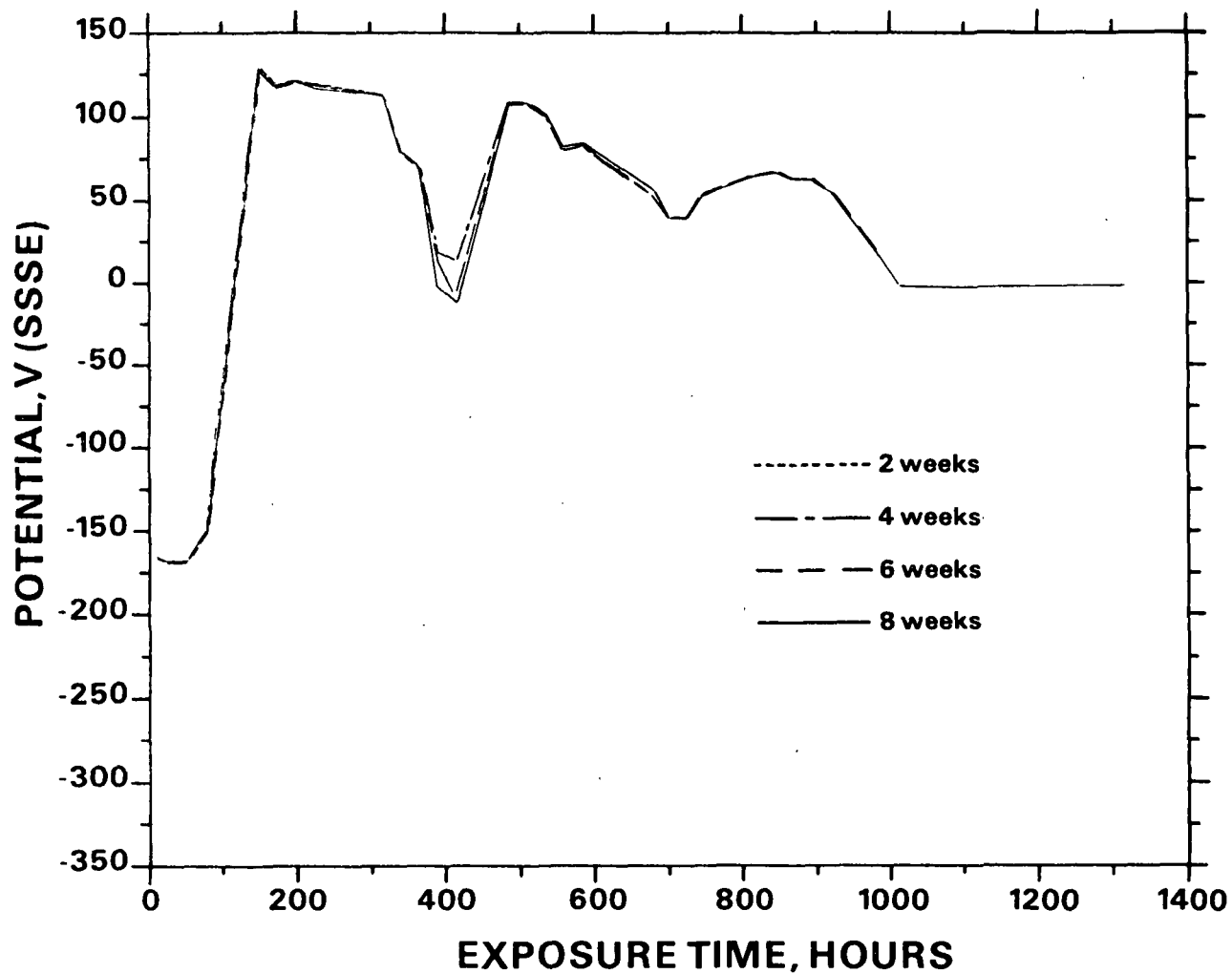


Figure AII-13. Corrosion potential in 80 g/L NaOH + 20 g/L Na₂S + 1 g/L S. Similar behavior was observed in solution containing 80 g/L NaOH + 20 g/L Na₂S + 1.5 g/L S.

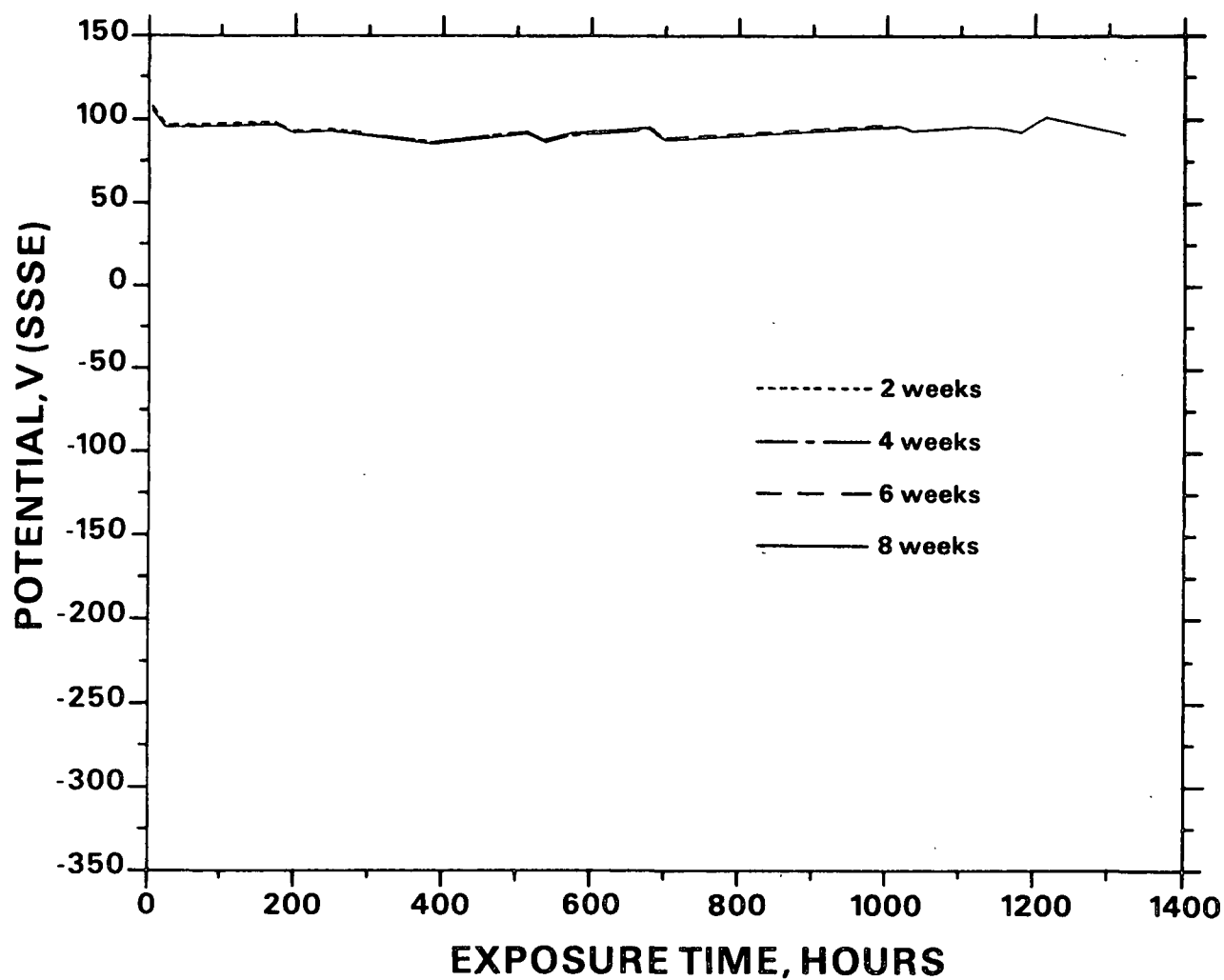


Figure AII-14. Corrosion potential in 80 g/L NaOH + 20 g/L Na₂S + 5 g/L S. Similar behavior was observed in solutions of the following compositions:

NaOH, g/L	Na ₂ S, g/L	S, g/L
80	20	10
80	30	5
80	30	10
100	40	10

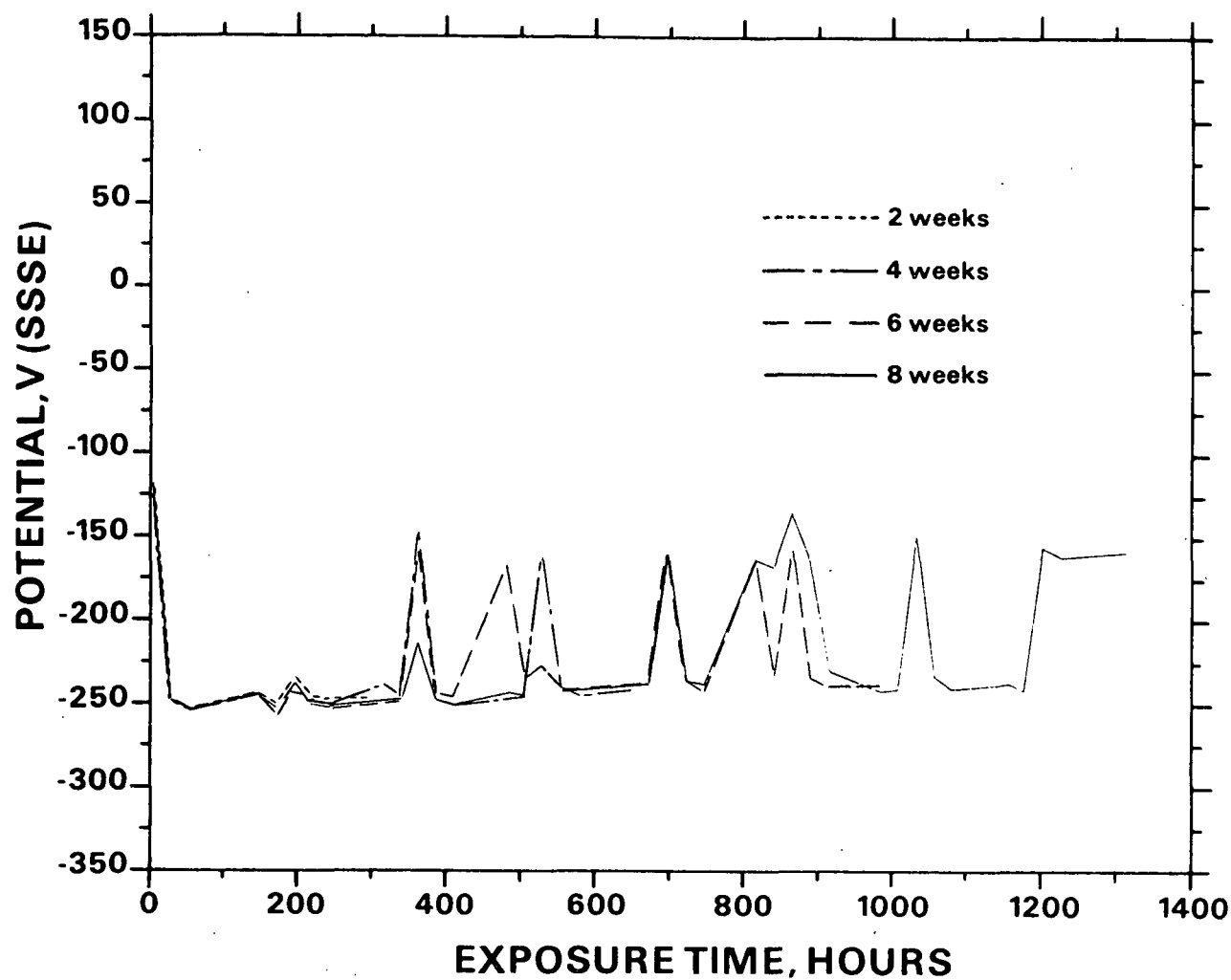


Figure AII-15. Corrosion potential in 80 g/L NaOH + 30 g/L Na₂S + 0.5 g/L S. Similar behavior was observed in solutions of the following compositions:

NaOH, g/L	Na ₂ S, g/L	S, g/L
100	20	0
100	40	1
120	30	1
120	40	1

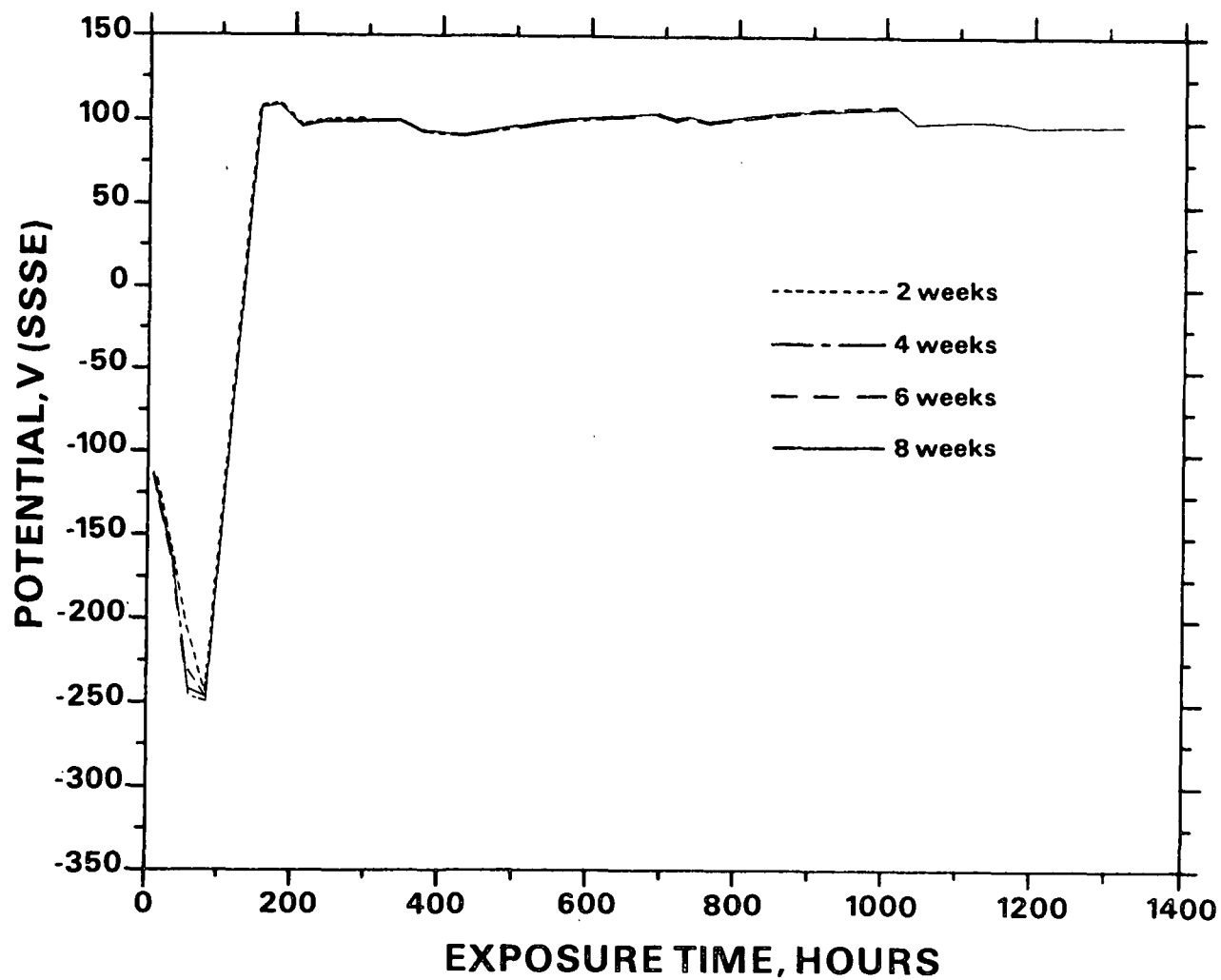


Figure AII-16. Corrosion potential in 80 g/L NaOH + 30 g/L Na₂S + 1.5 g/L S. Similar behavior was observed in solutions of the following compositions:

NaOH, g/L	Na ₂ S, g/L	S, g/L
80	40	1
100	20	1.5
100	20	2

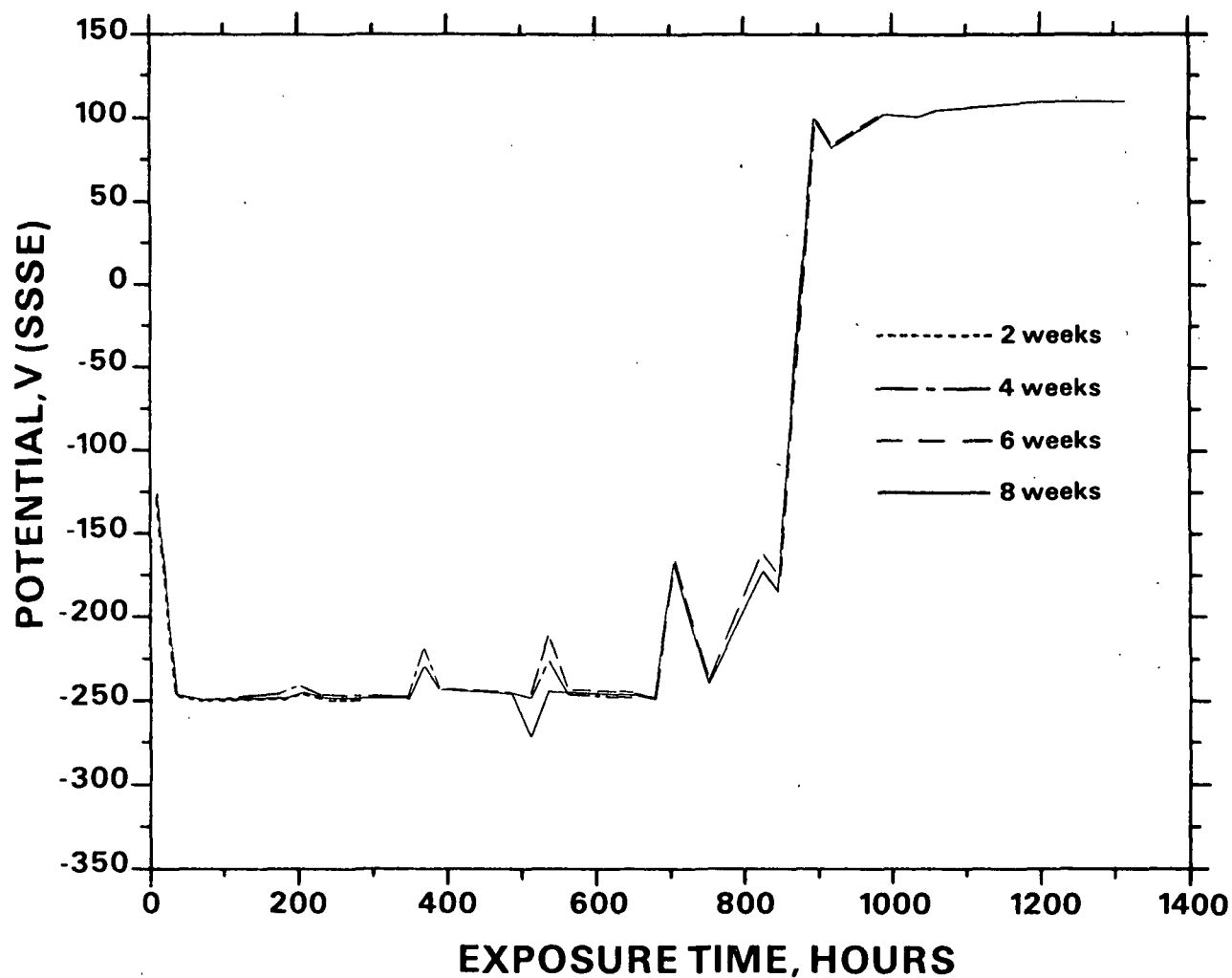


Figure AII-17. Corrosion potential in 80 g/L NaOH + 40 g/L Na₂S + 0.5 g/L S. Similar behavior was observed in 120 g/L NaOH + 40 g/L Na₂S + 0.5 g/L solution.

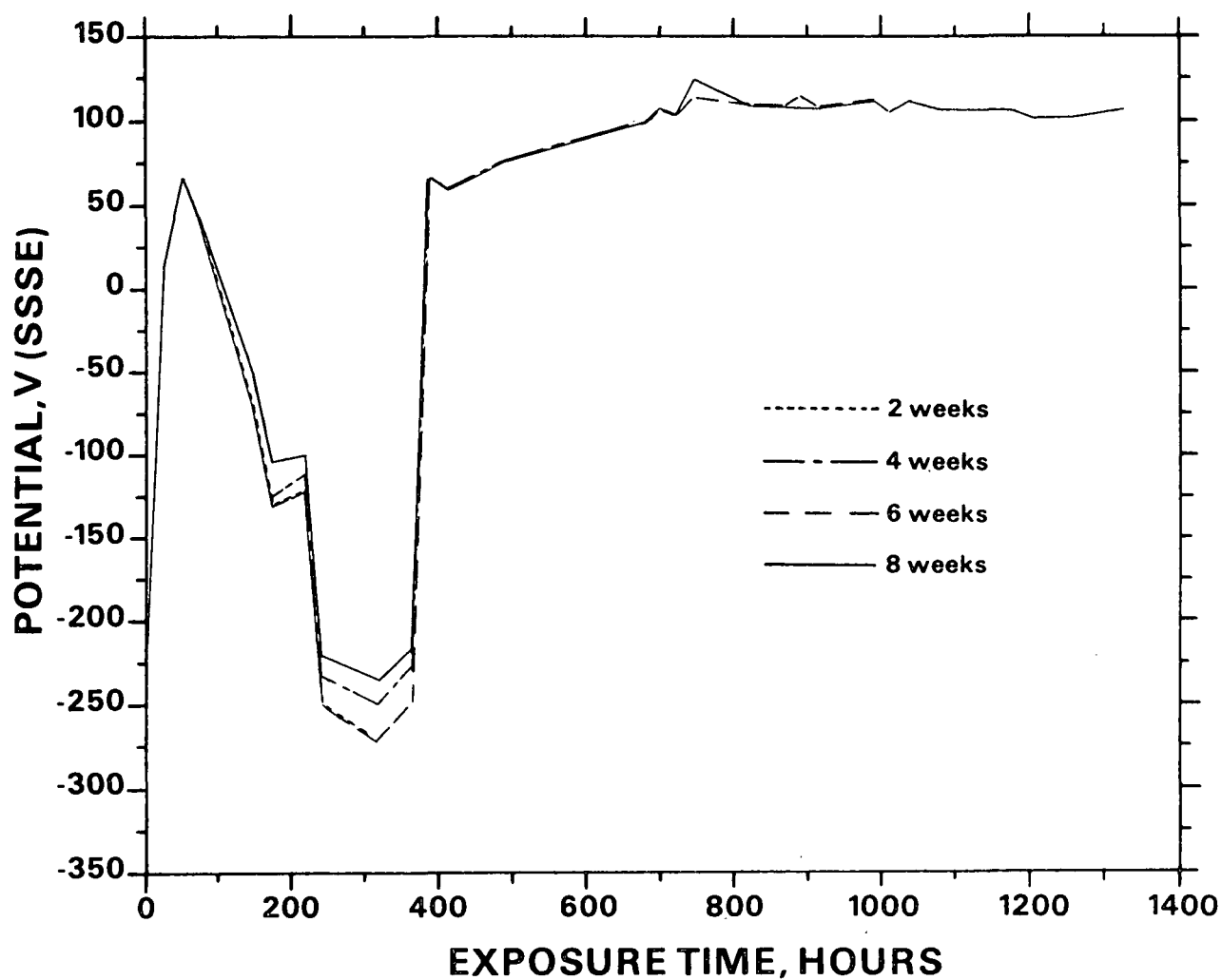


Figure AII-18. Corrosion potential in 100 g/L NaOH + 10 g/L Na₂S + 2 g/L S. Similar behavior was observed in solutions of the following compositions:

NaOH, g/L	Na ₂ S, g/L	S, g/L
100	20	0.5
100	20	1
120	20	0.5

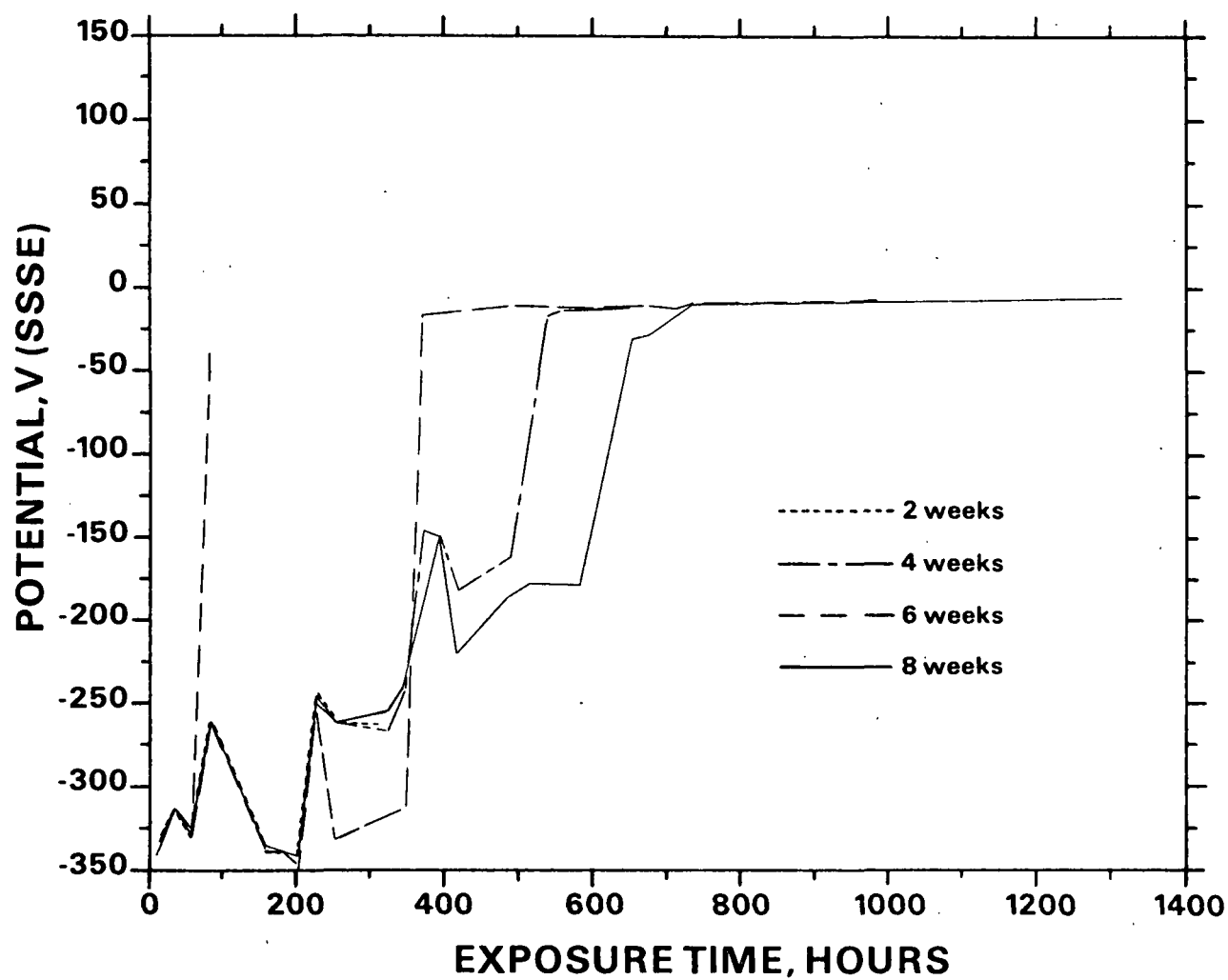


Figure AII-19. Corrosion potential in 100 g/L NaOH + 40 g/L Na₂S + 2 g/L S.

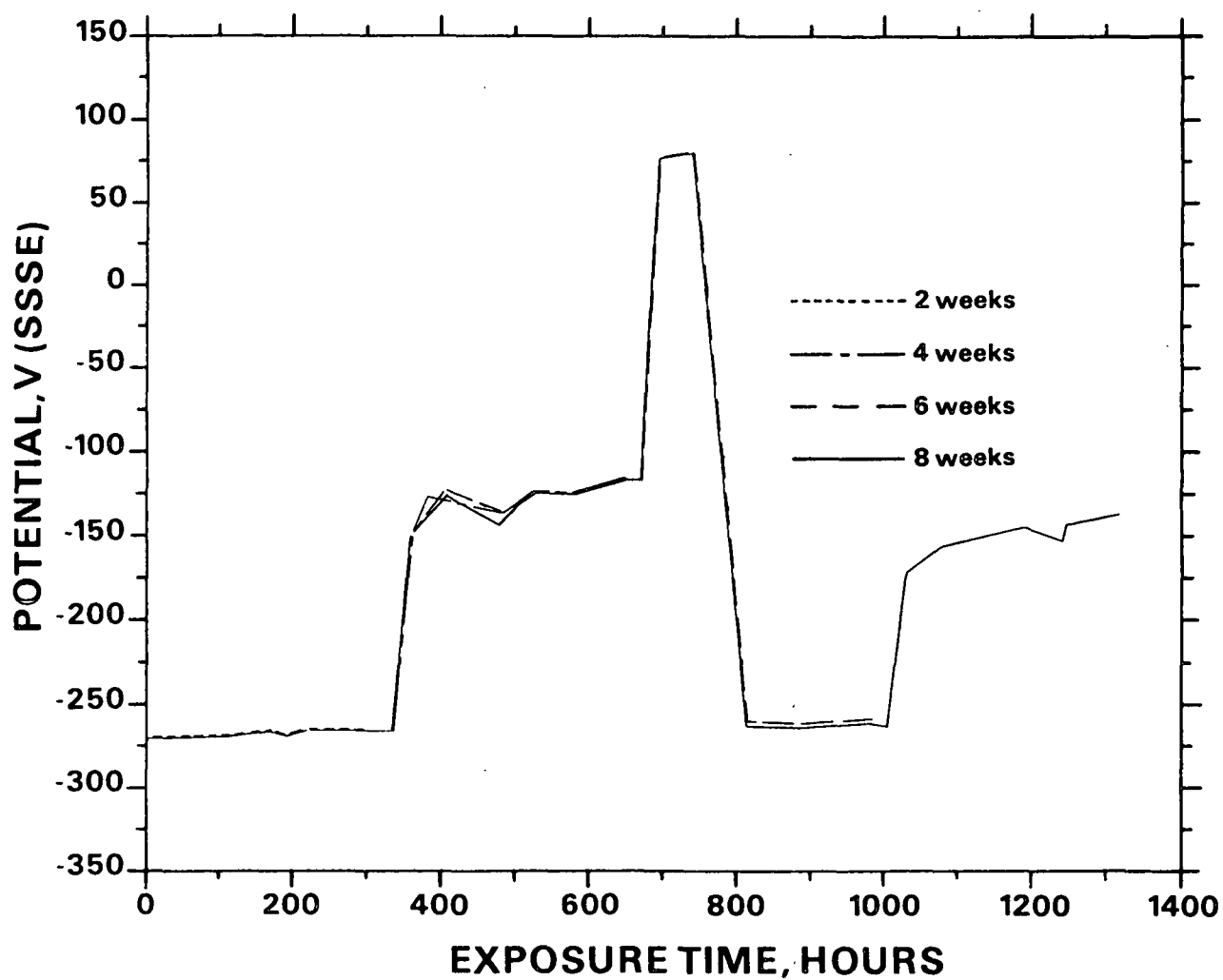


Figure AII-20. Corrosion potential in 120 g/L NaOH + 10 g/L Na₂S.

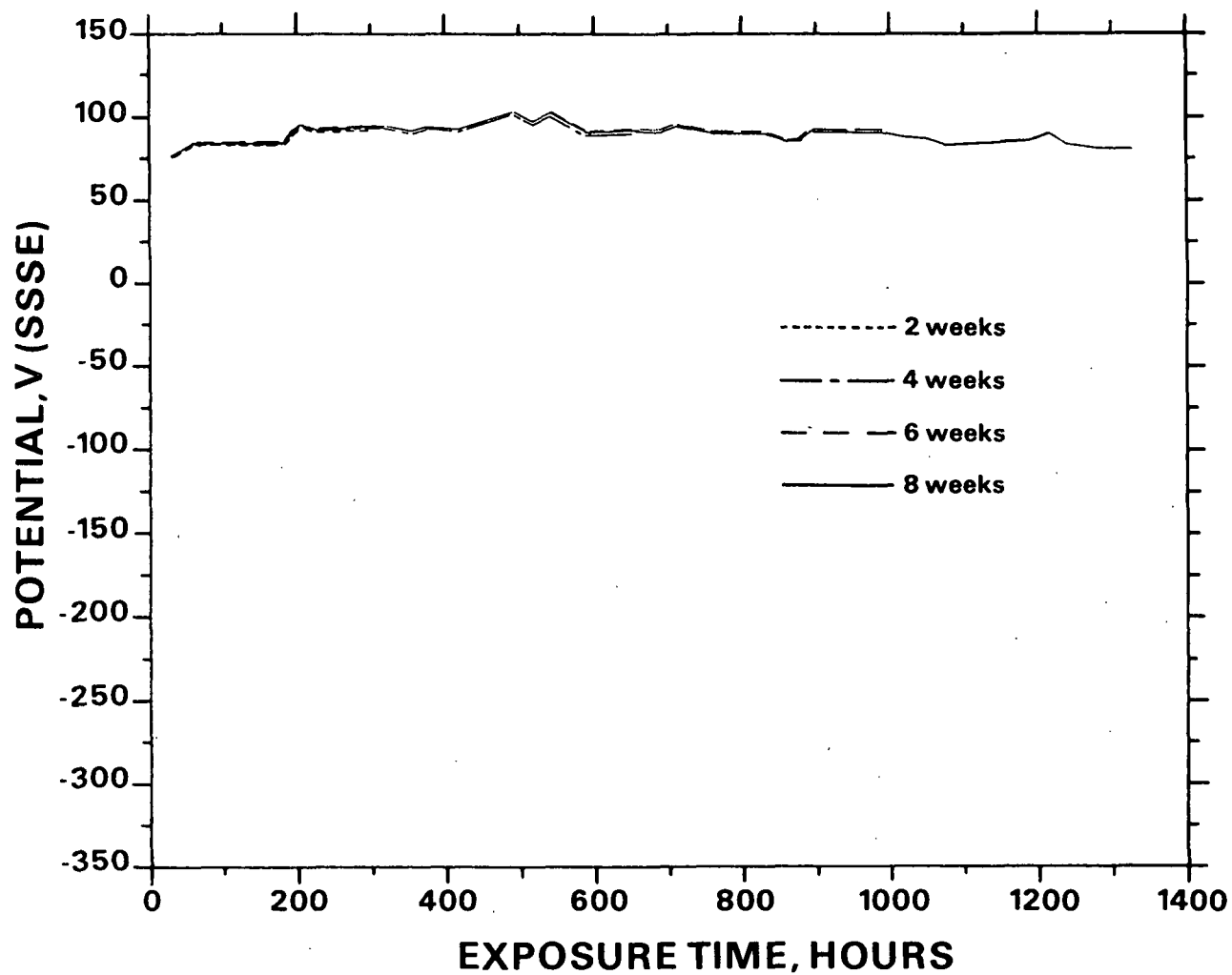


Figure AII-21. Corrosion potential in 120 g/L NaOH + 20 g/L Na₂S + 5 g/L S. Similar behavior was observed in 120 g/L NaOH + 30 g/L Na₂S + 10 g/L S.

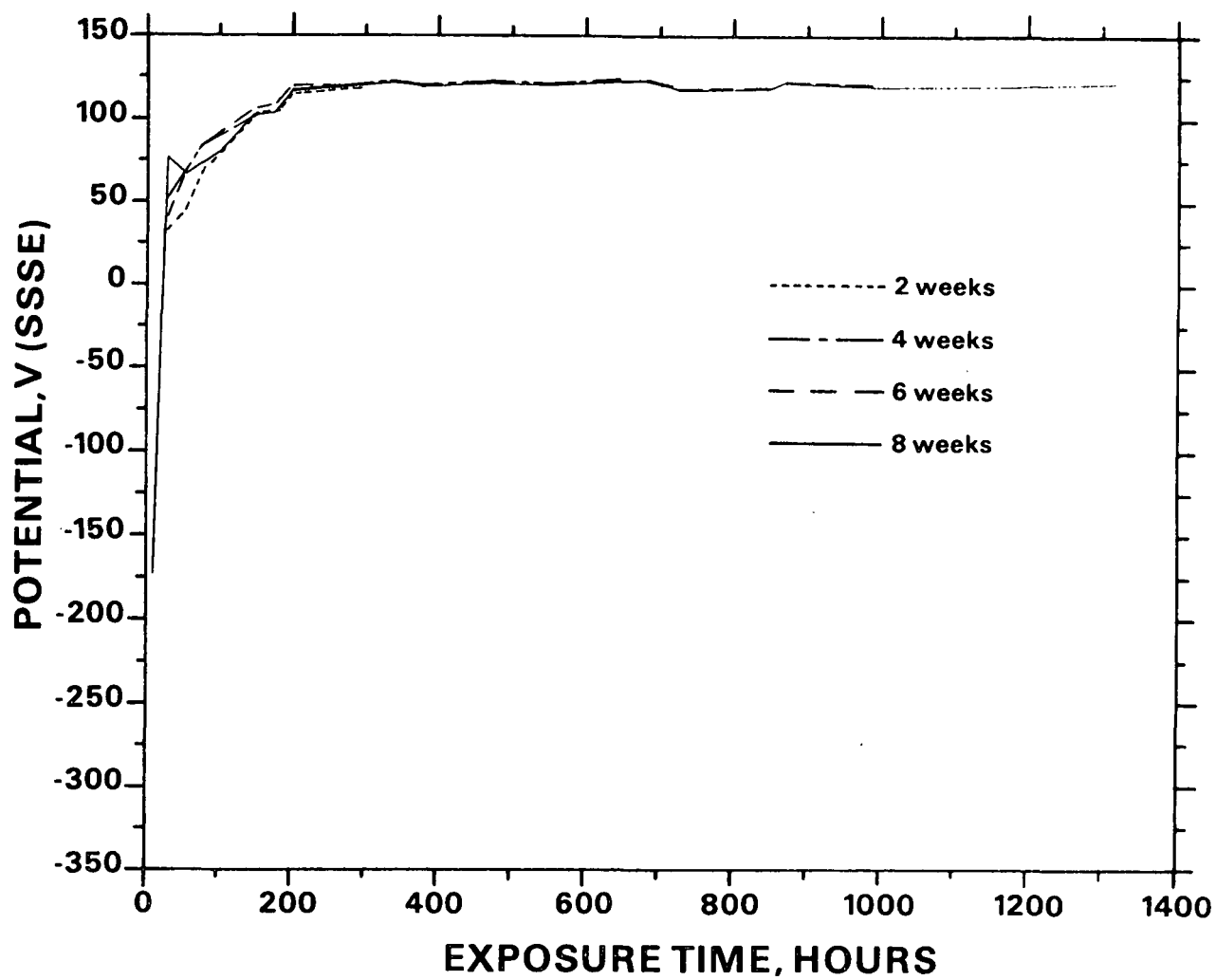


Figure AII-22. Corrosion potential in 120 g/L NaOH + 40 g/L Na₂S + 5 g/L S. Similar behavior was observed in 120 g/L NaOH + 40 g/L Na₂S + 10 g/L S.

SOLUTIONS CONTAINING THIOSULFATE ADDITIONS

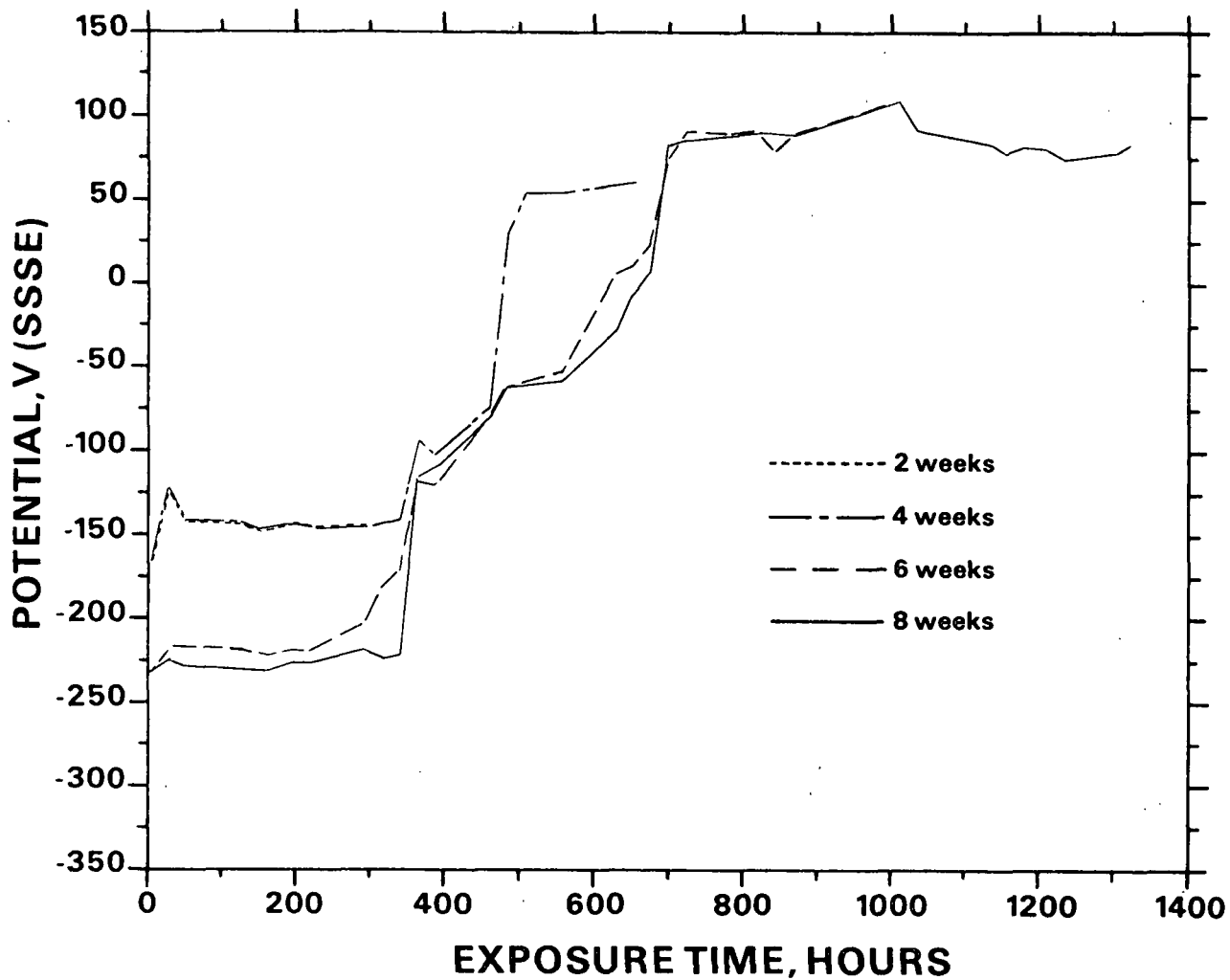


Figure AII-23. Corrosion potential in 60 g/L NaOH + 10 g/L Na₂S + 2.5 g/L Na₂S₂O₃. Similar behavior was observed in 80 g/L NaOH + 10 g/L Na₂S.

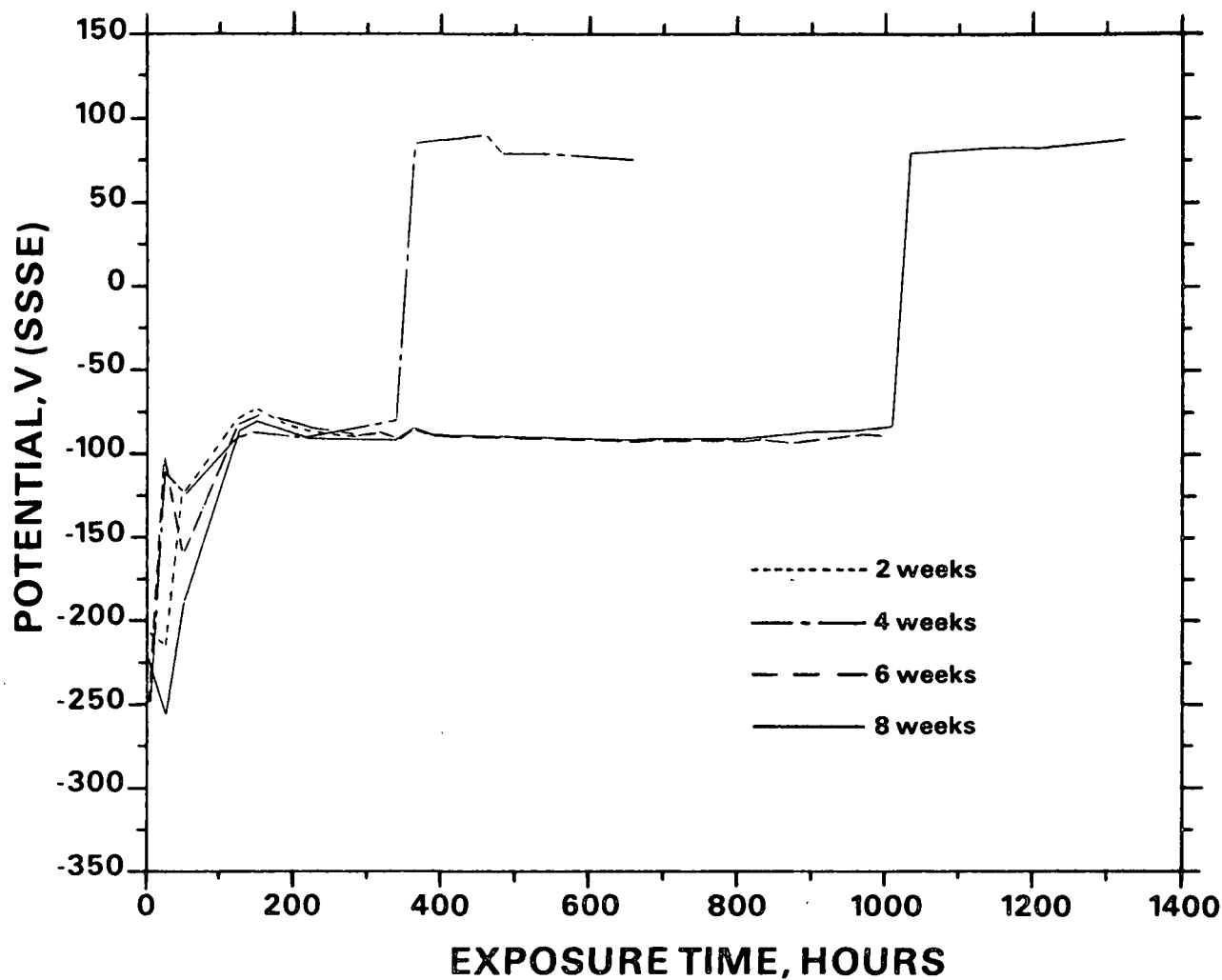


Figure AII-24. Corrosion potential in 60 g/L NaOH + 10 g/L Na₂S + 5 g/L Na₂S₂O₃. Similar behavior was observed in solutions of the following compositions:

NaOH, g/L	Na ₂ S, g/L	Na ₂ S ₂ O ₃ , g/L
60	10	10
60	10	25
80	10	2.5
100	10	10

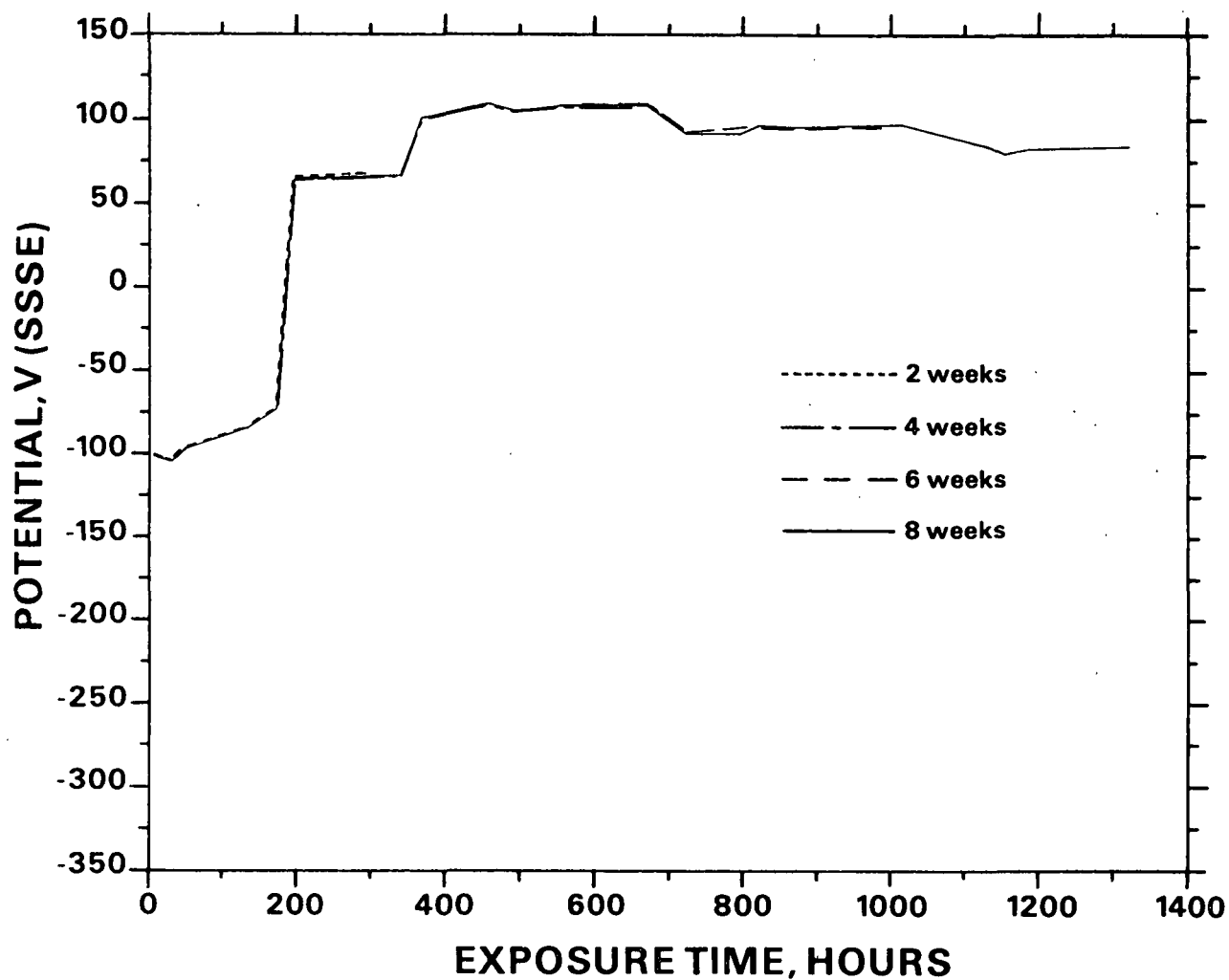


Figure AII-25. Corrosion potential in 60 g/L NaOH + 10 g/L Na₂S + 50 g/L Na₂S₂O₃. Similar behavior was observed in solutions of the following compositions:

NaOH, g/L	Na ₂ S, g/L	Na ₂ S ₂ O ₃ , g/L
80	10	25
80	10	50
100	10	25
100	10	50
120	10	25
120	10	50

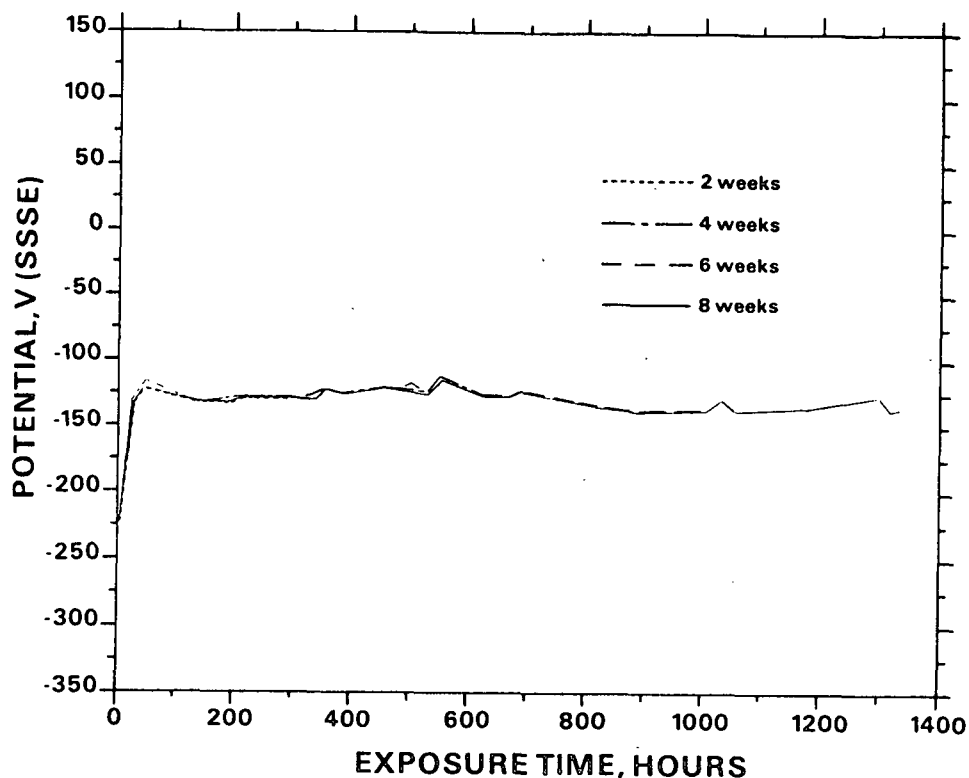


Figure AII-26. Corrosion potential in 60 g/L NaOH + 20 g/L Na₂S + 2.5 g/L Na₂S₂O₃. Similar behavior was observed in solutions of the following compositions:

NaOH, g/L	Na ₂ S, g/L	Na ₂ S ₂ O ₃ , g/L
60	20	5
60	20	10
60	20	25
60	20	50
60	30	2.5
60	30	5
60	30	10
60	30	50
60	40	25
60	40	50
80	20	10
80	20	25
80	20	50
80	30	25
80	40	25
80	40	50

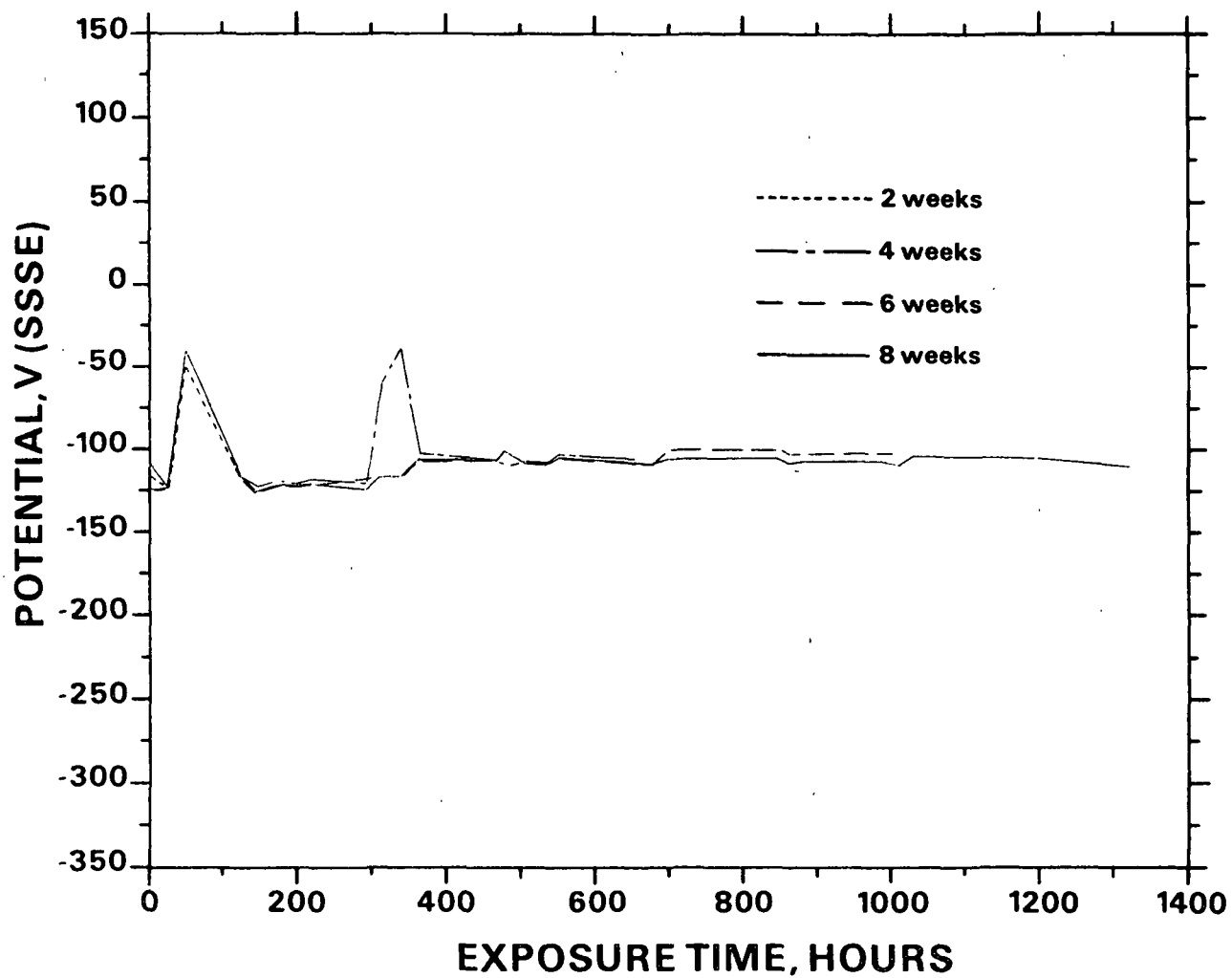


Figure AII-27. Corrosion potential in 60 g/L NaOH + 30 g/L Na₂S + 25 g/L Na₂S₂O₃. Similar behavior was observed in 100 g/L NaOH + 40 g/L Na₂S + 25 g/L Na₂S₂O₃.

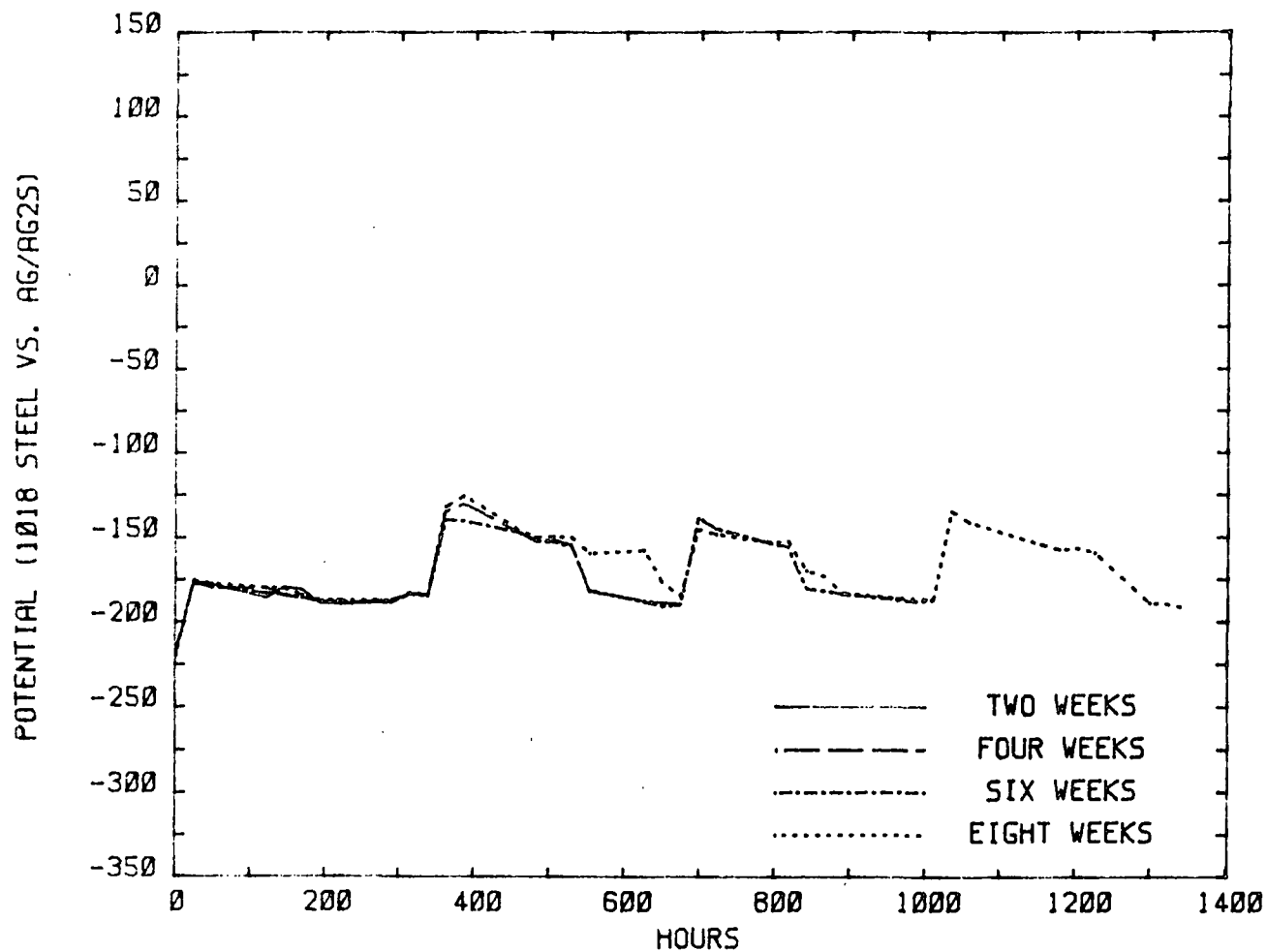


Figure AII-28. Corrosion potential in 60 g/L NaOH + 40 g/L Na₂S + 2.5 g/L Na₂S₂O₃. Similar behavior was observed in solutions of the following compositions:

NaOH, g/L	Na ₂ S, g/L	Na ₂ S ₂ O ₃ , g/L
60	40	5
60	40	10
80	40	10
100	20	2.5

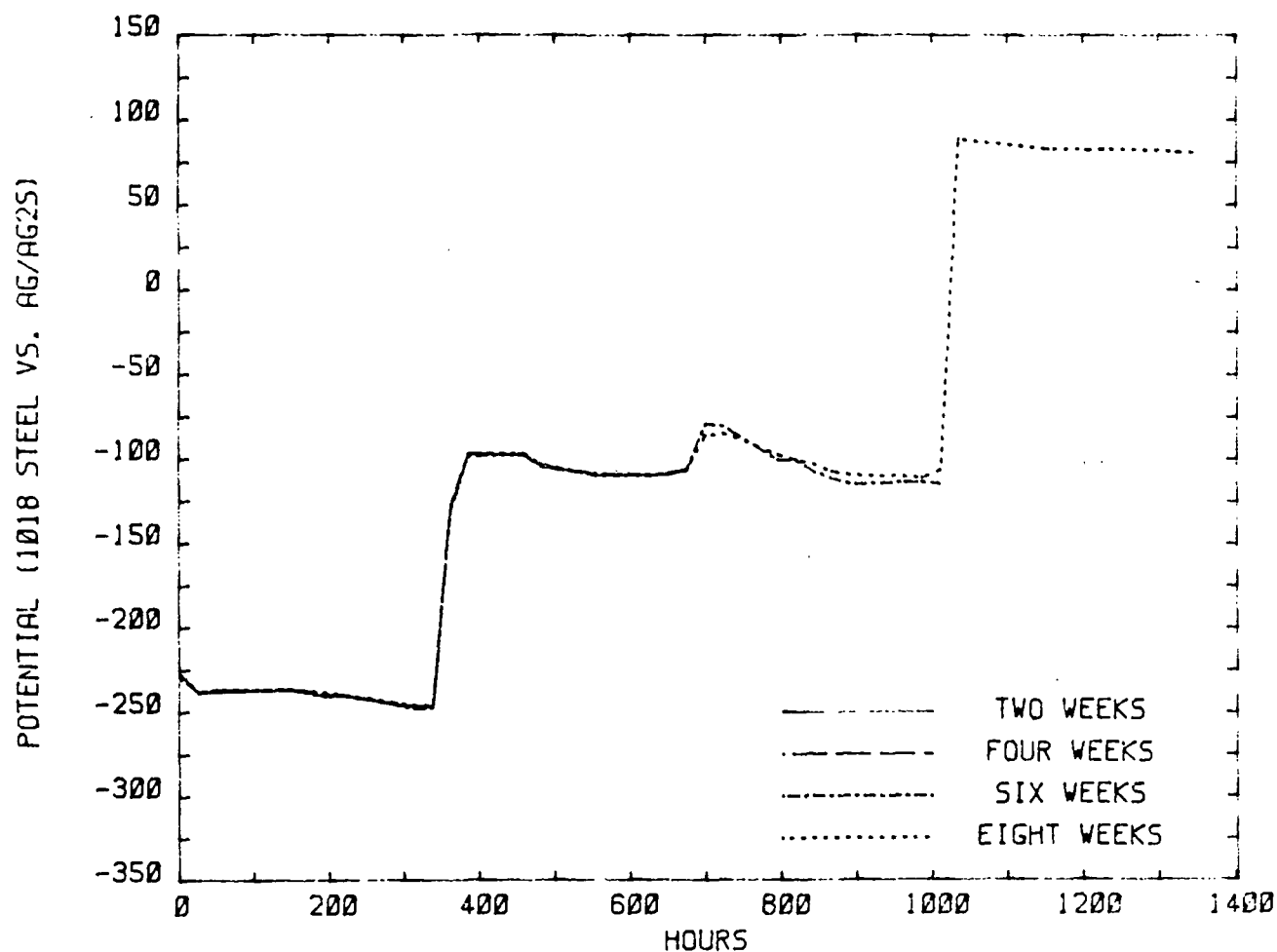


Figure AII-29. Corrosion potential in 80 g/L NaOH + 10 g/L Na₂S + 2.5 g/L Na₂S₂O₃. Similar behavior was observed in solutions of the following compositions:

NaOH, g/L	Na ₂ S, g/L	Na ₂ S ₂ O ₃ , g/L
80	10	5
80	10	10
80	30	5
80	40	5
100	10	2.5
100	10	5
100	20	5
100	10	10

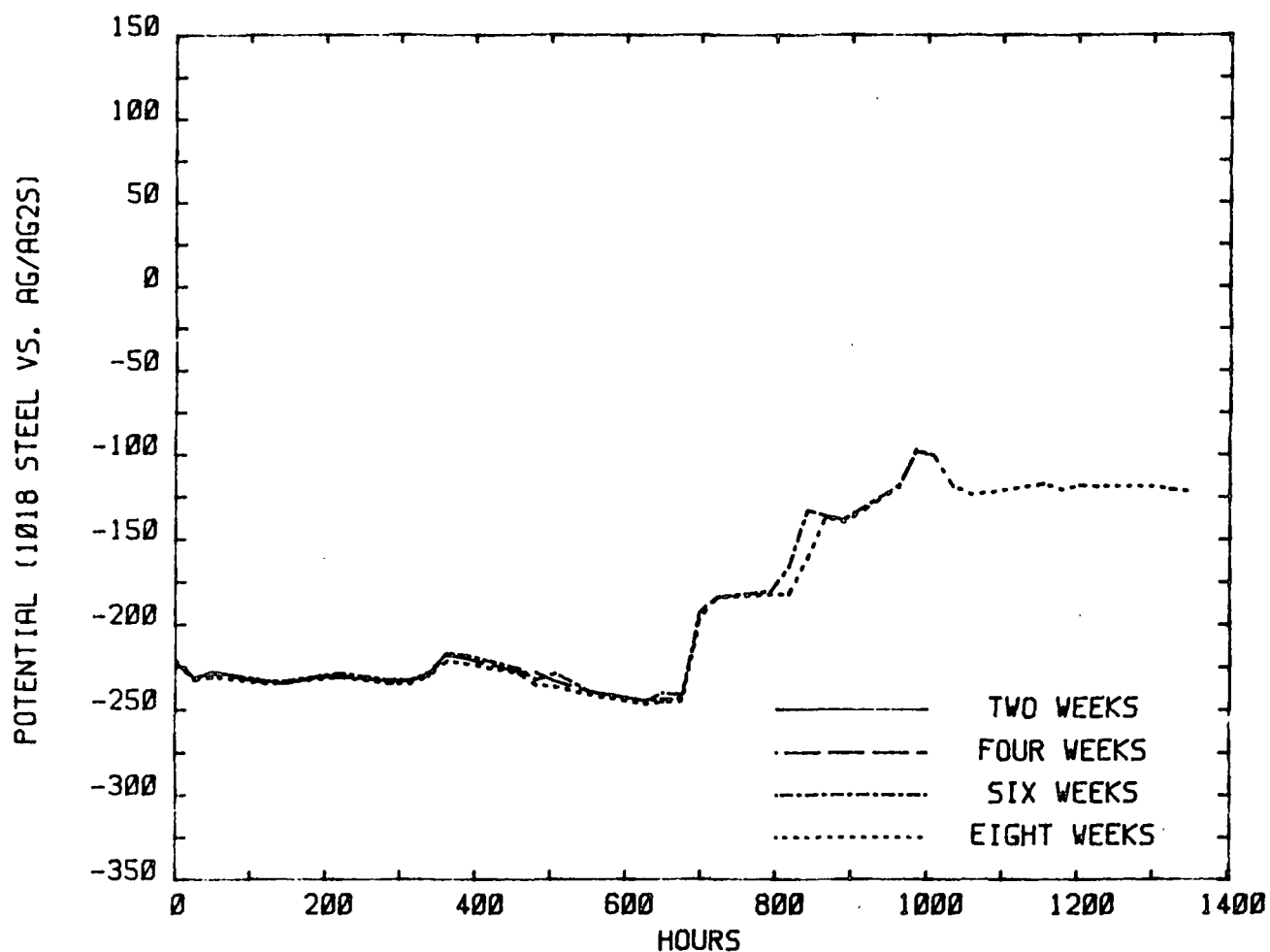


Figure AII-30. Corrosion potential in 80 g/L NaOH + 20 g/L Na₂S + 2.5 g/L Na₂S₂O₃. Similar behavior was observed in solutions of the following compositions:

NaOH, g/L	Na ₂ S, g/L	Na ₂ S ₂ O ₃ , g/L
80	20	5
100	10	2.5
100	30	5
100	40	10

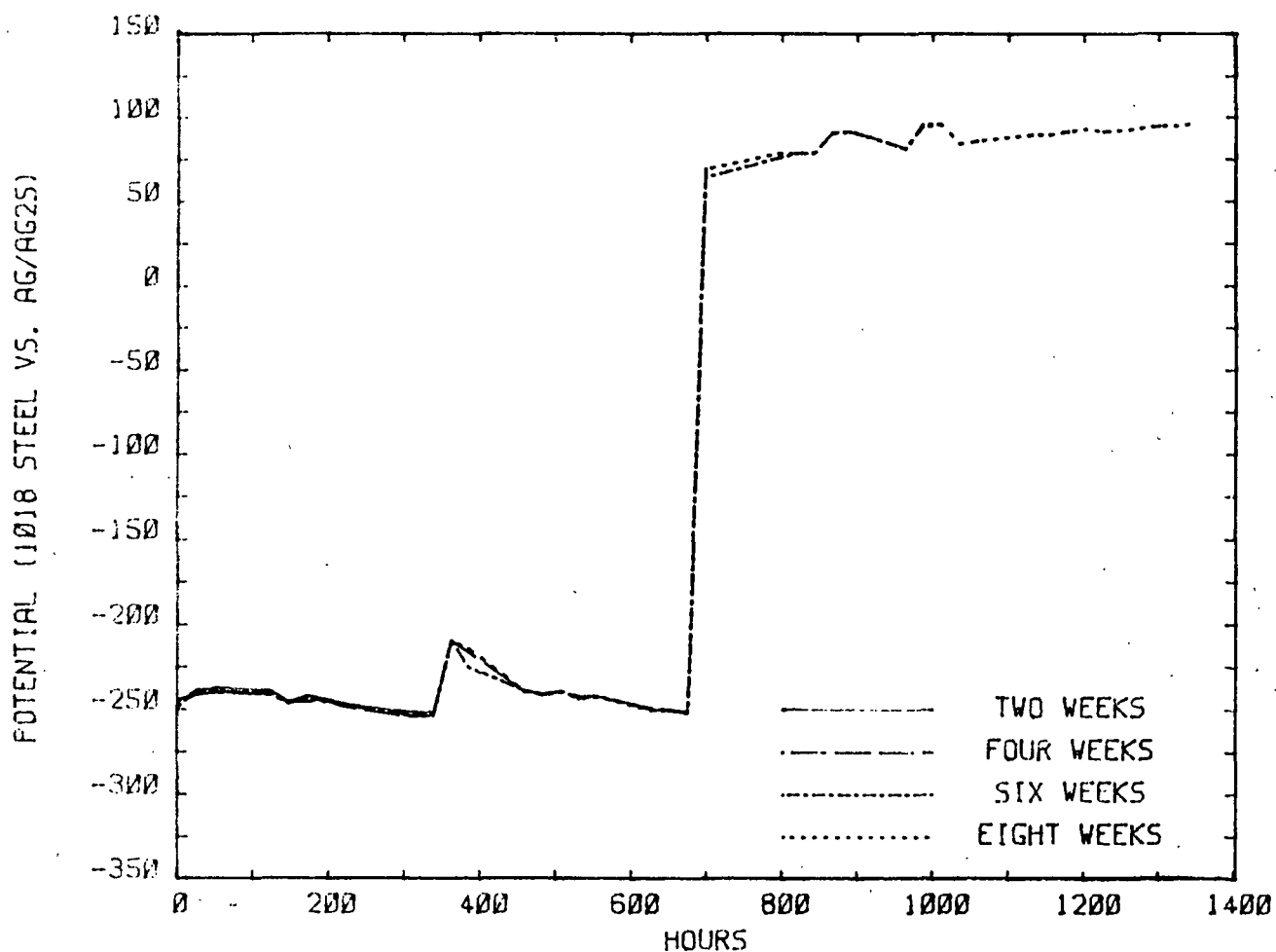


Figure AII-31. Corrosion potential in 80 g/L NaOH + 30 g/L Na₂S + 2.5 g/L Na₂S₂O₃. Similar behavior was observed in solutions of the following compositions:

NaOH, g/L	Na ₂ S, g/L	Na ₂ S ₂ O ₃ , g/L
80	40	2.5
100	40	2.5
100	40	5
120	20	2.5

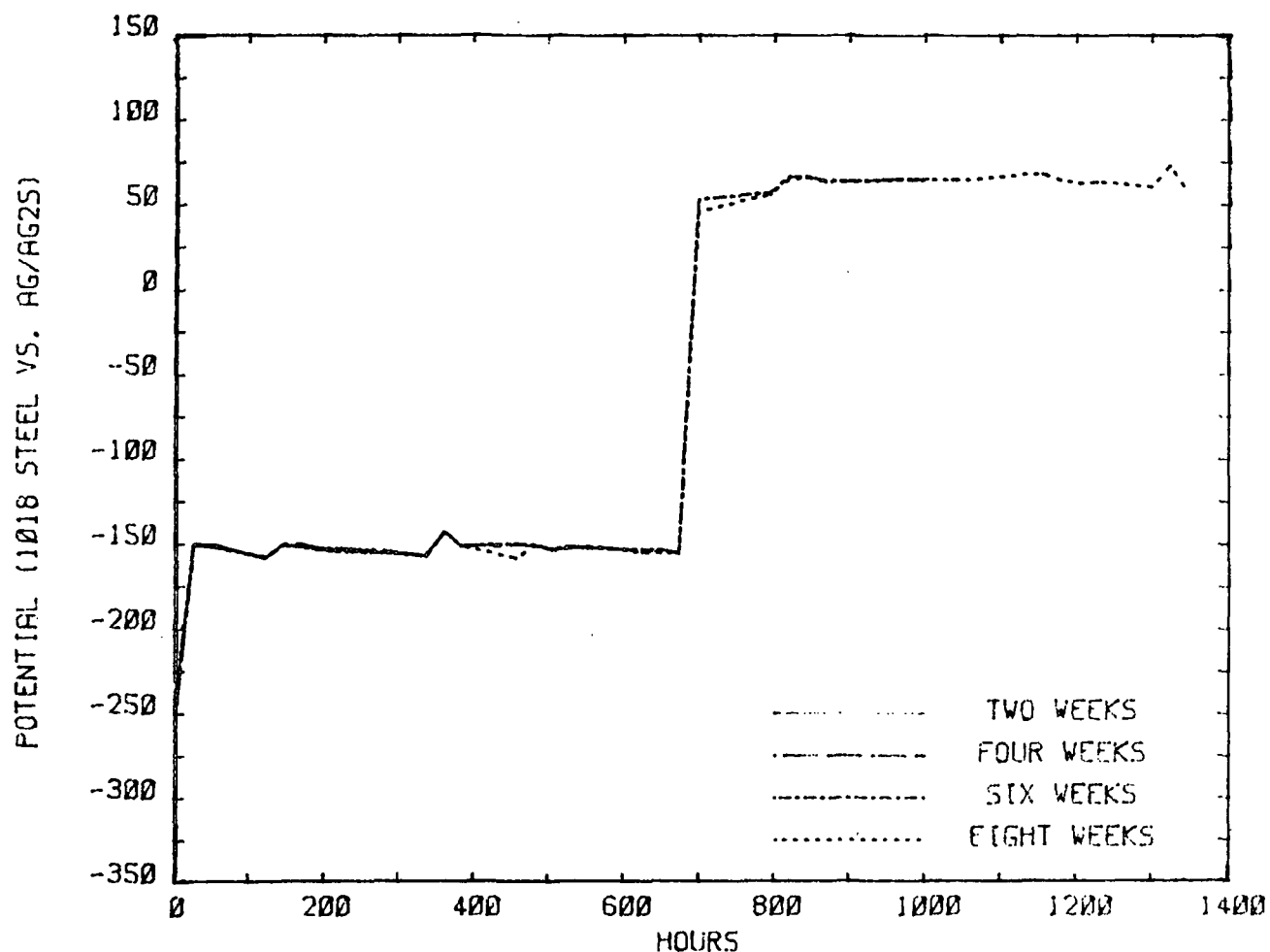


Figure AII-32. Corrosion potential in 80 g/L NaOH + 30 g/L Na₂S + 10 g/L Na₂S₂O₃. Similar behavior was observed in solutions of the following compositions:

NaOH, g/L	Na ₂ S, g/L	Na ₂ S ₂ O ₃ , g/L
80	30	25
80	30	50

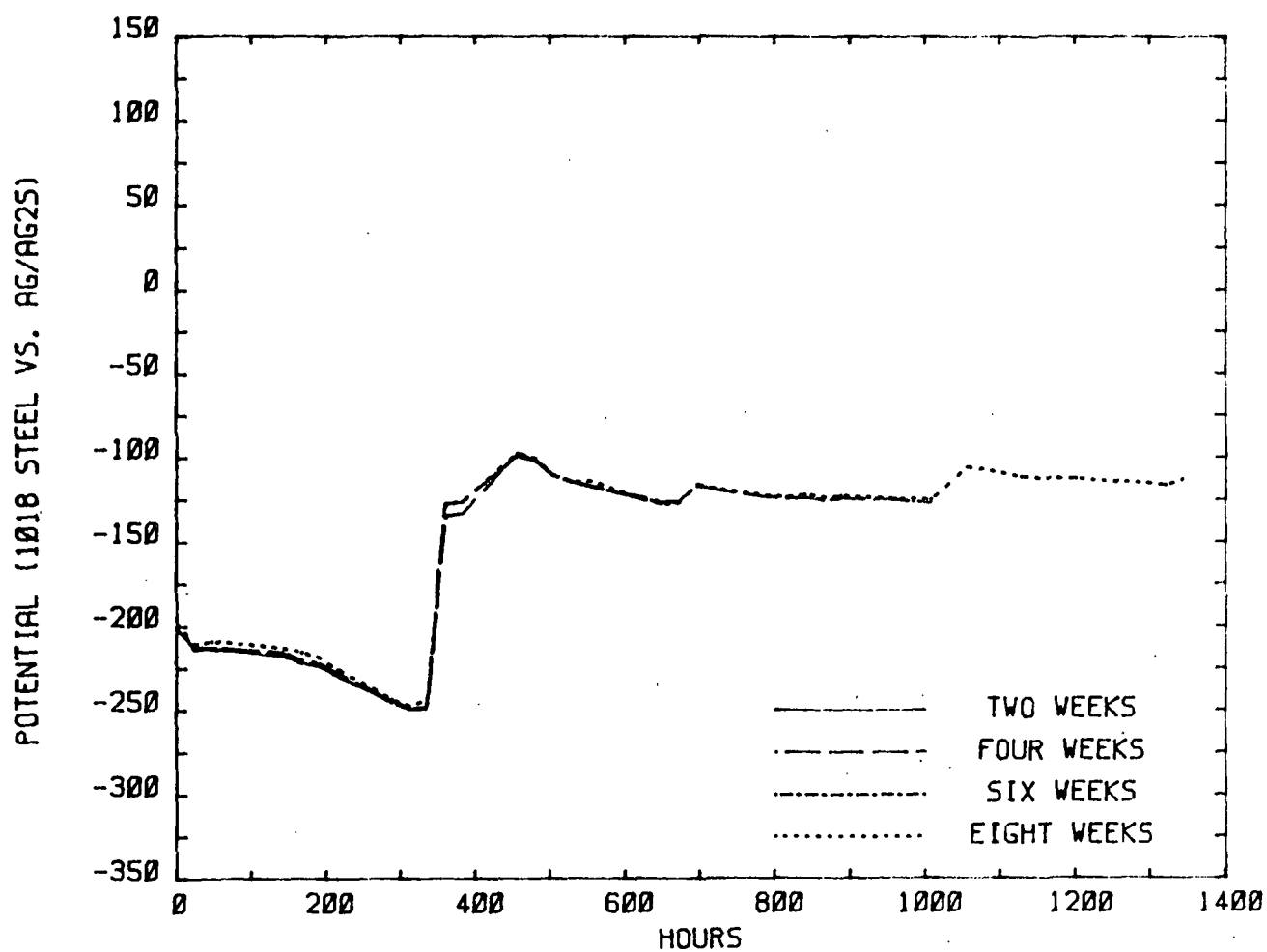


Figure AII-33. Corrosion potential in 100 g/L NaOH + 20 g/L Na₂S + 10 g/L Na₂S₂O₃.

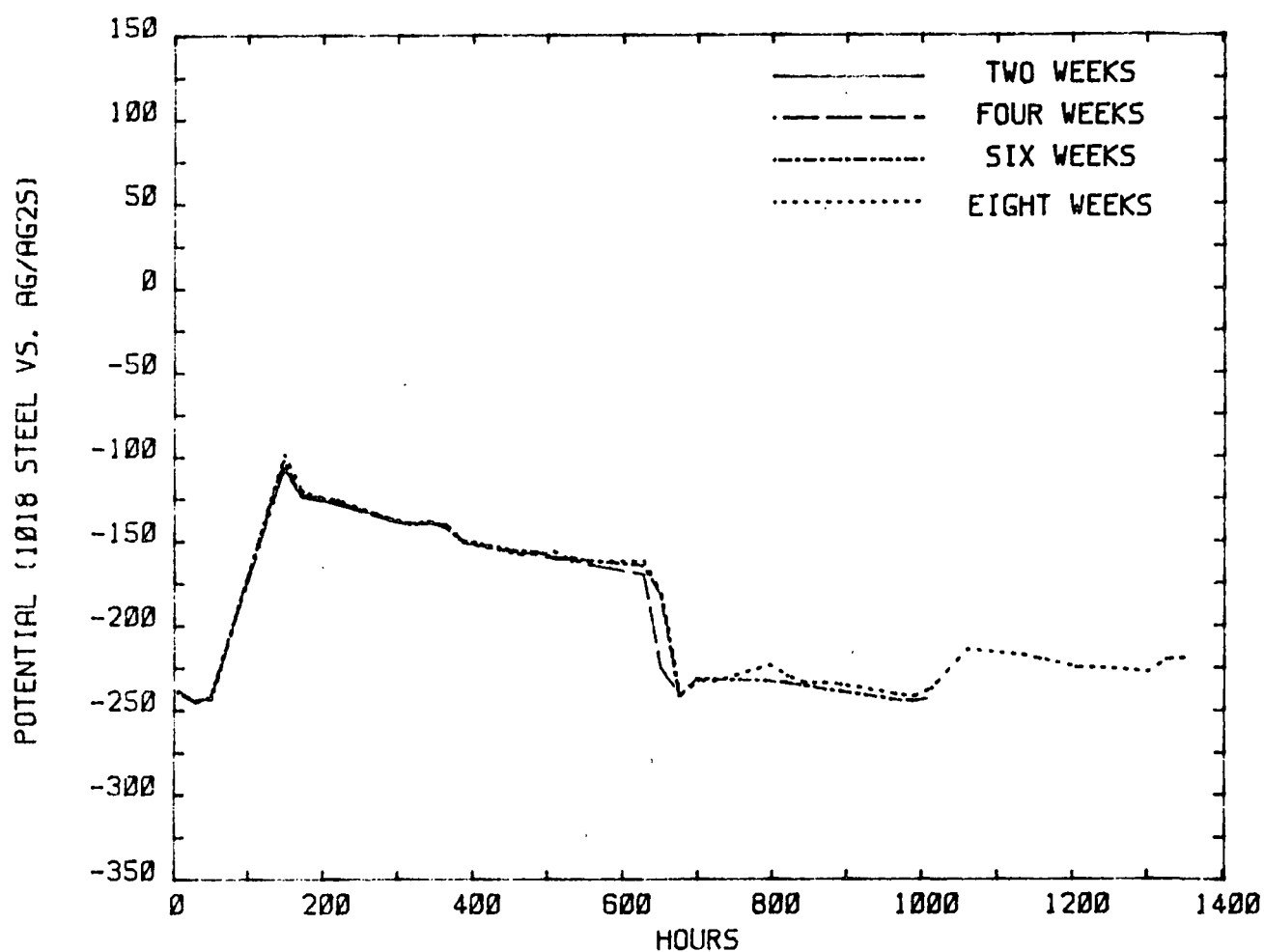


Figure AII-34. Corrosion potential in 100 g/L NaOH + 30 g/L Na₂S + 2.5 g/L Na₂S₂O₃. Similar behavior was observed in 100 g/L NaOH + 30 g/L Na₂S + 10 g/L Na₂S₂O₃.

APPENDIX III

DATA FROM POLARIZATION CURVES

SOLUTIONS WITH SULFUR ADDITIONS

Table AIII-1. Data from polarization curves. A. Solutions with sulfur additions; polarization curves on gold.

NaOH	Na ₂ S	S	Anodic E _{CORR}	β_A	Cathodic E _{CORR}	β_C	β_C	β_C
60	10	0	112		108	266		
		0.5	116		118	114		
		1	116		118	95		
		1.5	114		114	106		
		2	114		114	110		
		5	100		100	114		
		10	96		98	114		
60	20	0	104		108	311		
		0.5	116	104	118	110		
		1	118	97	118	108		
		1.5	114	90	116	114		
		2	118	86	120	120		
		5	116	69	114	140		
		10	112	81	112	133		
60	30	0	94		102			
		0.5	104	114	104	112		
		1	102	93	100	98		
		1.5	96		102			
		2	94	110	92	106		
		5	86	66	84	124		
		10	134	66	134	95		
60	40	0	100		62			
		0.5	109	106	108	91		
		1	110	100	110	91		
		1.5	96		104	110		
		2	102	106	104	104		
		5	106	66	106	130		
		10	92	66	80	104		
80	10	0	96	114	104	150		
		0.5	122	88	124	102		
		1	120	88	118	95		
		1.5	122	81	122	112		
		2	122	75	122	112		
		5	124		124	95		
		10	128		126	106		

Table AIII-1 (Continued). Data from polarization curves. A.
Solutions with sulfur additions;
polarization curves on gold.

NaOH	Na ₂ S	S	Anodic E _{CORR}	β_A	Cathodic E _{CORR}	β_C	β_C	β_C
80	20	0	90	118	96	193		36
		0.5	92	102	94	124		
		1	90	106	92	104		
		1.5	128	75	122	140		
		2	130	74	130	126		
		5	134	66	134	114		
		10	100	53	100	102		
80	30	0	82	135	94	250		34
		0.5	118	106	114		89	
		1	112	81	114	131		
		1.5	122	60	122	145	124	
		2	120	56	122	126	78	
		5	132	73	130	135	88	
		10	124	73	120	131	85	
80	40	0	86	122	84	225		36
		0.5	102	107	98		88	
		1	110	71	114	208		41
		1.5	116	70	118	135	89	
		2	126	71	124	142		
		5	118	57	120	124	78	
		10	132	73	130	135	91	
100	10	0	126	107	128			39
		0.5	112	—	114			34
		1	122	55	124	153		
		1.5	132	—	132	167		
		2	124	57	126	164		
		5	136	53	134	161		
		10	138	114	138			33
100	20	0	118		122	122		
		0.5	122	66	122	278		47
		1	126	69	126	217		
		1.5	124	78	124	134		
		2	126	66	126	165		
		5	126	60	126	135		
		10	128	56	128	174		
100	30	0	112	60/118	106			33
		0.5	112	75/114	114			44
		1	124	69	122	167		
		1.5	122	71	122	190	114	
		2	126	64	124	149		
		5	130	58	130	149		
		10	134	56	136	149		
100	40	0	88	85	110			39

Table AIII-2. Polarization curves of steel.

NaOH	Na ₂ S	S	Anodic E _{CORR}	β_A	Cathodic E _{CORR}	β_C	Anodic Peaks					
							A	B	C	D	E	F
60	10	0	-254	45	-242	284	-137	-27		89	198	
		0.5	-82	--	-74	--		-50				
		1	116	--	116	--						
		1.5	114	--	114	--						
		2	112	--	114	--						
		5	100	--	102	--						
		10	96	--	116	--						
60	20	0	-244	45	-282	108	-140		20	80		
		0.5	-90	--	-90	--			0			
		1	-90	--	-86	--		-89	1	40		
		1.5	-90	34	-82	--		-29	7	130		344
		2	-84	57	-84	--		-30	5	129		346
		5	116	--	114	--						
		10	112	--	112	--						
60	30	0	-242	--	-192	--	-136	-21		98		
		0.5	-116	36	-98	--		-42		116		
		1	-104	28	-74	--		-48		106		
		1.5	-158	--	-142	--		-25				
		2	-126	28	-128	--		-53		112		
		5	86	--	84	--						
		10	136	150	136	--						
60	40	0	-238	59	-242	108	-133	-21				
		0.5	-100	19	-104	--	-99					
		1	-98	49	-100	--			17		137	
		1.5	-146	--	-144	--		-48				
		2	-108	--	-110	--		-57		119		
		5	58	--	42	--				103		
		10	86	--	84	--						
80	10	0	-248	65	-246	--	-143	-37		65	165	
		0.5	-80	--	-84	--		-48				
		1	120	83	120	--						
		1.5	122	--	120	--						311
		2	122	--	122	--						
		5	124	62	124	114						
		10	130	--	130	118						
80	20	0	-246	63	-248	122	-137		-9	73	167	
		0.5	-124	--	-124	--		-34		99		
		1	-290	--	-120	--	-169	-67	11	90	139	
		1.5	124	--	122	91						
		2	132	--	128	93						
		5	134	--	132	108						
		10	100	--	98	120						

Table AIII-2 (Continued). Polarization curves of steel.

NaOH	Na ₂ S	S	Anodic E _{CORR}	β_A	Cathodic E _{CORR}	β_C	Anodic Peaks					
							A	B	C	D	E	F
80	30	0	-248	69	-182	131	-140		4	70		
		0.5	-102	---	-104	---		-20				
		1	28	---	0	---						
		1.5	58	---	60	---						
		2	60	---	66	---						
		5	52	---	52	---					143	
		10	48	---	46	---						
80	40	0	-224	66	-220	127						
		0.5	-124	---	-124	---			0			
		1	-166	98	-166	---		-34				334
		1.5	-152	---	-150	---	-93	-51		103		348
		2	-158	---	-164	---	-116			67		
		5	-116	---	-150	---				72		
		10	42	---	42	---						
100	10	0	-260	---	-260	---	-142	-41		76	222	
		0.5	-142	---	-144	---	-86				213	
		1	-144	---	-156	---	-125		28	79		
		1.5	84	---	-130	---						
		2	60	---	52	---						
		5	52	---	50	---						
		10	142	---	142	---						
100	20	0	-256	43	-258	114	-137	-43		69		
		0.5	-104	---	-104	---		-50		101		
		1	-94	---	-92	---		-57		105		
		1.5	-90	---	-92	170		-61		109		
		2	-84	49	-86	205		-54	24	132		277
		5	132	80	136	---						
		10	136	112	136	104						
100	30	0	-254	78	-254	94	-137	-42			191	
		0.5	-204	19	-202	---	-145	-41	50			260
		1	-108	---	-108	---	-97	-44		123		
		1.5	122	158	104	---						
		2	-100	---	-98	---		-69	-6	100		
		5	-90	---	-80	---		-54		106	180	325
		10	134	---	136	---						
100	40	0	-252	66	-254	95		-37				

Table AIII-3. Polarization curves on gold.

NaOH	Na ₂ S	Na ₂ S ₂ O ₃	Anodic E _{CORR}	β_A	Cathodic E _{CORR}	β_C	β_C
60	10	0	128	36	118		40
		2.5	128	57	127		45
		5	128		132	370	50
		10	116		112	161	52
		25	138		120	167	60
		50	120	49	126	190	66
60	20	0	130	58	138		40
		2.5	118	55	122	393	42
		5	132	50	130	505	45
		10	118	52	112		48
		25	114	53	112	190	47
		50	114	50	116	163	58
60	30	0	118	61	116		40
		2.5	126	56	122		41
		5	112	56	116		44
		10	120	55	118		52
		25	114	58	110	173	50
		50	110	53	110	161	60
60	40	0	108	55	112		36
		2.5	116	57	112		44
		5	118	60	122		45
		10	110	57	112	208	49
		25	114	61	120	235	58
		50	114	58	114	170	69
80	10	0	138		136		37
		2.5	140	48	136		45
		5	126	45	134	310	48
		10	142	57	140	255	52
		25	130	58	132	255	60
		50	136	41	126	201	78
80	20	0	136	53	126		41
		2.5	122	56	120	417	43
		5	128	83	132	319	49
		10	114	75	124	250	56
		25	122	54	114		56
		50	112		118		67
80	30	2.5	152	57	124	352	41
		5	146	63	126	417	49
		10	128	60	108	505	44
		25	136	56	120	290	64
		50	104	61	118	183	61

Table AIII-3 (Continued). Polarization curves on gold.

NaOH	Na ₂ S	Na ₂ S ₂ O ₃	Anodic E _{CORR}	β _A	Cathodic E _{CORR}	β _C	β _C
80	40	2.5	106	78	118	335	47
		5	112	74	110	278	45
		10	110	69	110	212	57
		25	102	66	110	170	56
		50	100	66	108	161	73
100	10	2.5	182	57	136	393	42
		5	142		126	250	48
		10	130	47	138		44
		25	114	48	128	235	57
		50	114	56	130	201	60
100	20	2.5	138	63	122	319	45
		5	126	60	116	230	28
		10	112	45	118	239	52
		25	110	57	124	216	56
		50	102	55	118	193	70
100	30	2.5	106	61	118	335	41
		5	110	66	116	250	53
		10	114	69	114	235	57
		25	104	66	118	201	69
		50	114	64	120	180	55
100	40	2.5	102	75	114	255	47
		5	92	72	106	235	44
		10	102	67	114	240	52
		25	110	69	116	255	63
		50	102	69	108	156	70
120	10	2.5	120	66	142	472	42
		5	116	60	136	393	44
		10		60		319	48
		25		55		208	57
		50		52		173	66
120	20	2.5		63		300	45

Table AIII-4. Polarization curves of steel.

NaOH	Na ₂ S	Na ₂ S ₂ O ₃	Anodic	β_A	Cathodic	β_C	Anodic Peaks					
			E _{CORR}		E _{CORR}		β_A	B	C	D	E	F
60	10	0	-260	40	-262	94	-150	-44	82	175		
		2.5	-250	--	-252	78	-151	-42	77			
		5	-216	--	-214	--	-154	-44	62	179	261	
		10	-102	--	-98	--		-49	107	174		
		25	-92	--	-90	102		-54	97	143	282	
		50	-90	13	-88	--		-53	111	169	247	
60	20	0	-240	69	-250	126	-152	-45	72	182		
		2.5	-232	79	-230	--	-149	-50	72	180		
		5	-222	78	-224	--	-151	-47	67	175		
		10	-174	--	-108	--	-139	-46	118			
		25	-110	23	-112	50		-51				
		50	-114	20	-120	78		-53				
60	30	0	-238	66	-238	88	-144	-42				
		2.5	-232	74	-234	167	-146	-41	74			
		5	-230	77	-228	161	-146	-44	79			
		10	-122	--	-138	--		-47				
		25	-104	--	-128	--		-58	97			
		50	-128	--	-120	--		-56				
60	40	0	-242	69	-244	93		-36				
		2.5	-224	91	-228	170		-37				
		5	-170	--	-202	--		-38				
		10	-140	--	-114	72		-41				
		25	-132	--	-128	--		-39				
		50	-122	--	-120	--		-42				
80	10	0	-246	33	-246	83	-152	-49		159		
		2.5	-234	53	-232	--	-154	-54	55	155		
		5	-102	27	-100	98		-53		166	244	
		10	-206	53	-212	205	-154	-50	55	165	244	
		25	-100	34	-98	120		-52		170	247	
		50	-104	--	-110			-63	94	173	242	
80	20	0	-240	66	-242	170	-149	-51	63			
		2.5	-224	63	-232	176	-151	-53	65	168		
		5	-204	20	-202	--	-149	-51	55		261	
		10	-128	27	-194	335		-59			257	
		25	-118	20	-118	67		-59			255	
		50	-112	--	-110	88		-59			259	
80	30	2.5	-210	57	-216	255		-39				
		5	-186	37	-204	393	-145	-39			269	
		10	-190	--	-192	--	-165	-39	58		266	
		25	-126	--	-128	--		-56			263	
		50	-116	--	-114	57		-52	96		269	

Table AIII-4 (Continued). Polarization curves of steel.

NaOH	Na ₂ S	Na ₂ S ₂ O ₃	Anodic	β_A	Cathodic	β_C	Anodic Peaks					
			E _{CORR}		E _{CORR}		β_A	B	C	D	E	F
80	40	2.5	-204	48	-216	335		-50				
		5	-200	49	-196	112					236	
		10	-166	--	-182	98	-146				271	
		25	-132	--	-132	78	-111	-41			269	
		50	-126	28	-132	94		-59		113	270	
100	10	2.5	-234	49	-234	--	-160	-59	45	145		
		5	-214	52	-208	34	-157	-57	48	159	246	
		10	-218	53	-216	230	-159	-56	40	155	251	
		25	-206	50	-204	190	-157	-54	43	159	241	
		50	-100	19	-106	118		-65				
100	20	2.5	-218	53	-218	--	-147	-47	49		257	
		5	-226	55	-224	--	-150	-53	48		259	
		10	-212	50	-210	255	-146	-49	46	190	255	
		25	-186	--	-186	78		-47	35		254	
		50	-118	--	-116	104		-60			264	
100	30	2.5	-232	54	-234	180	-146	-45	45	192		
		5	-202	49	-202	167	-143	-43			258	
		10	-194	--	-194	--	-146	-43	91		259	
		25	-128	--	-136	--		-47	91		263	
		50	-124	--	-120	44	-102	-52	100		265	
100	40	2.5	-206	55	-208	--		-40				
		5	-204	54	-204	142		-42			263	
		10	-180	86	-180	--		-41			261	
		25	-169	88	-166	116		-59	85		251	
		50	-138	36	-140	110		-50	83			
120	10	2.5	-246	42	-244	278	-162	-59	31			
		5	-232	--	-230	--	-162	-59	33	143		
		10		41		205						
		25		--		--						
		50		--		--						
120	20	2.5		47		--						

IPST HASELTON LIBRARY



5 0602 01057255 2